5-12-2005

Provenance and Depositional History of Late Pleistocene New Jersey Shelf Sediments

Roxie Jessica Turner

PROVENANCE AND DEPOSITIONAL HISTORY OF LATE PLEISTOCENE NEW JERSEY SHELF SEDIMENTS

by

ROXIE JESSICA TURNER

Under the Direction of Beth A. Christensen

ABSTRACT

Pleistocene New Jersey shelf sedimentology is strongly influenced by glacially driven sea level changes. A combination of regressive shoreline processes, subaerial exposure, fluvial downcutting, and deposition and reworking during transgression has influenced the NJ shelf sediment composition. Sediment provenance and transport history may be determined on a shelf environment through analysis of grain size distribution, heavy mineral content, magnetic mineral concentrations, and isotopic dating methods. A combination of surface grab and stratigraphic samples were analyzed within the study area. Relatively high percentages of heavy minerals were found in the 2ϕ and 3ϕ size fractions and hornblende grains provided K-Ar age values indicating two groups of sediment sources. The first source is Grenville with apparent ages above 900 Ma deposited during marine OIS 1. The second source is a mixed assemblage of Grenvillian and Paleozoic sources deposited during marine OIS 3, with apparent ages of approximately 850 ± 20 Ma.

INDEX WORDS: New Jersey shelf, Provenance, Heavy minerals, IRD, Grain size analysis, Sedimentology, Hudson Highlands

PROVENANCE AND DEPOSITIONAL HISTORY OF LATE PLEISTOCENE NEW JERSEY SHELF SEDIMENTS

by

ROXIE JESSICA TURNER

A Thesis Submitted in Partial Fulfillment of Requirements for the Degree of
Master of Science
Georgia State University

2005

PROVENANCE AND DEPOSITIONAL HISTORY OF LATE PLEISTOCENE NEW JERSEY SHELF SEDIMENTS

by

ROXIE JESSICA TURNER

Major Professor: Dr. Beth A. Christensen
Committee: Dr. Eirik Krogstad
Dr. Clark Alexander
Dr. J. Marion Wampler

Electronic Version Approved:

Office of Graduate Studies
College of Arts and Sciences
Georgia State University
May 2005

ACKNOWLEDGEMENTS

This study is supported by the Office of Naval Research (ONR) grant N00014-04-1-0036 to Dr. Beth Christensen with analyses at Georgia State University and Georgia Institute of Technology. Additionally, Georgia State University financially assisted through a teaching assistantship granted in the Fall 2003 and Spring 2004 academic semesters. A writing consultant position granted for Spring 2005 semester provided additional financial support for this research. I thank Dr. Beth Christensen, my thesis advisor, for all of her help, support, direction, and encouragement. I thank Dr. Marion Wampler for his help with the K-Ar isotopic dating of hornblende grains, his support during the writing of my thesis, and participation on my thesis committee. I thank Dr. Eirik Krogstad for logistical assistance with the zircon dating and magnetic mineral separations at Georgia State University and for his participation on my thesis committee. I thank Dr. Clark Alexander for his participation on my thesis committee. I thank John Goff, Hilary Olson, Sean Gulick, and Sylvia Nordfjord, all from the University of Texas at Austin working under ONR grant N00014-00-1-0844, who wet sieved the grab samples used in this study. I thank Robert Neurath, Vanessa Donnelly, Jennifer Fisher, and Donald Hardison who assisted with sample preparation of the downcore samples and with a portion of the heavy mineral separations. I thank all of the faculty and staff in the Georgia State University Geology Department for their assistance and encouragement. I thank Alex Turner, my husband, and our friends and family for their support and encouragement.

TABLE OF CONTENTS

Page

LIST OF TABLES

LIST OF FIGURES

LIST OF ABBREVIATIONS AND SYMBOLS

IRD	ice-rafted debris	m	Meter
HM	heavy minerals	cm	centimeter
ONR	Office of Naval Research	mm	millimeter
LGM	Last glacial maximum	μm	micrometer
THM	Total heavy minerals	nm	nanometer
RHM	Recovered heavy minerals	ft.	foot
EHM	Economic heavy minerals	g	gram
H1	Heinrich layer 1	mg	milligram
H2	Heinrich layer 2	kg	kilogram
H3	Heinrich layer 3	yr	year
H4	Heinrich layer 4	ka	thousand years ago
H5	Heinrich layer 5	My	million years
H6	Heinrich layer 6	Ma	million years ago
ZTR	zircon-tourmaline-rutile	Ga	billion years ago
°C	degrees Celsius	B.P.	before present (or 1950)
ρ	density	mL	milliliter
N	north	A	ampere
S	south	mA	milliampere
HF/LC	high fine/low coarse	MeV	megaelectron volt
		mol	mole
AAS	atomic absorption spectrophotometer	AEI	Associated Electrical

			Industries
^{38}Ar	argon-38	NJ	New Jersey
$^{40}Ar_i$	initial amount of ^{40}Ar	UK	United Kingdom
λ_{total}	total decay constant of ^{40}K	*R/V*	research vessel
λ_{EC}	partial decay constant for decay of ^{40}K to ^{40}Ar	*CHS*	Canadian Hydrographic Survey
t	time		

CHAPTER 1: INTRODUCTION

1.0 Objectives

Detrital sediments on a continental shelf can provide evidence of provenance and transport history through geochronological determinations and mineralogical assessment. By establishing the provenance, or source region, of marker minerals, the sediment history will be better understood. Additionally, transport history leading to the final deposition of sediment grains on the shelf may be established from the compositional and textural maturity of individual grains. Transport history can answer questions about the timing and nature of surface features such as sand ridges and sand ribbons. If proximal and distal basin sediment sources are identified, ice rafting may have been a mechanism of transport. Ice rafted debris (IRD) consists of sediments transported by icebergs that are deposited onto the seafloor as the iceberg melts.

This study seeks to establish the provenance and transport history of New Jersey shelf sediments and address the possible presence of IRD on the New Jersey shelf by study of mineral assemblages, grain size distributions, and radiometric ages of mineral grains. Through this study, the formation of large- and small-scale features on the New Jersey shelf such as the outer shelf wedge and sand ribbons will also be evaluated. The ultimate goals of this study are to determine 1) the age and provenance of New Jersey shelf sediments; 2) the transport history of the sediments; and 3) any presence of IRD on the New Jersey shelf. If IRD is identified on the New Jersey shelf, a new southerly extent of iceberg transport will have been established.

1.1 Study Area

The survey area for this study is located on the New Jersey shelf, to the south of the submerged portion of the Hudson River Valley (Figure 1.1), and includes the outer shelf wedge and the Franklin scarp (Goff et al., 1999). The Office of Naval Research (ONR) STRATAFORM (STRATA FORmation on Margins) swath survey area represents the extent of multibeam bathymetry and backscatter data collected aboard the *CHS Creed* in 1996 (Goff et al., 1999). This region has been previously studied and imaged as a part of the ONR Geoclutter program, an initiative to better understand and model bedforms and stratigraphic features that respond to acoustic energy. Nearly 100 grab samples were collected along transect lines perpendicular to the shoreline (Figure 1.2) from aboard the *R/V Cape Henlopen* in 2001 (Goff et al., 2004). In addition, three sites were drilled for stratigraphic sampling from aboard the *R/V Knorr* in 2002. A group of 31 grab samples and samples from two core sites were targeted for analysis in this study.

River-transported materials eroded from the glacial deposits to the north and IRD are thought to be major contributors to the existing mineralogical diversity of the New Jersey shelf sediments. Additionally, iceberg keel marks have been reported in the New Jersey study area (Duncan and Goff, 2001). If icebergs have grounded on the New Jersey shelf in the past, they would have released IRD at the grounding sites upon melting. The New Jersey shelf sediment is dominated by terrigenous medium to fine quartz sands that are equivalent in grain size to the IRD found in deep marine environments. Thus, IRD identification methods that use grain size as a marker are not useful in this area. Methods that trace provenance, such as those used by Hemming et al. (1998), can be applied to this study.

FIGURE 1.1 Study area on the New Jersey Shelf (from Goff et al., 1999). The gray area represents the Strataform Swath Survey Area. Contours are in meters.

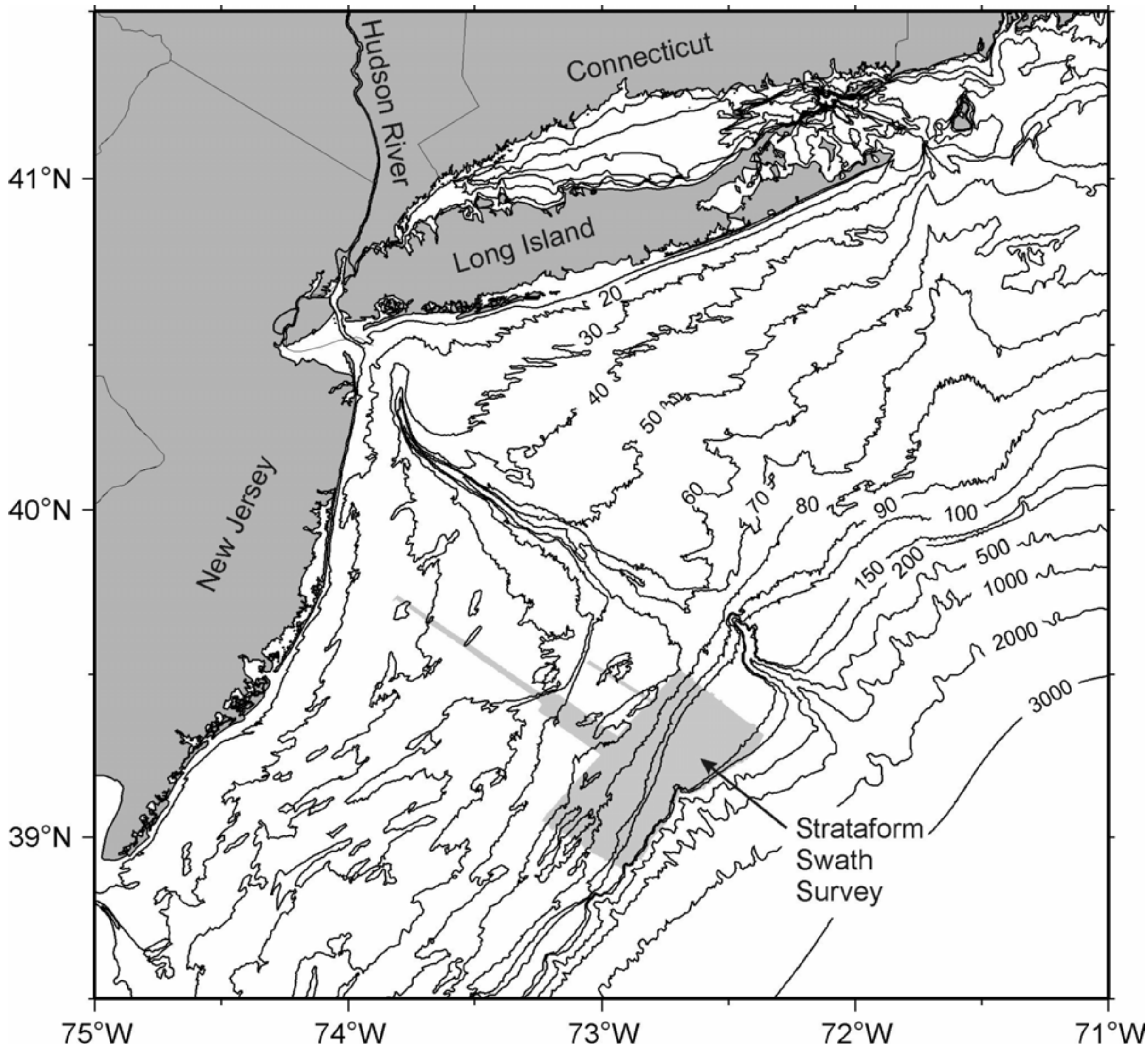

FIGURE 1.2 Survey area with grab sample and core locations with contours in meters, adapted from Goff et al. (1999).

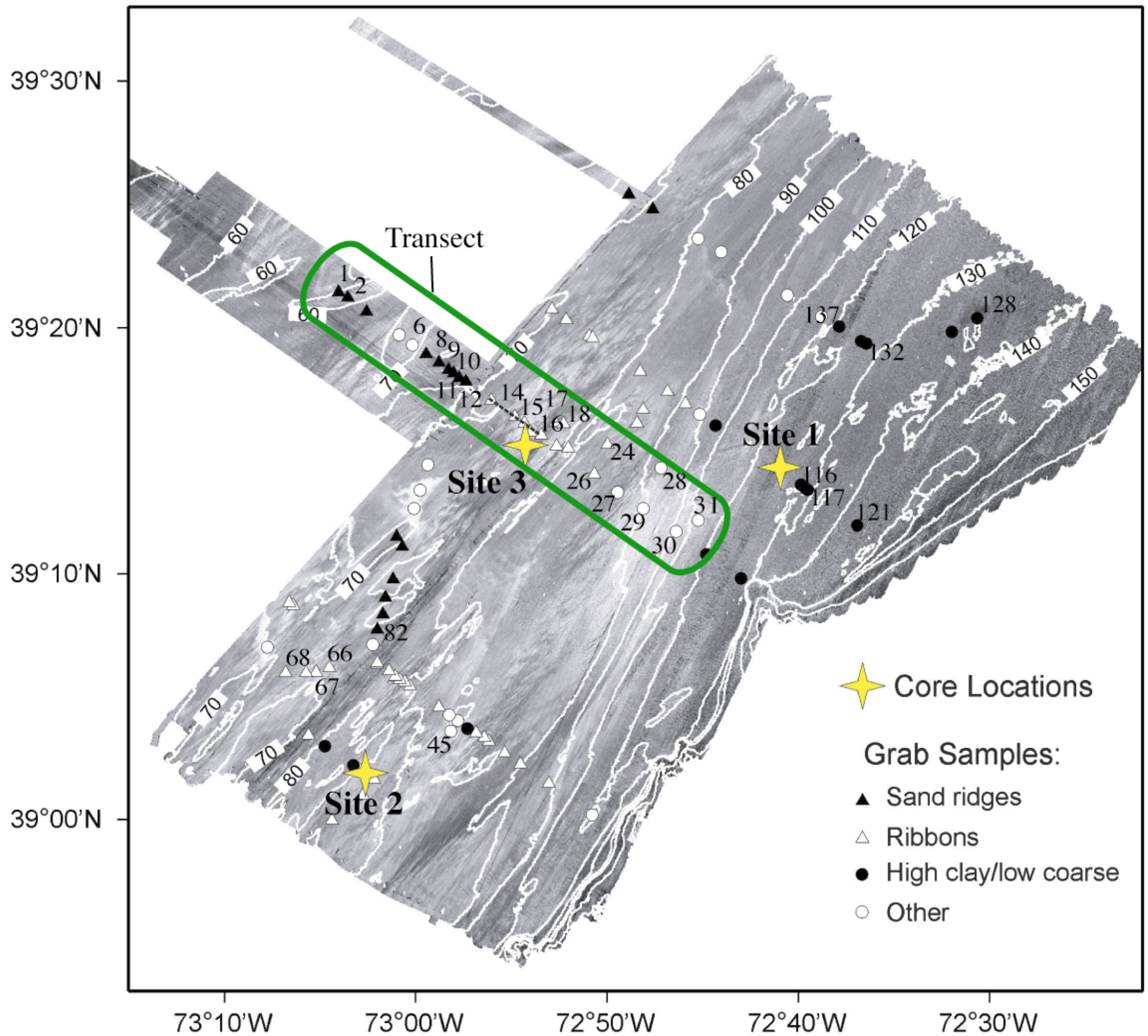

1.2 Regional Geology

The continental region that surrounds the New Jersey shelf includes New York, New Jersey, and Pennsylvania. Within these states, numerous geologic units of a vast array of geologic ages and mineralogy outcrop. The Appalachians, the Highlands, the Taconic Mountians, the Ramapo Mountains, and the Manhattan, Reading and Trenton Prongs (Figure 1.3) provide exposed rock that is eroded and transported to form sediments found today on the New Jersey continental shelf. Additionally, glacial advances over some of the region surrounding the New Jersey shelf have scraped up weathered rock, soil, and blocks of bedrock, periodically increasing the rate of erosion.

The geology of the Hudson Valley is important to consider for this study because the Hudson River is the primary drainage channel emptying into the study area, both historically and presently. Fluvial sediment discharge through this drainage system has been a significant source of sediment to the New Jersey shelf over time. The Hudson River valley is underlain by rock units of varying in age from Grenvillian to Jurassic.

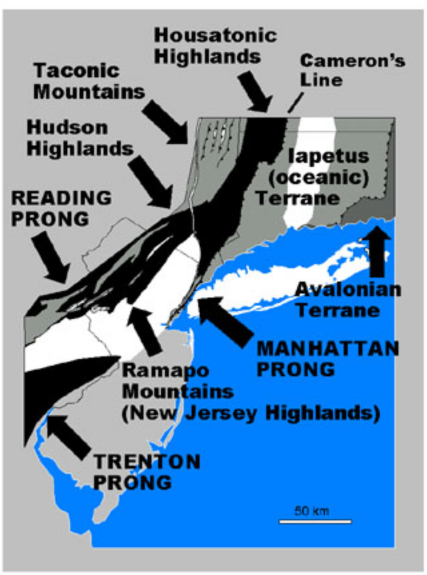

FIGURE 1.3 Map of mountain ranges of New Jersey and New York from USGS (2003).

Figure 1.3 illustrates the extent of the Hudson Highlands and related rock features representing an outcrop belt of crystalline basement rocks, which are largely Precambrian in age. The Hudson Highlands are a part of the Reading Prong that extends northeastward from Reading, Pennsylvania, meeting the Taconic Mountains in New York State (USGS, 2003).

Gates and Krol (1998) and Gates et al. (2000) studied

the faults and associated fractures within the Hudson and New Jersey Highlands. They found that hornblendes within mineralized fracture zones have $^{40}Ar/^{39}Ar$ ages of 915 $\pm$ 9 Ma while those from in and around granitic pegmatites have ages of 896 $\pm$ 8 Ma.

The Cortlandt Complex (Figure 1.4) is an oval-shaped igneous body approximately 40 km2 in area that intrudes rocks of the Manhattan Prong along the eastern margin of the Hudson River approximately 50 km north of New York City (Dallmeyer, 1975). It consists of six discrete, sequentially intruded plutons of mafic rocks. Two smaller mafic intrusions, the Rosetown and Stony Point complexes, are extensions of the Cortlandt Complex found on the western side of the Hudson River.

Several studies have been completed to determine the mineralogy and age of the different rock units found along the Hudson River. Dallmeyer (1975) determined the ages of the Cortlandt and Rosetown plutons using $^{40}Ar/^{39}Ar$ incremental-release dating on biotite and hornblende. The Cortlandt complex, which contains a diverse assemblage of igneous rocks ranging from peridotite to diorite, was dated with hornblendes, which recorded ages of 420 Ma and biotites, with ages of 390 Ma. The Rosetown pluton has an older core of hornblendite, hornblende-pyroxeneite, and hornblende-diorite that is crosscut by a younger phase of biotite- and hornblende-diorite, lamprophyre, cortlandtite, and granodiorite (Dallmeyer, 1975). The younger phase of Rosetown hornblende samples provided ages of 463 $\pm$ 10 Ma and 483 $\pm$ 10 Ma and biotites recorded an average age of 420 Ma. The older phase of the Rosetown pluton was determined with biotites to be 473 $\pm$ 10 My (Dallmeyer, 1975). Bender et al. (1982) summarized the isotopic dating using K-Ar, $^{40}Ar/^{39}Ar$, and Rb-Sr procedures completed by Long and Kulp (1962), Dallmeyer (1975), Ratcliffe et al. (1982), and Bender (1980). These studies show that the Cortlandt, Stony Point, and Rosetown complexes are approximately 430 Ma old. Domenick

and Basu (1982) obtained a Sm-Nd isochron age for the Cortlandt Complex of 430 $\pm$ 34 Ma, which they interpreted to be the crystallization age.

FIGURE 1.4 Regional geologic map of the Hudson Valley illustrating the Cortlandt, Stony Point, and Rosetown complexes in relation to the Hudson River with sample locations analyzed by Bender et al., 1984. CC – Cortlandt Complex; C-O – Cambro-Ordavician; PC – Precambrian; PG – Peekskill Granodiorite; RT – Rosetown; SP – Stony Point; TR – Triassic (from Bender et al., 1984).

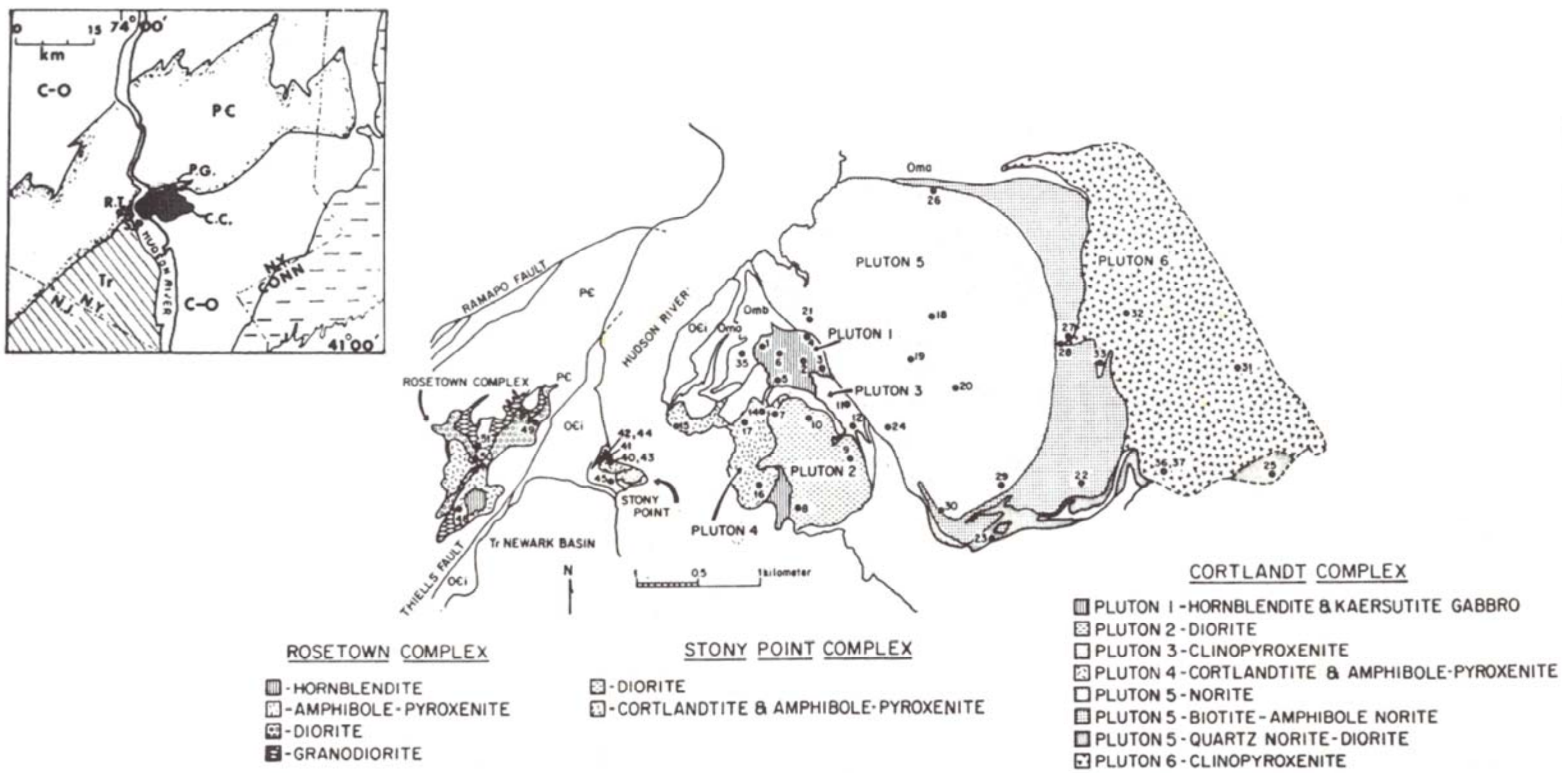

1.3 Geologic History of New Jersey

New Jersey is divided into four physiographic provinces based on distinctive geology and landforms (Figure 1.5). The geologic map of New Jersey is shown in Figure 1.6. Precambrian units outcrop throughout the Highlands Province and are underlain by the oldest rocks in the state (ages of 1,320 My to 750 My). These Precambrian rocks are part of the aforementioned Reading Prong that extends to the northeast and southwestinto New York and Pennsylvania (Smith, 1969). Six major rock types have been described for the majority of the Highlands Province: hypersthene-quartz-andesine gneiss, pyroxene-quartz-feldspar gneiss, quartz-feldspar-biotite gneiss, amphibolite, marble, and granite (Smith, 1969). Petrologically, the Precambrian rocks found in the New Jersey Highlands are unlike those found in the Blue Ridge Mountains to the south, but are very similar to rocks found in the Adirondacks of New York and the Grenville province of Canada (Drake, 1969).

The Valley and Ridge Province is underlain by Paleozoic sedimentary units of siltstones, shales, sandstones, conglomerates, and limestones. These rocks originated as sediments on former seabeds and coastal plains (New Jersey Geological Survey, 1999). During the Ordovician, Pennsylvanian, and Permian Periods, compressional forces and thrust faults deformed these sedimentary units, resulting in folded and tilted bands of alternating erosion-resistant sandstone and more easily eroded shale and limestone (New Jersey Geological Survey, 1999). Differential erosion of these alternating bands, oriented in a northeast-southwest direction, created the valley and ridge features for which this province is named. Paleozoic

FIGURE 1.5 Physiographic provinces of New Jersey (New Jersey Geological Survey, 2004).

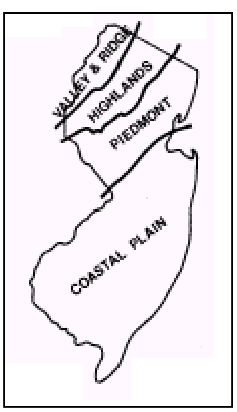

FIGURE 1.6 Geologic map of New Jersey (New Jersey Geological Survey, 2004).

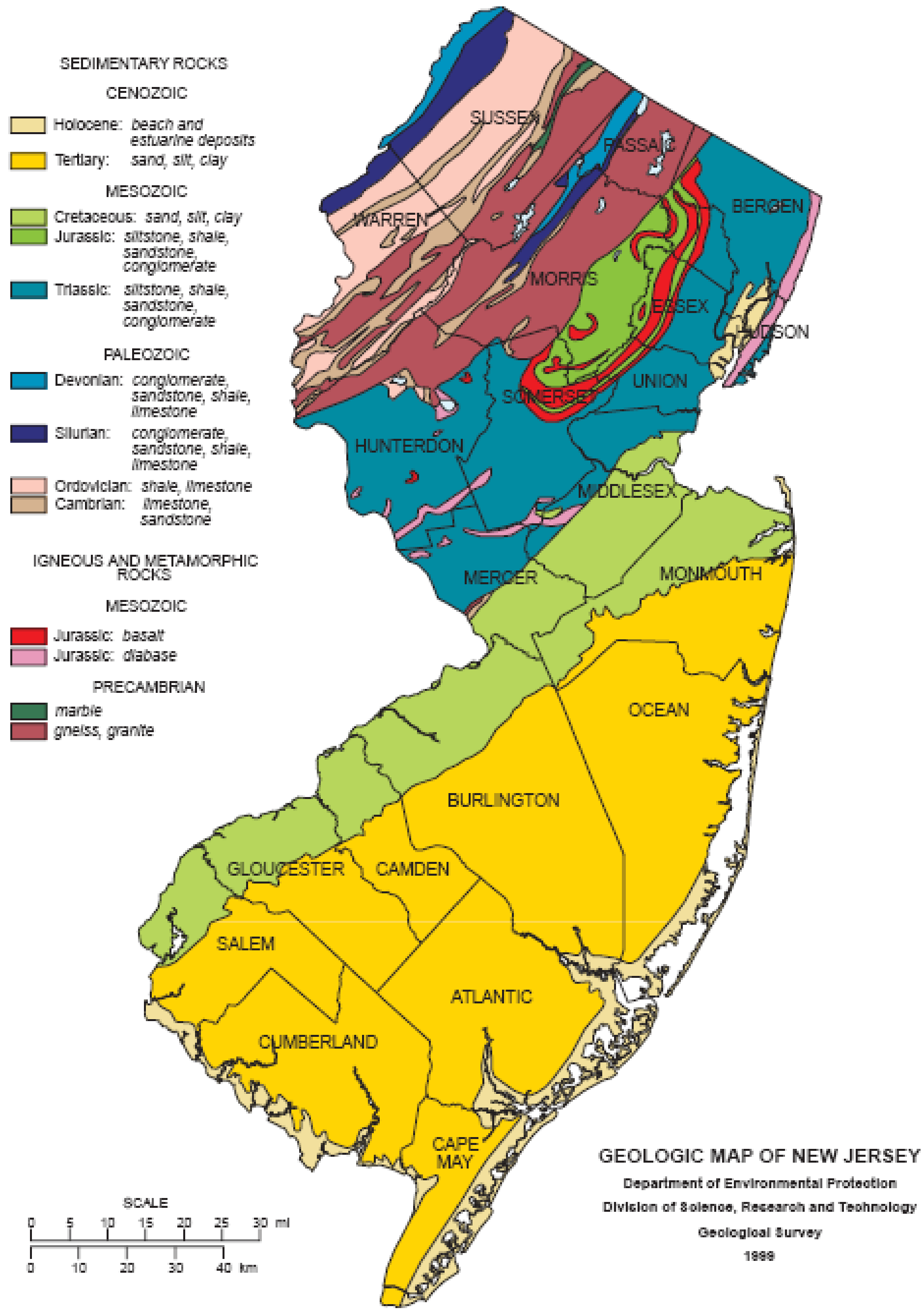

sedimentary rocks are also found in the Highlands, providing the most productive aquifers in the area (New Jersey Geologic Survey, 1999).

Mesozoic siltstones, shales, sandstones, and conglomerates are the dominant rock types found in the Piedmont Province. These formed within rift basins created between 230 and 190 My ago in advance of the opening of the Atlantic Ocean. Volcanic activity accompanied the rifting, resulting in Jurassic units of diabase and basalt in the Piedmont (New Jersey Geological Survey, 1999). The diabase units comprise notable features such as the Palisades Sill, Rocky Hill, Sourland Mountain, and the Cushetunk Mountains. Basalt units form the Watchung Mountains, Long Hill, and Hook Mountain (New Jersey Geological Survey, 1999).

Sand, silt, and clay of Cretaceous to Miocene age were deposited in the Coastal Plain Province in association with fluctuating sea levels and remain as unconsolidated sediment. As sea level changed, alternating deposits of deltaic and marine sediments were distributed in bands that trend northwest to southeast. These sediments are important sources of economic resources such as iron, glass and foundry sand, ceramic and brick clays, and minerals such as glauconite used in fertilizers and ilmenite for titanium production (New Jersey Geological Survey, 1999).

The Pleistocene Epoch is well represented in New Jersey in consequence of three major glaciations and related sea level fluctuations. Glacial sediment deposits are distributed throughout the northern part of the state. The first Pleistocene glaciation, known as the Jerseyan (or pre-Illinoian), left till that is at least 800,000 years old. The Illinoian glaciation occurred about 150,000 years ago and the Wisconsinan glaciation about 21,000 years ago (White, 1998). See Figure 1.7. Glacial meltwater deposits consisting of sand and gravel in buried or filled river channels and silt and clay in glacial lake beds are found primarily in the northern portion of the Piedmont province and are found in the Valley and Ridge and Highlands provinces in lesser

abundance (New Jersey Geological Survey, 1999). Both glacial and non-glacial sediments found throughout all provinces are rich in mineralogical diversity, are important sources of construction materials, and include productive aquifers (New Jersey Geological Survey, 1999).

During the late Pleistocene, the Laurentide ice sheet extended over half of North America reaching a terminal position that extended across northern New Jersey (lW in Figure 1.7) and Long Island, New York and out onto what is now the continental shelf east of Cape Cod. The glaciers eroded the rocks in and around northern New Jersey, and the products of that erosion became the dominant source of the Pleistocene and Recent sediments now on the New Jersey shelf. After sediment was transported to the coast, longshore currents, tidal currents, and dynamic effects of storm energy further transported the sediment. Sea level changed in response to cycles of expanding and retreating glaciers. During the last glacial maximum (LGM), the sea level was between 120 and 140 m lower than today along the New Jersey shore (Gulick et al., 2005). As the Laurentide ice sheet retreated, the sea transgressed (the shoreline moved landward) quickly although stillstands appear to have occurred. At sea level stillstands, sediments that can be seen on the shelf today were deposited.

FIGURE 1.7 Limits of Pleistocene glaciations in New Jersey: lW – Wisconsinan (LGM), I – Illinoian (150 ka), and pI – pre-Illinoian, or Jerseyan (800 ka) from White (1998).

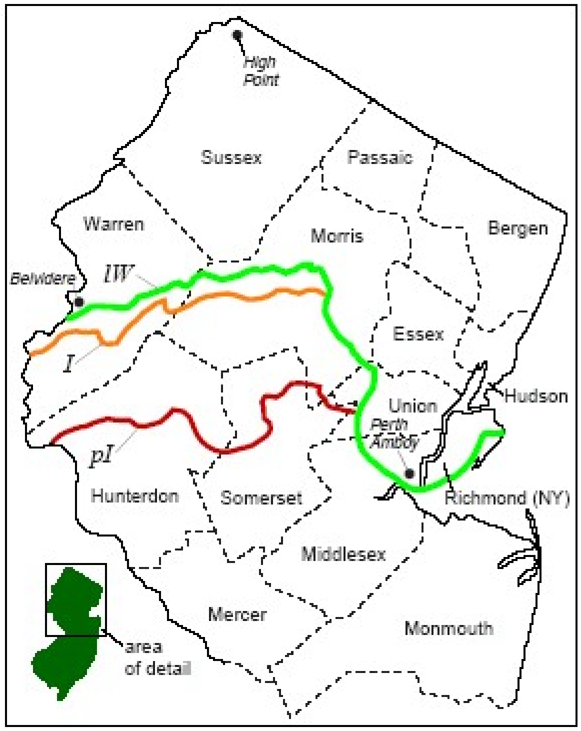

1.4 New Jersey Shelf Sediments

The depositional history of the New Jersey shelf is controversial. Sea-level change is thought to have created a series of features through deposition and erosion, but the mechanisms are under debate. Both large- and small-scale features define the region. Large scale features include the outer shelf wedge, the Franklin paleo-shore, and the mid-shelf wedge, while the small-scale features are described as sand ridges and sand ribbons. See Figure 1.8. An outer shelf wedge, known as the Hudson Apron, is clay-rich. It is found just landward of the modern shelf break south of the Hudson Canyon (Ewing et al., 1963). The Hudson Apron marks the edge of the continental shelf and was deposited in a deltaic environment at the mouth of the

FIGURE 1.8 Map of New Jersey continental shelf and surrounding areas, from Duncan et al. (2000).

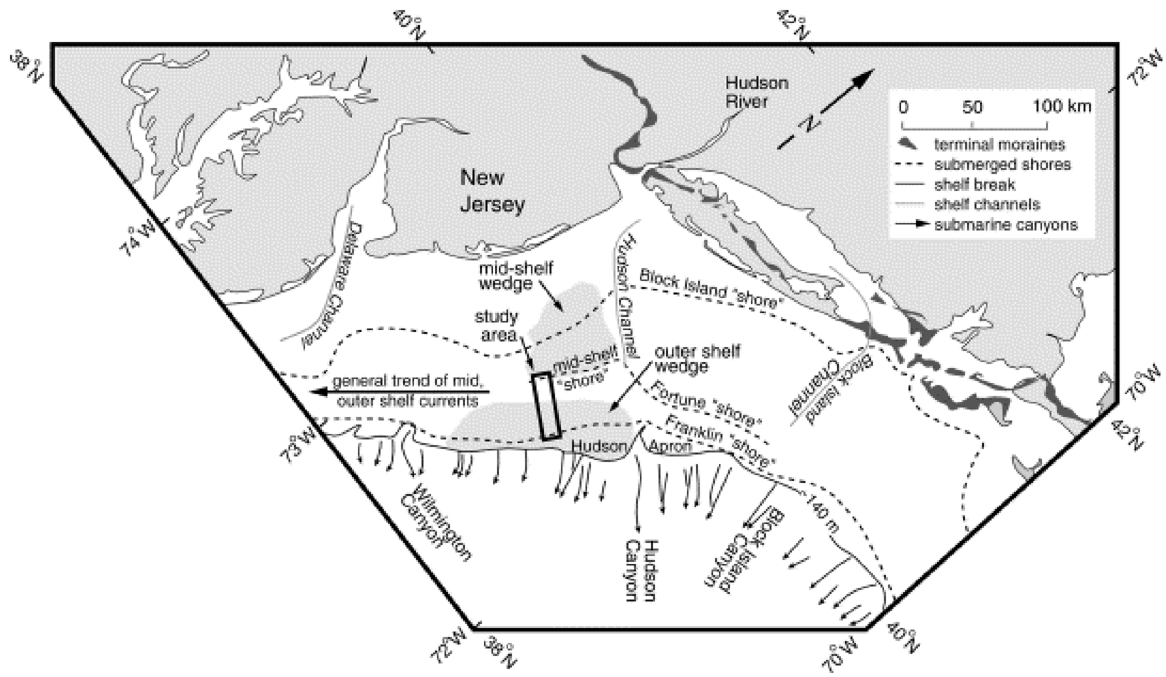

Hudson River when the shelf was exposed during the LGM (Ewing et al., 1963). The Franklin paleo-shore, located just landward of the outer shelf wedge at approximately the 100 m isobath, and the mid-shelf shore (also called the Fortune shore) located approximately at the 45 m isobath, are an additional indicators of past stillstands which were deposited during a pause in the transgression of the ocean after the LGM (Duncan et al., 2000; Emery and Uchipi, 1984; Veatch and Smith, 1939).

In 1972, Frank and Friedman reported a study of 150 New Jersey surface sediment samples collected along four transects extending from and perpendicular to the shore (Figure 1.9). Sediment mean grain size was calculated by the mathematical method of moments, which uses statistics rather than graphical measurements. Frank and Friedman concluded that most of the New Jersey continental shelf sediments were likely transported by an ancient Hudson River

FIGURE 1.9 Sample map from Frank and Friedman (1972). Black dots are surface grab sample locations, contours show moment mean grain size, and depth contour lines are given in fathoms (1 fathom = 6 ft. = 1.83 m).

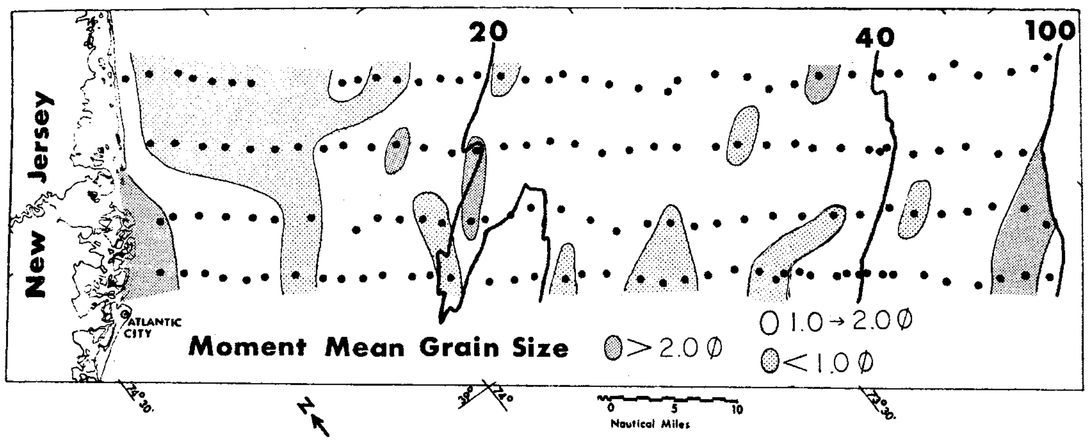

system. The heavy mineral fractions of the coastal plain sediments are rich in ilmenite and leucoxene and are lacking in hornblende and garnet (McMaster, 1954; Owens and Sohl, 1969; Isphording, 1970), and thus do not match the heavy mineral fractions of continental shelf sediments, which are dominated by hornblende and garnet (Frank and Friedman, 1972).

The bedform categories described by Goff et al. (1999) are used to classify the samples sites in this study. Sand ridges are the dominant morphologic feature of the Atlantic continental shelf and are from 1-12 m tall, from 1-5 km wide, and up to 20 km long and are oriented at oblique angles to the modern shoreline of New Jersey (Swift and Field, 1981; Figueiredo et al., 1981; Stubblefield and Swift, 1981; Goff et al., 1999). Sand ridges are thought to be formed in near shore environments and continue to be modified after transgression in water depths to 50 m or more by storm activity and shelf bottom currents (Goff et al., 2004). Sand ridges are found on the inner, middle, and outer continental shelf.

Stubblefield et al. (1984) studied New Jersey shelf sediments using data from grab samples, vibracores, and bathymetric maps to theorize how the sand ridges formed. The authors differentiated two groups of sand ridges in respect to process of formation. The first group of ridges includes the nearshore and outer shelf ridges that are aligned obliquely (approximately 30^{o}) to the coast and were interpreted to have formed in a nearshore environment. The mid-shelf ridges lie parallel to the modern coast, and thus were considered to have formed through a different process, most likely as a barrier island complex. Swift et al. (1984) argued against the conclusions drawn by Stubblefield et al. (1984) claiming there is not enough evidence to support the idea that the mid-shelf ridges are degraded barrier beach complexes. Rine et al. (1991) completed a study with vibracore samples from the New Jersey inner- and mid-shelf using grain size, statistical, and paleontological analyses. Their results show significant differences in sediment texture and paleontology between the nearshore and mid-shelf ridges, thus the current working hypothesis is that mid-shelf ridges are formed in a mid-shelf environment and near-shore ridges are formed in a near-shore environment (Rine et al., 1991).

Sand ribbons are smaller, linear features reaching heights greater than 1 m, typically with less than 0.2 km spacing between each, and are oriented parallel to tidal flow (Goff et al., 1999). Areas between the sand ridges and ribbons appear as areas of low backscattered energy when imaged by sidescan sonar. Interpretation and application of sidescan backscatter data can be potentially useful, as variations in backscatter response tend to be associated with variations in intrinsic properties (i.e., impedance, texture, grain size) of surface sediments (Goff et al., 1999). Grab samples described as high fine / low coarse (HF/LC) are defined as having >10% fine fraction (<0.0625 mm) and <5% coarse-grained sediment (>4 mm sieve mesh size). Several

sample sites in this study were categorized as "other" by Goff et al. (2004) as they do not fit neatly into the categories of sand ridge, sand ribbon, or HF/LC.

Goff et al. (2005) investigated erosional forces acting on the New Jersey shelf sediments. Their study shows that at depths of approximately 40 m and greater, sand ridge development changes from that of evolution to strictly erosional processes affected by bottom currents. Analysis of sediment samples indicates that all sand ridge samples have been extensively reworked, as evident by the presence of abraded mineral grains and relict foraminiferal assemblages. Sand ribbons show both relict and pristine populations of grains and microfauna. This bimodal distribution may be explained by previously undisturbed sediment having been eroded from scour pits and then deposited within reworked sediment assemblages (Goff et al., 2005). The study by Rine et al. (1991) showed that foraminiferal assemblages found in the upper portions of both nearshore and mid-shelf ridges were deposited in or near their present settings, which is contradictory to the conclusions drawn by Goff et al. (2005).

Seismic analysis has been employed in addition to sediment and bathymetric analyses to better understand sea level fluctuations and their influence on sediment deposition and transport on the New Jersey continental shelf (Austin et al., 1996; Davies and Austin, 1997; Duncan et al., 2000; Nordfjord et al., 2005). A new study by Fulthorpe and Austin (2004) identifies steep-sided incisions that have been filled in with sediment on the New Jersey shelf. Episodic flooding that occurred between 19-12 ka is believed to be the best scenario to explain the creation and subsequent infilling of these channels. During the retreat of the Laurentide ice sheet, massive amounts of glacial outwash would have swept across the coastal plains of New Jersey and New York creating numerous fluvial drainage systems, including the ancestral Hudson River Valley, deeply incising the exposed New Jersey shelf. Fulthorpe and Austin (2004) propose that this

outwash built up in lakes behind natural dams formed by terminal moraines. During glacial melting, the glacial dams collapsed releasing large amounts of meltwater and sediment that had been eroded from a proximal source such as New York and New Jersey bedrock (Fulthorpe and Austin, 2004), which filled the deep incisions. Donnelly et al. (2005) also found evidence of a catastrophic meltwater discharge through the Hudson Valley at about 13,350 yr B.P. It is believed that Glacial Lake Iroquois breached its ice dam and then flowed into Glacial Lake Vermont and Glacial Lake Albany, breaching their terminal moraine dams (Figure 1.10). This massive outwash event is believed to be large enough to diminishing thermohaline circulation in the North Atlantic Ocean (Donnelly et al., 2005). If sediment grains characteristic of freshly weathered rock are identified on the shelf in this study, such a catastrophic outwash event may provide a likely explanation.

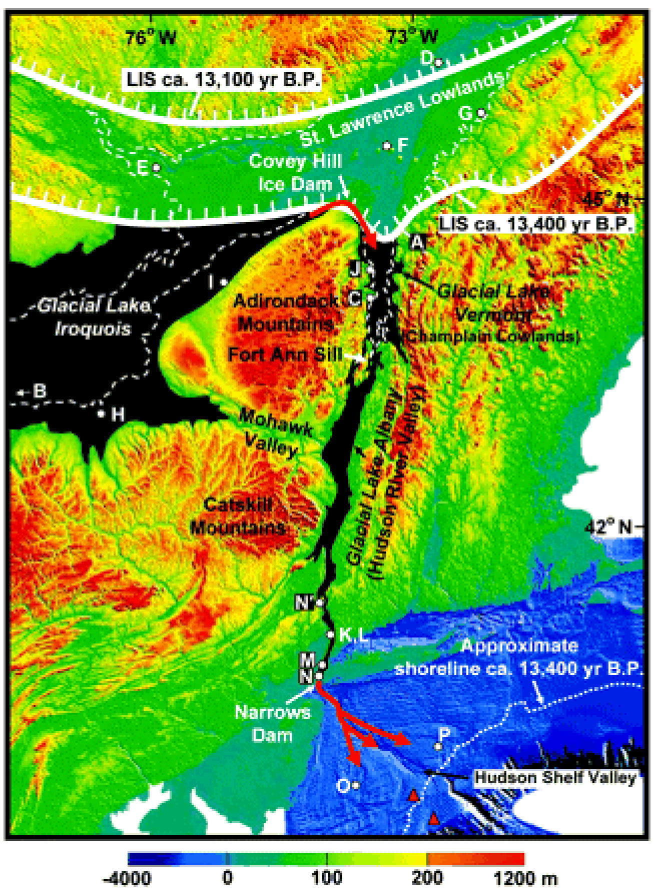

FIGURE 1.10 Map of the northeastern North America between 13,500 and 13,100 years B. P. illustrating the areas covered by Glacial Lake Iroquois, Glacial Lake Vermont, and Glacial Lake Albany (from Donnelly et al., 2005).

1.5 History of IRD studies

Many IRD studies have been published to expand understanding of past glacial extents and paleocurrents, particularly during the Pleistocene. Episodes of anomalously high ice-rafting in the North Atlantic, named Heinrich events, occurred at irregular intervals throughout the late Pleistocene. Provenance studies of IRD associated with Heinrich events in the North Atlantic indicate continental sediment sources of Archean age surrounding the Labrador Sea (Hemming et al., 1998). Six distinct Heinrich layers (H6-H1) have been identified for this time range in northern Atlantic marine sediment deposits. Heinrich layer H6, is dated to between 65 ka and 60 ka, approximately, H5 at 44.0 ka, H4 to between 33.2 ka and 35.1 ka, H3 at 26.0 ka, H2 at 22.0 ka, and H1 to between 15 ka and 13 ka (Cronin, 1999). The ages provided for Heinrich events are best approximations, as the timing of iceberg rafting associated with the deposition of Heinrich layers is difficult to constrain because of the slow sedimentation rate during non-IRD periods. Heinrich layers are also characterized in deep marine cores by intervals of high abundance of terrigenous detritus in coarse fractions that in most cases are easily identifiable as bright white layers within core samples (Hemming et al., 1998). Heinrich layers H1, H2, H4, and H5 are classified as the carbonate-bearing Heinrich layers. They have high IRD%, high sediment flux, high amounts of detrital carbonate (providing the white coloring), and extreme isotopic compositions (Hemming et al., 1998). Heinrich layers H3 and H6 have high IRD% identifiable in the core samples, but exhibit little to none of the other features found in the carbonate-bearing layers.

Hemming et al. (1998) studied core V28-82 from within the North Atlantic IRD belt. Their goal was to use an integrated approach to evaluate the four carbonate-bearing Heinrich layers in order to establish similarities between the layers and resolve provenance discrepancies

that had arisen in other studies. The sediment was sampled at 1 cm intervals throughout the core for lithic-grain counts and IRD percentage calculation on the >150 mm (>2.75ϕ) fraction (Hemming et al., 1998). Black to dark green mineral grains were identified as hornblende and picked from the >150 mm (>2.75ϕ) fraction for $^{40}Ar/^{39}Ar$ dating. Feldspar grains were picked from the >250 μm (>2.0ϕ) fraction for Pb isotope measurement. Finally, Sr and Pb isotope analyses were completed on the >63 μm (>4ϕ) fraction of the bulk de-carbonated samples (Hemming et al., 1998). By use of this diverse array of methods, the IRD grains were shown to have come from a terrain formed during the Late Archaen (~2.7 Ga) and metamorphosed in the Early Proterozoic (~1.75 Ga). This led to a provenance interpretation of the Churchill region of Canada with transport through the Labrador Sea (Hemming et al., 1998). Only conventional K-Ar dating has been used in this study.

IRD has also been identified in deep marine study areas outside of the North Atlantic, such as offshore Antarctica (Diekmann and Kuhn, 1998) and the North Pacific (St. John and Krissek, 1999). Diekmann and Kuhn (1998) studied the mineralogy and grain properties of surface sediments from the Weddell Sea floor. The goals of their study were to determine the spatial variations of provenance and the transport paths of Antarctic-derived IRD, to constrain mechanisms of glacial-marine sedimentation, and to estimate modern accumulation rates of IRD versus surface-transported mud. The floating ice sheets surrounding Antarctica release terrigenous debris into the sea, however there are markedly different source rocks from which these sediments were derived. Their grain size data show nearly equal proportions of coarse and fine grain-size fractions that were very poorly sorted. The HM suites of sand size fractions show low mineralogical maturity (they are dominated by hornblende, garnet and clinopyroxene), linking them to a specific source rock from which the sand was transported as IRD (Diekmann

and Kuhn, 1998). The clay fractions, however, have a different provenance and were carried to the study area by the Weddell Gyre rather than as IRD (Diekmann and Kuhn, 1998).

The study of IRD in the North Pacific by St. John and Krissek (1999) used mass accumulation rate determination methods. The authors combined their results for DSDP site 580 and ODP sites 882 and 887 with previous IRD mass accumulation rate studies to form a synthesis of Pleistocene ice-rafting episodes in the North Pacific. The 0.25–2.0 mm (2.0ϕ through -1.0ϕ) size fraction was dried and weighed for calculation of weight percent and grain size analyses. The results indicate that coastal Alaska and coastal Siberia (including the Kamchatka Penninsula) are the two primary sources of IRD for this study area. Additionally, an attempted correlation across multiple core sites shows variations in timing of IRD supply across the North Pacific, suggesting that multiple rafting events have occurred in this region (St. John and Krissek, 1999). Grain size analysis and HM assessment are used in this study to constrain provenance of New Jersey sediments.

Relict iceberg keel marks identified by Duncan and Goff (2001) suggest that ice rafted debris may be present on the New Jersey shelf. The furrows vary in width between 100 m and 400 m, in depth between approximately 0.5 m and greater than 4 m, and in length up to several kilometers. The shorter keel marks are interpreted to be older and formed in shallower water, while the longer keel marks are believed to be younger and formed in deeper water. The older keel marks, in some case, have overlapping younger keel marks that cut across them. These keel marks were interpreted to be from icebergs that calved off the Laurentide ice sheet south of Maine or southern Canada and were transported southwestward (Duncan and Goff, 1999). Heinrich events H2 and H1 were proposed by Duncan and Goff (2001) as possible alternate

contributors to icebergs that grounded on the New Jersey shelf, although the dates were incorrectly cited for these events in their work.

The possibility of late Pleistocene IRD on the New Jersey shelf originating from either Maine, which had a sufficient ice sheet at the time, or from a more northerly source region in Canada, is an attractive hypothesis. At its peak, the Laurentide ice sheet covered the entire area of what is now the State of Maine, reaching a thickness of several thousand feet to cover the highest mountains found there (Kaplan, 1999). The most recent glacial expansion in Maine began about 25,000 years ago. Shortly after reaching its terminal position between 22 ka and 21 ka, the ice sheet began to retreat (Kaplan, 1999; Sirkin, 1986). The Laurentide ice sheet terminal position was approximately 240 km from the New Jersey study area; however, the southernmost point of ice sheet contact with the ocean was along what is now the continental shelf of Maine between 22 ka and 21 ka (Duncan and Goff, 2001; Marvinney and Thompson, 2000). The timing of iceberg release from this area would be constrained by the approximately one thousand-year period during which the Laurentide ice sheet reached the ocean there. According to the Late-Pleistocene sea-level diagram adapted for the New Jersey shelf by Gulick et al. (2005), from the global sea-level curve by Lambeck and Chappell (2001), sea level was more than 100 m lower than today, so the entire outer shelf wedge was exposed (Figure 1.11) between 26 and 18 ka. Therefore, icebergs that calved from the Laurentide ice sheet off the coast of Maine would not have been transported to the exposed New Jersey shelf.

Icebergs that strayed from the most likely paths described by Hemming et al. (2002) could have veered southwestward towards New Jersey. Duncan and Goff (2001) proposed H2 and H1 as possible sources for IRD; however sea level was too low during the H2 event for contribution from it on the New Jersey shelf. From the sea level curve of Figure 1.11, which

indicates higher sea levels before around 30 ka and after about 18 ka, an older Heinrich event, possibly H4, or the youngest event H1 could have contributed to IRD on the New Jersey shelf. The likelihood of preservation of iceberg keel marks incised during H4 over the period of shelf exposure is questionable. Numerous flooding events and other erosional processes would likely alter keel marks previously incised.

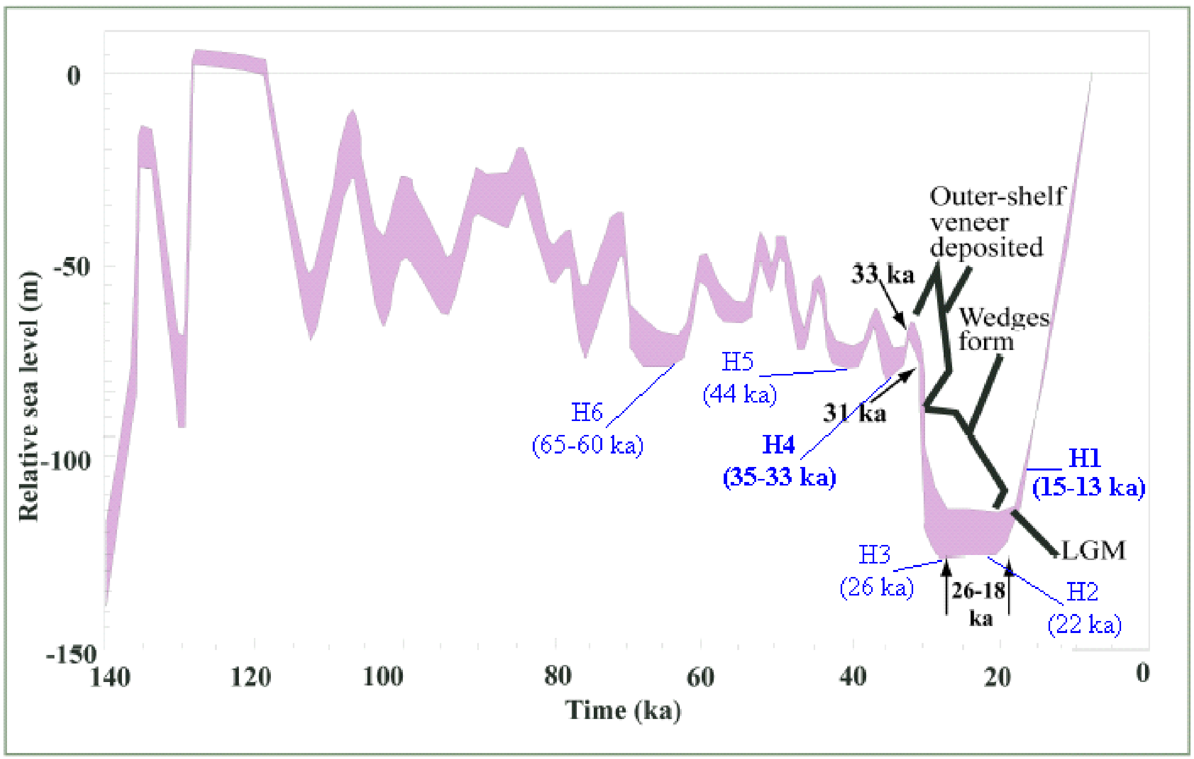

FIGURE 1.11 Late-Pleistocene sea-level curve of Lambeck and Chappell (2001), adapted for the New Jersey shelf; timing of depositional changes are from Gulick et al. (2005); Heinrich events are shown in blue.

1.6 Previous Heavy Mineral Studies

Heavy mineral (HM) assemblages can be used to relate sediments to their parent rocks by the relative abundances and other characteristics of key minerals. For example, grains of heavy minerals that are highly stable, such as zircon and rutile, can survive multiple weathering cycles and consequently become rounded in shape. Such mineral grains are indicative of high mineralogical maturity, quantitatively described by the zircon-tourmaline-rutile (ZTR) index (Hubert, 1962). Other HMs such as magnetite, pyroxenes, and amphiboles are less stable and are diagnostic of proximal source rocks (Pettijohn et al., 1987). Heavy mineral analysis provides information on parent rock by constraining the source-terrain mineralogy (Morton, 1999).

Many studies have shown successful use of HM assemblages to identify provenance. Recent investigations have combined identification of HM assemblages with one or more absolute dating methods to better constrain source areas. Hallsworth et al. (2000) used two HM analysis methods to identify several mineralogical groups with distinct provenances within Carboniferous sandstone in the Pennine Basin, UK. The first method involves determining the ratios of abundance of specific HMs with similar hydraulic and diagenetic behaviors and the second relies on the properties of a single mineral population, in this case garnet (Hallsworth et al., 2000). In conjunction with HM data, U-Pb isotopic dating of single zircon grains from each mineralogical assemblage with a sensitive, high-resolution ion microprobe (SHRIMP) placed constraints on source terrain geochronology (Hallsworth et al., 2000). This particular absolute dating method facilitated the identification of four different source terrains and sediment transport paths that changed through time. The methods employed by Hallsworth et al. (2000) are useful to consider for this study as New Jersey shelf sediments have been shown to be rich in garnet and contain smaller concentrations of zircon grains (Uptegrove et al., 1991).

Frank and Friedman (1972) studied heavy minerals along four traverses on the New Jersey shelf (Figure 1.9) and found varying amounts of HMs, between 0.6% and 14.4% of the total sample weight, with garnet and hornblende comprising approximately 50% of the non-magnetic HM fraction in the majority of samples. No regional trend regarding HM deposition was identified along the traverses (Frank and Friedman, 1972). Uptegrove et al. (1994) reported the average content of economic heavy minerals (EHM) in 76 surface grab samples as 1.3% by weight of bulk grab samples and a corresponding average of 0.98% by weight in bulk vibracore samples. The New Jersey shelf economic HMs are ilmenite, altered ilmenite, rutile, zircon, monazite, and aluminosilicates. Additional HMs identified by Uptegrove (1994) include garnet, pyroboles, epidote, staurolite, tourmaline, and magnetite. See Figure 1.12 from Uptegrove et al. (1994) for the overall distribution of HMs in the grab and vibracore samples. In general, New Jersey shelf sediments contain higher percentages of heavy minerals than sediments of

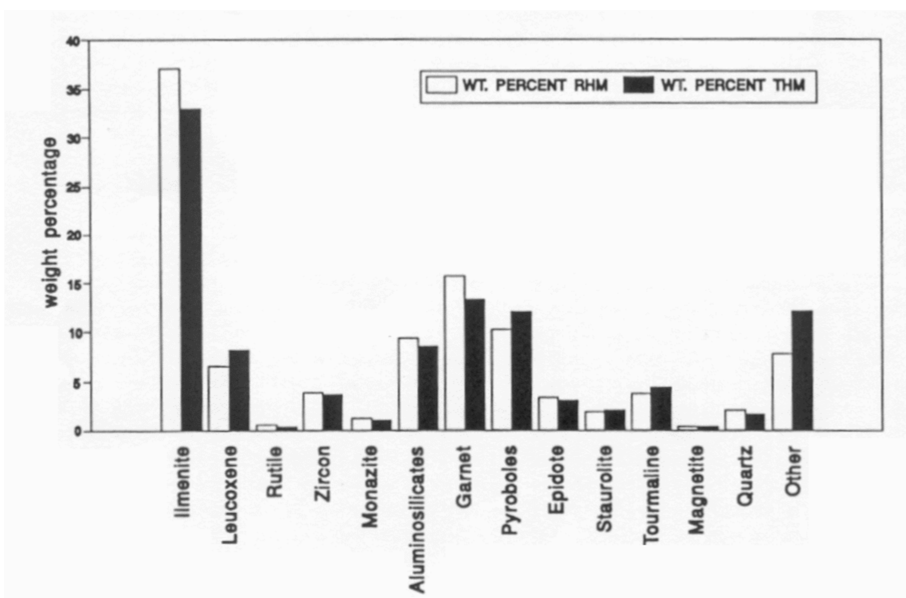

FIGURE 1.12 Distribution of heavy minerals on the New Jersey shelf, from Uptegrove et al., 1994. RHM – Recovered Heavy Minerals following spiral concentration and heavy liquid separation, THM – Total Heavy Minerals based on rejected materials by spiral concentrator plus RHM.

surrounding northern (New York) and southern (Maryland, Virginia, North Carolina, South Carolina and Florida) shelf study areas (Uptegrove et al., 1994).

Ockay and Hubert (1996) studied mineralogy and provenance of Pleistocene outwash-plain deposits and modern beach sands in outer Cape Cod, Massachusetts. Coastal cliffs reaching up to 57 m in height extend along the shoreline of Cape Cod for 26 km. These cliffs are retreating through erosion at a rate of approximately 0.8 m/yr (Ockay and Hubert, 1996). An estimated 20% of the eroded material is transported seaward and removed from the coastal system. The coarse-grained erosional material is transported northward of the cliffs through longshore transport, while the fine-grained sediments are transported southward (Ockay and Hubert, 1996). The goal of their study was to trace the Cape Cod beach and outwash-plain sands to their pre-glacial sources by using light and heavy mineral assemblages as indicators. Approximately 0.5 kg samples of sand were taken from 21 beaches from depths not less than 15 cm below the surface in trenches dug at the middle of the foreshore slope (Ockay and Hubert, 1996). Ten samples, each with an approximate mass of 0.5 kg, were collected from each of the four outwash plain sites along coastal cliffs. Approximately 100 g of each sample was sieved through ¼-phi interval Tyler sieves and rotapped for 15 minutes (Ockay and Hubert, 1996). Heavy minerals were separated with heavy liquids, and then proportions of minerals in the assemblages were measured by the Fleet method of ribbon traverses (Ockay and Hubert, 1996). This involves mounting the mineral grains onto a slide and counting the grains of each different mineral within particular elongate bands (Galehouse, 1971). Twenty-three distinct heavy minerals were identified within the beach and outwash sand samples. The proportions of heavy mineral species varied from sample to sample, but the color varieties of specific minerals were uniform among all samples (Ockay and Hubert, 1996). The mineral composition of the 0.25-0.5

mm fraction of the light mineral fraction was also determined. Thin section analysis showed that the quartz grains had been modified by glacial transport. This inference was based on characteristic shape and surface features such as conchoidal fractures, flat or slightly concave to convex surfaces, abundant plate-like and sliver-like grains of fine and very fine sand, "razor sharp" edges, curving pressure cracks, and grooves (Ockay and Hubert, 1996). Similar surface features and shapes were also identified for heavy mineral grains. A common provenance was determined for the beach and the outwash-plain sands from the similarity of heavy and light mineral assemblages. Some of the methods utilized by Ockay and Hubert (1996) will be applied to sediment samples in this study.

These previous heavy mineral studies suggest that identification of the source region or regions for sediments found on the New Jersey shelf will be facilitated by study of the heavy mineral suite. The HM assemblage may also be used to identify IRD. If the heavy mineral assemblage in certain New Jersey shelf sediments do not match the signature of the nearby Hudson or New Jersey Highlands, the Paleozoic units in New York, or the Jurassic lava flows in New Jersey, then the presence of IRD in those sediments is likely.

1.7 Previous Isotopic Studies of Detrital Hornblende Grains

The K-Ar method of dating minerals utilizes the radioactive decay of atoms of the naturally occurring potassium isotope ^{40}K (Z=19) to either ^{40}Ca or ^{40}Ar. About 11% of the decaying ^{40}K atoms decay by electron capture to an excited state of ^{40}Ar. The excited ^{40}Ar then emits a gamma ray with an energy of 1.46 MeV to decay to the ground state of ^{40}Ar. As long as a mineral grain remains a closed system, the amount of ^{40}Ar within it will grow through time as the amount of ^{40}K decreases. Assuming that the grain had not been completely outgassed of Ar

at mineral formation, the growth of ^{40}Ar in a K-bearing mineral grain is represented by (Dickin, 1995):

$$^{40}Ar = {}^{40}Ar_i + \frac{\lambda_{EC}}{\lambda_{total}} {}^{40}K(e^{\lambda_{total}t} - 1)$$

where the symbol for each species stands for its amount in the mineral at time *t*, $^{40}Ar_i$ is the initial amount of ^{40}Ar in the mineral, λ_{EC} is the partial decay constant for decay of ^{40}K to ^{40}Ar (5.81×10^{-11} yr^{-1}), and λ_{total} is the total decay constant of ^{40}K (5.543×10^{-10} yr^{-1}).

Using samples from a series of sites within and near a contact metamorphic zone, Hart (1964) studied argon loss from K-feldspar, biotite, and hornblende grains. Hornblende was shown to have high ^{40}Ar retention ability in comparison to the other minerals, with argon loss confined to samples from within a distance of approximately 3 m feet from the contact (Hart, 1964). Hornblende is often useful for dating by the K-Ar method in volcanic, plutonic, and metamorphic rock types (Dalrymple and Lanphere, 1969).

Jappy et al. (2001) studied the relationships between hornblende K-Ar ages and their chemical composition and hydrogen isotopes. The results of their study show correlations of hornblende K-Ar age values with FeO, MgO, Mg/(Mg + Fe), K_2O, and δD. The largest hornblende age values were found in the samples with greatest packing density within the crystalline structure. Additionally, δD shows a correlation with age value where intrusion of hot fluids has influenced the cooling history of the rocks. Such correlations indicate that the hornblende K-Ar apparent age is not a reliable measure of time of uplift and cooling as a result of exhumation (Jappy et al., 2001). The level of detail investigated by Jappy et al. (2001) is interesting but in provenance studies, the knowledge of K-Ar age values of potential source rocks is the most important consideration.

Hemming et al. (2002) used $^{40}Ar/^{39}Ar$ isotopic dating methods in a provenance study to establish ice sheet history at the last glacial maximum. Hornblende grains, along with a few biotite and muscovite grains, were picked from samples collected from the Laurentide margin on the east coast of North America, the Norwegian margin, and the Greenland margin for this study. Along the eastern coast of North America, terranes increase in age from south to north. Grenville and Paleozoic grains are dominant in sediments from along the southern extent of the Laurentide ice sheet, while in sediments from the northeastern portion Paleoproterozoic and Archean grains are dominant (Hemming et al., 2002).

Isotopic analyses of hornblende have been successfully applied to determine provenance age and transport history of a broad range of sediments. In most cases, detrital hornblendes provide reliable geochronological markers relating the detrital grains to source terranes where the history of crystallization and cooling of plutonic rocks is reasonably well known. In this study, detrital hornblende grains will be analyzed in an effort to trace the geological source(s) of New Jersey shelf sediments.

TABLE 1.1 Source Rocks for Detrital Hornblende and other Marker Mineral Grains on the New Jersey Shelf

Rock Type	Location	Mineral Assemblage	Reference
Granite group	Throughout NJ Highlands	Mesoperthite-quartz-hornblende granite	Smith, 1969
		Granite gneiss with microcline, albite-oligoclase, quartz and hornblende	
Amphibolite	Throughout NJ Highlands	Amphibolite and pyroxene amphibolite	Smith, 1969
Hypersthene-quartz-andesine gneiss	Throughout NJ Highlands	Andesine, quartz, hypersthene, clinopyroxene, hornblende, biotite	Smith, 1969
Cortlandt-Beemerville magmatic belt	Southeastern New York to	Hornblendite and kaersutite gabbro	Ratcliffe et al., 1982
	Northern NJ Valley and Ridge	Diorite	Eby, 2004
		Clinopyroxenite	
		Amphibole pyroxenite	
		Granodiorite	
Pyroxenes	Palisades Sill, NJ Piedmont	Ferrozugite, hypersthene, olivine, biotite, hornblende	Walker et al., 1973

CHAPTER 2: METHODS

2.0 Sample Collection

Grab samples were collected aboard the *R/V Cape Henlopen* in 2001 and washed by Goff et al. (2004). Table 2.1 provides the types and specific geographic locations of the grab samples analyzed. The stratigraphic or core samples were collected from aboard the *R/V Knorr* during research cruise KN167-KN168AB (Alexander and Austin, 2002). Core Site 1 was drilled in water depth of 127 m at 39.2391^{o}N, 72.6863^{o}W. Site 3 was drilled in water depth of 75 m at 39.2533^{o}N, 72.8998^{o}W. Sediment analysis of the sand fraction of grab and core samples consisted of several steps including separation into whole phi size fractions, heavy mineral separations, magnetic-mineral percentage determinations, K-Ar dating of hornblende grains, and comparison to foraminiferal analyses. See Table 2.2 for listing of methods employed in this study.

Table 2.1 Grab Sample Locations

Sample	*Type*	*Longitude*	*Latitude*
1	Ridge	-73.067123	39.357460
2	Ridge	-73.059158	39.353775
6	Other	-73.002640	39.321632
8	Ribbon	-72.979919	39.309845
9	Ridge	-72.971283	39.304974
10	Ridge	-72.966919	39.302567
11	Ridge	-72.962227	39.299389
12	Ridge	-72.956355	39.297058
14	Ridge	-72.913864	39.273205
15	Ribbon	-72.905045	39.268677
16	Ribbon	-72.900009	39.262600
17	Ribbon	-72.890396	39.260719
18	Ribbon	-72.878212	39.269058
24	Ribbon	-72.833061	39.254406
26	Ribbon	-72.844376	39.234299
27	Ribbon	-72.823982	39.222019
28	Other	-72.786377	39.238647
29	Other	-72.801834	39.210869
30	Other	-72.773201	39.195469
31	Ridge	-72.753754	39.203125
45	Scour	-72.969650	39.059872
66	Scour	-73.075203	39.103008
67	Ridge	-73.086533	39.100090
68	Ridge	-73.095558	39.099693
82	Ridge	-73.033638	39.128933
116	Ridge	-72.660316	39.224602
117	Scour	-72.658730	39.223690
121	Scour	-72.615479	39.199749
128	Outer Shelf	-72.510750	39.339985
132	Outer Shelf	-72.607719	39.322735
137	Outer Shelf	-72.646614	39.341042

TABLE 2.2 Methods employed in this study.

Proxy	Method	Interpretation	Reference
Grain Size	Mode	Most frequent grain size	McBride, 1971
	Mean	Average grain size	
	Standard deviation	Sorting of sample	
	Skewness	Sorting in tails	
	Kurtosis	Peakedness	
Heavy mineral concentration	Total amount of heavy minerals	Transport history, Depositional environment	Ahern, 1995; Uptegrove et al., 1991 Grosz et al., 1990; Friedman and Johnson, 1983
	Identification of prominent minerals	Provenance	
Magnetic mineral weight %	Frantz Isodynamic Magnetic Separator, Model L-1, slope 0^o	Constituent mineral abundance, Provenance	Grosz et al., 1990, Uptegrove et al., 1991
K-Ar Isotopic Dating	Apparent age determination of hornblende samples	Age of source rock Provenance of source region	Jappy et al., 2001; Hemming et al., 1998; Dalrymple and Lanphere, 1969
Foraminiferal comparison	Qualitative assessment of rounding	Transport history	Christensen et al., 2003

2.1 Grain Size Separations

Heavy minerals and other key identifying minerals are often found in particular size fractions of sediment samples. The sand fractions of grab and core samples were analyzed for grain size distribution in this study. Complete grab sample grain size analysis was completed by Goff et al. (2004). Complete core sample grain size distribution was analyzed by Alexander et al. (2003).

A set of three-inch W. S. Tyler standard sieves was used with each grab sample for separation into whole phi fractions for analysis based on size groupings. The sieve opening ranges employed to separate the sample fractions (with corresponding maximum phi (ϕ) values) are > 1 mm (0.0ϕ), 1.0 - 0.5 mm (1.0ϕ), 0.5 - 0.25 mm (2.0ϕ), 0.25 - 0.125 mm (3.0ϕ), 0.125 - 0.063 mm (4.0ϕ), and < 0.063 mm (fines). As the fines from all the samples had been previously washed through a 0.063 mm sieve and discarded, the fines are minimal and not considered for further analysis. Mean, standard deviation, skewness, and kurtosis were calculated in a Microsoft Excel spreadsheet using moment statistics formulae below (McBride, 1971):

$$\text{Mean} \quad \bar{x}_a = \frac{\Sigma f m_m}{100}$$

$$\text{Standard deviation} \quad \sigma_a = \sqrt{\frac{\Sigma f (m_m - \bar{x}_a)^2}{100}}$$

$$\text{Skewness} \quad Sk_a = \frac{\Sigma f (m_m - \bar{x}_a)^3}{100{\sigma_a}^3}$$

$$\text{Kurtosis} \quad K_a = \frac{\Sigma f (m_m - \bar{x}_a)^4}{100{\sigma_a}^4}$$

where f = weight percent (frequency) in each grain-size grade present,
m = midpoint of each grain-size grade in phi values
n = total number in each sample, which is 100 when f is in percent.

The mean is the average of all particles sizes in a sample (Folk and Ward, 1957). The standard deviation is the primary measure of sorting within a sample (Folk, 1974). Skewness is a value that represents an aspect of the sorting related to the tails of the grain size population as seen on a grain size frequency curve. If a sample has a tail of fine particles (higher phi sizes) substantially larger than the tail of coarse particles, it is positively (or fine) skewed. If the population has a tail of coarse particles substantially larger than the tail of fine particles, it is negatively or (coarse) skewed. If skewness values are between +0.10 and –0.10, the sample is considered to be near symmetrical (Folk, 1974). Kurtosis measures the degree of concentration of the grains relative to the average (or peakedness) but has little value for interpretive grain-size studies (Boggs, 2001).

2.2 Heavy Mineral Separations

Systematic investigations of the heavy mineral fractions of grab and core sediment samples help determine distribution patterns and narrow down possible parent materials. A mineral assemblage that is different than that of the typical New Jersey coastal sediments, as described by Uptegrove et al. (1998) and Frank and Friedman (1972) allows for identification of possible IRD. To facilitate mineral assemblage identification, heavy mineral separation procedures were employed. Heavy minerals are those denser than about 2.9 g/cm^3. Heavy mineral analyses of sediments begin with separation of heavy mineral grains from light mineral grains, the latter predominantly quartz on the New Jersey shelf, in a heavy liquid (Grosz et al., 1990; Ahern, 1995). Figure 2.1 is a picture of the apparatus setup. Open-top separatory funnels

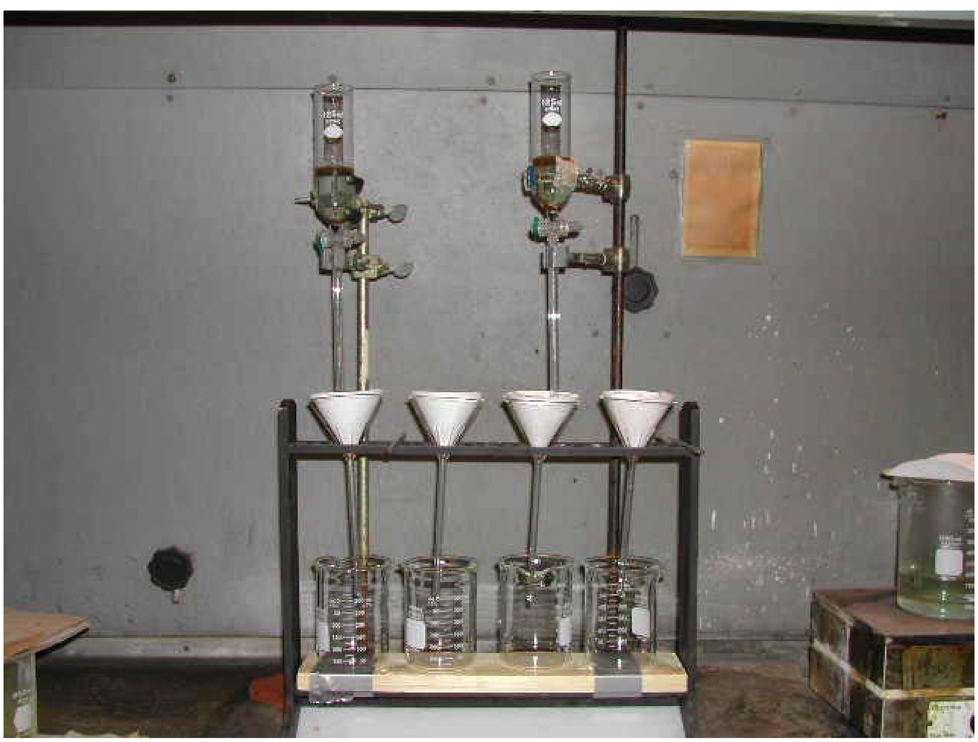

FIGURE 2.1 Heavy mineral separation apparatus.

are placed above a set of funnels with filter papers labeled “heavy” and “light.” Sodium polytungstate solution, $\rho = 2.90$ g/ml, is used in the separatory funnels. Sediment sample fractions by phi size are placed inside the separatory funnels, allowing the light minerals to float and heavy minerals to sink. To perform each separation the separatory funnel stopcock is opened, allowing the heavy minerals to flow through to the filter paper marked “heavy.” The separatory funnel is then moved over the filter paper marked “light” and the remaining minerals are released. Any mineral grains remaining in the separatory funnel are washed through to the “light” filter paper for collection of the entire sample. All sodium polytungstate solution is collected for reuse. The portion of the solution that has become dilute is evaporated back to the correct density, determined with a hydrometer. The samples are washed, dried, and weighed.

2.3 Magnetic Mineral Percentage

A total of 17 grab samples were selected for determination of magnetic mineral percentages. This provides a semi-quantitative assessment of the magnetic portion of these samples. Heavy mineral grains were divided into six magnetic susceptibility categories controlled by a Frantz Isodynamic magnetic separator, model L-1: ferromagnetic (separated as “magnetic” at 0.05 A or less); and four groups “magnetic” at current setting of 0.2, 0.4, 0.6, and 1.8 A; and nonmagnetic at 1.8 A (Grosz, 1990). The Frantz isodynamic separator is mounted on a universal mount, which allows it to be rotated to a desired slope setting (Carver, 1971). A slope setting of 0^{o} was used for these separations. Each sample was dropped in front of the magnet at each magnetic setting three times, except for the setting of 1.8 A. At 1.8 A, each sample was dropped four times as three times was not adequate to capture all the grains that are

"magnetic" at that setting. The ferromagnetic mineral grains are primarily magnetite, ilmenite, and pyroboles (undifferentiated pyroxenes and amphiboles) (Uptegrove et al., 1991). The fraction magnetic at 0.2 A is dominated by ilmenite, garnet, and pyroboles. The fraction magnetic at 0.4 A includes ilmenite, garnet, pyroboles, tourmaline, epidote, and leucoxene (Uptegrove et al., 1991). The fraction magnetic at 0.6 A contains primarily pyroboles, tourmaline, leucoxene, and staurolite, and contains less ilmenite than the two previous fractions. The fraction magnetic at 1.8 A includes leucoxene and aluminosilicates such as sillimanite, kyanite, and andalusite. The last fraction contains the non-magnetic mineral residuum including some aluminosilicates, leucoxene, zircon, and rutile (Uptegrove et al., 1991).

2.4 K-Ar Age Determination of hornblende grains

2.4.1 Sample Preparation

Hornblende was identified by its cleavage, fracture, color and needle-like form. By visual identification under the microscope within the 2ϕ and/or 3ϕ heavy mineral fractions, hornblende grains were selected for isotopic dating at the School of Earth and Atmospheric Sciences at Georgia Institute of Technology under the direction and supervision of Dr. J. M. Wampler. Approximately 3 to 5 mg (between 80 and 120 grains) of hornblende was picked from each sample targeted for K-Ar age determination. Five grab and six core samples were selected for K-Ar age determination.

Each sample was submerged in dilute nitric acid and agitated with an ultrasonic probe to ensure all grains were free of solid precipitated from the heavy liquid. The grains were rinsed following the acid bath and then crushed under ethanol using a small, glazed, alumina mortar and

pestle. Each sample was crushed to ensure that the separate samples taken from it for potassium measurement and for argon isotope measurement were equivalent in respect to potassium and argon content. The samples were dried under a heat lamp. For potassium determinations, approximately 1 mg of each sample was weighed in a copper-foil capsule and transferred to a fluoropolymer (FEP Teflon®) container for digestion. For argon determinations, approximately 3 mg of each sample was weighed into a copper capsule and kept therein until it was melted for argon extraction.

To further prepare for the potassium determinations, the samples were digested in concentrated HF-$HClO_4$ solution in the small Teflon® containers. An equivalent amount of acid was put into a container for a blank potassium determination. The closed containers were gently heated overnight and then heated more strongly with lids off, resulting in nearly all of the acid being evaporated away. The residual materials remaining in the Teflon® containers were transferred into pre-weighed 125 mL bottles with a Cs-bearing (0.01 mol/kg) diluting solution. The volume of solution in each bottle was brought to approximately 50 mL with additional diluting solution, and the mass of each bottle with solution was determined by weighing.

2.4.2 Potassium Determinations

The potassium content of each sample solution was determined by flame atomic absorption spectrophotometry with a Perkin Elmer AAS 3100 against reference solutions prepared from a KCl standard. A potassium hollow-cathode lamp was operated at 6 mA. The absorbance within an air-acetylene flame was measured at the wavelength 766.5 nm. A red filter was used with a slit of 0.7 nm.

The approximate potassium content of each sample solution was determined in preliminary measurements in order to place the sample solutions in order of K-content among K-reference solutions containing 0.000, 0.500, and 1.000 mg/kg. Absorbance during aspiration of sample, blank, and reference solutions was measured with 10× expansion in a sequence in which the entire ordered set of solutions was scanned four times.

The data values were entered into a Microsoft Excel worksheet developed by Dr. J. M. Wampler to calculate the K-content of the samples. The worksheet calculates a value of K-content of each sample solution by linear interpolation of K-content as a function of absorbance. The absorbance function is based on the two readings of reference solutions that, in the sequence of measurements, bracketed the particular reading of the sample solution. The worksheet provides four independent values for the K-content of each sample solution, from which the standard error is calculated. The relative standard error ranged from 0.24% to 1.02% for the grab samples and between 0.32% and 0.95% for the core samples. The estimated overall relative error for each K-content determinations includes an estimate of the error in weighing, which is the largest source of error for these very small samples. The estimated values for overall relative error in K-content of the grab samples range between 1.8% and 4.5% at the 95% (2σ) confidence level. For the K-content of the core samples, these values range between 1.7% and 3.2% at the 95% confidence level.

2.4.3 Argon Isotopic Analyses

Figure 2.2 illustrates the argon extraction line used for these analyses. To prepare for Ar extractions and isotopic analyses, the copper-foil capsules containing the samples were loaded into a glass holding tube in a recorded sequence. The open end of the holding tube was sealed and the Ar-extraction line was evacuated by a mechanical vacuum pump and a mercury diffusion pump in series. The furnace was preheated prior to extraction of argon from the first sample.

In order to release the Ar from a sample, the copper-foil capsule containing it was dropped into a resistance-heated furnace and heated stepwise until the copper melted at about 1070 ^{o}C, at which temperature the sample also was melting. Further heating to near 1500^{o}C ensured that the argon was completely released from the melt. The argon gas from the sample was mixed ("spiked") with a known amount of ^{38}Ar. The sample and spike mixture passed through a liquid-nitrogen cooled trap to collect any water and other condensable vapors.

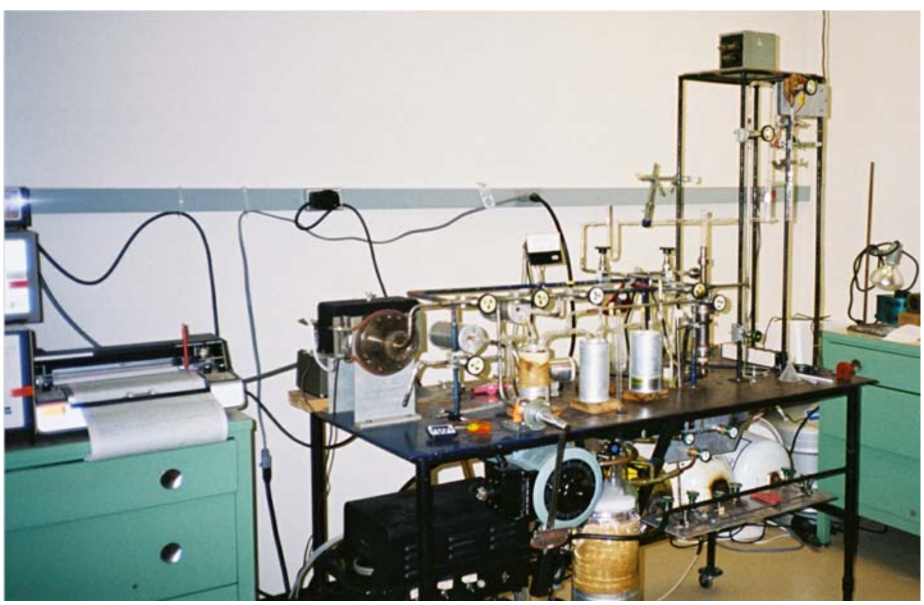

FIGURE 2.2 Argon extraction line at the Georgia Institute of Technology.

Following this, the gas mixture was exposed to a hot (~800^{o}C) titanium getter. The titanium getter was cooled, allowing it to react with impurities such as hydrogen. After three minutes, a second cold finger trap was cooled with liquid nitrogen. Then the first trap was allowed to warm up so the originally trapped ice could evaporate, releasing any argon that may have been occluded in it. This procedure ensured complete mixing of the sample argon with the spike argon.

The sample gas mixture was transferred to a mass spectrometer (AEI MS-10) where, after final gas cleanup by a second titanium getter, it was analyzed for ^{36}Ar, ^{38}Ar, and ^{40}Ar. The Ar mass spectrum was scanned forward and backward, twice in each direction. The mass spectrometer output signal (a voltage proportional to the ion-beam current) was recorded on a strip chart. The peak heights were measured in millimeters with a ruler and the two values recorded for each of the three Ar isotopes in a forward and backward sweep through the mass spectrum were averaged. The two sets of average peak heights, along with the appropriate electrometer range factors, were entered into a Microsoft Excel workbook, which includes the potassium worksheet mentioned above, that calculates the radiogenic argon content and the apparent age for each sample. The worksheet also provides for correction of the measured peak heights for mass discrimination and for background signals due to species other than argon isotopes. The ^{40}K decay constant used has the value 5.543×10^{-10} yr^{-1}, the (partial) constant for decay to ^{40}Ar is 5.81×10^{-11} yr^{-1}, and the isotopic abundance of ^{40}K is 0.01167%. The estimate of overall relative error (2σ) in radiogenic argon determination is about 2% for most samples, but is substantially higher in one case because the amount of sample used was only 0.57 mg and in another case because no spike was added. In the latter case the calculated amount of radiogenic

argon was based on an estimate of the ^{38}Ar signal that would have been measured if the spike had been added. That estimate was possible, as also was a judgment of the uncertainty of the estimate, because the ^{38}Ar signal was nearly constant from one argon measurement to the next in this series of argon isotope analyses.

2.5 Comparison to Foraminiferal Studies

As a supplemental step, mineralogical data were collected to compare with data from the foraminiferal studies completed by Christensen et al. (2003) grab samples classified according to bedform features described by Goff et al. (1999). Specifically, relict versus modern mineral assemblages are correlated to foraminifera data to identify similarity. Core samples are also compared to mineralogical and sediment descriptions from the point count procedures. A qualitative assessment of angularity and roundness of sediment grains as functions of depth are used in comparison with foraminiferal data (relict verses modern).

CHAPTER 3: RESULTS

3.0 Grain Size Distribution

The groups of grab samples show differences in mean grain size among the major shelf bedform features. The results of the moment statistical analyses and interpretations are found in Tables A-1 and A-2, respectively. The eight sand ridge samples appear to fall into two separate groups by grain size. This group (samples 1, 2, 8, 9, 10, 11, 12, and 82) has medium to coarse sand mean grain size ranging from 1.08ϕ to 1.45ϕ. The standard deviations range from 0.50ϕ to 0.79ϕ, indicating the sand in this group is moderately well to moderately sorted. The ten sand ribbon samples have mean grain sizes ranging from 1.27ϕ to 2.11ϕ with standard deviations ranging from 0.46ϕ to 0.86ϕ, indicating the sand is in general moderately well sorted. The six samples collected from the areas of high fine / low coarse sediment have mean grain sizes ranging from 1.59ϕ to 2.32ϕ, with standard deviations ranging from 0.78ϕ to 1.01ϕ, indicating the sand is moderately sorted. The seven "other" samples have mean grain sizes ranging from 1.29ϕ to 1.93ϕ, with standard deviations ranging from 0.58ϕ to 0.95ϕ, indicating the sand is moderately well to moderately sorted. Results of grain size analysis by mass per unit range in phi size for grab samples are presented in Table 3.1. Cumulative weight percent results for grab samples are found in Table 3.2. See Figure 3.1 for cumulative frequency plots. Grab sample frequency distribution is plotted as histograms found in the appendix.

Core Site 1 has mean grain sizes ranging from 1.52ϕ to 1.63ϕ, with standard deviations ranging from 0.87ϕ to 1.05ϕ, indicating the sand in this core is moderately sorted to poorly sorted. Site 3 has mean grain sizes ranging from 1.61ϕ to 2.54ϕ, with standard deviations

ranging from 0.36ϕ to 0.75ϕ, indicating the sand in this core is well to moderately well sorted. Results of grain size analysis by mass per phi size for core samples are presented in Table 3.3. Cumulative weight percent results for core samples are found in Table 3.4. See Figure 3.2 cumulative frequency plots for the core samples. Core frequency distribution data are plotted in histograms available in the appendix.

TABLE 3.1 Mass of Grab Sample Phi Size Fractions

		Mass of Sand Fraction (grams)					
Sample	Type	Sample	0 phi	1 phi	2 phi	3 phi	4 phi
1	Ridge	32.81	3.58	9.23	17.13	2.73	0.01
2	Ridge	28.27	2.58	7.30	16.01	2.28	0.02
6	Other	19.22	0.66	4.47	11.08	2.89	0.06
8	Ridge	35.79	1.35	9.70	22.35	2.35	0.01
9	Ridge	40.71	1.00	11.50	26.03	2.14	0.02
10	Ridge	28.94	1.36	9.99	16.29	1.30	0.05
11	Ridge	33.95	0.43	9.14	22.95	1.40	0.00
12	Ridge	35.30	0.80	7.38	24.14	2.92	0.01
14	Ribbon	20.07	0.14	0.99	16.21	2.71	0.02
15	Ribbon	19.95	0.45	1.92	10.27	6.94	0.39
16	Ribbon	23.87	0.42	3.56	18.28	1.57	0.02
17	Ribbon	33.30	0.06	1.22	24.11	7.84	0.07
18	Ribbon	27.70	0.00	0.72	19.54	7.29	0.11
24	Ribbon	39.70	1.90	8.05	27.13	2.49	0.10
26	Ribbon	25.03	0.21	4.50	16.86	3.18	0.23
27	Other	31.45	0.55	3.83	22.74	3.93	0.18
28	Other	30.28	0.60	4.62	11.87	12.21	0.94
29	Other	11.45	1.15	2.67	5.23	2.11	0.25
30	Other	20.22	0.78	2.50	7.42	8.64	0.83
31	Other	22.27	0.88	2.63	6.89	9.85	2.04
45	Other	5.19	0.17	0.85	2.65	1.36	0.17
66	Ribbon	9.62	0.41	0.97	3.65	4.34	0.26
67	Ribbon	19.35	0.07	0.45	6.52	12.12	0.10
68	Ribbon	20.26	0.33	2.07	9.53	7.77	0.52
82	Ridge	19.81	0.07	2.76	15.12	1.83	0.04
116	HF/LC	5.08	0.24	0.50	2.10	1.87	0.39
117	HF/LC	52.10	2.41	7.12	22.12	16.80	3.61
121	HF/LC	52.09	3.16	10.26	22.24	11.69	4.71
128	HF/LC	26.84	0.59	2.87	6.94	11.06	5.29
132	HF/LC	8.84	0.35	1.30	4.24	2.39	0.56
137	HF/LC	9.98	0.19	0.45	1.52	6.57	1.20

Note: Ridge, Ribbon, Other, and HF/LC (high fine/low coarse material) as defined by Goff et al., 2004.

TABLE 3.2 Grab Sample Cumulative Weight Percent by Phi Fraction

		Sand Size Fraction					Bulk Sample*	
Sample	Type	coarser than 0 phi	1 phi	2 phi	3 phi	4 phi	% coarser than 0 phi	% finer than 4 phi
1	Ridge	11.0%	39.2%	91.6%	100.0%	100.0%	10.8%	1.8%
2	Ridge	9.1%	35.0%	91.8%	99.9%	100.0%	21.6%	2.2%
6	Other	3.4%	26.8%	84.6%	99.7%	100.0%	13.5%	4.3%
8	Ridge	3.8%	30.9%	93.4%	100.0%	100.0%	8.8%	0.9%
9	Ridge	2.5%	30.7%	94.7%	100.0%	100.0%	8.7%	0.6%
10	Ridge	4.7%	39.1%	95.2%	99.7%	99.9%	7.4%	0.2%
11	Ridge	1.3%	28.2%	95.9%	100.0%	100.0%	5.0%	0.6%
12	Ridge	2.3%	23.2%	91.7%	100.0%	100.0%	5.6%	2.1%
14	Ribbon	0.7%	5.6%	86.4%	99.9%	100.0%	2.7%	1.6%
15	Ribbon	2.3%	11.9%	63.2%	97.9%	99.9%	18.0%	7.9%
16	Ribbon	1.8%	16.7%	93.3%	99.9%	100.0%	6.6%	1.1%
17	Ribbon	0.2%	3.8%	76.2%	99.8%	100.0%	0.7%	0.7%
18	Ribbon	0.0%	2.6%	73.2%	99.6%	100.0%	0.3%	4.6%
24	Ribbon	4.8%	25.1%	93.5%	99.7%	100.0%	13.6%	3.5%
26	Ribbon	0.8%	18.9%	86.3%	99.1%	100.0%	14.0%	7.1%
27	Other	1.8%	14.0%	86.8%	99.4%	100.0%	3.8%	2.5%
28	Other	2.0%	17.3%	56.5%	96.9%	100.0%	8.1%	5.0%
29	Other	10.1%	33.5%	79.3%	97.8%	100.0%	29.4%	6.2%
30	Other	3.9%	16.3%	53.0%	95.8%	100.0%	34.4%	3.4%
31	Other	3.9%	15.7%	46.6%	90.8%	100.0%	13.5%	14.4%
45	Other	3.3%	19.6%	70.4%	96.5%	99.8%	24.8%	14.8%
66	Ribbon	4.3%	14.3%	52.2%	97.2%	99.9%	21.8%	6.7%
67	Ribbon	0.4%	2.7%	36.5%	99.4%	99.9%	4.4%	2.6%
68	Ribbon	1.6%	11.9%	59.0%	97.4%	100.0%	13.6%	6.6%
82	Ridge	0.4%	14.3%	90.6%	99.8%	100.0%	0.3%	2.3%
116	HF/LC	4.7%	14.5%	55.6%	92.2%	99.8%	4.2%	17.0%
117	HF/LC	4.6%	18.3%	60.8%	93.0%	99.9%	3.0%	16.3%
121	HF/LC	6.1%	25.8%	68.5%	90.9%	100.0%	4.2%	24.0%
128	HF/LC	2.2%	12.9%	38.8%	80.1%	99.9%	0.9%	54.7%
132	HF/LC	4.0%	18.6%	66.5%	93.5%	99.8%	3.7%	20.1%
137	HF/LC	1.9%	6.4%	21.7%	87.7%	99.8%	3.5%	16.1%

Note: * % coarser than 0 phi and % finer than 4 phi determined from bulk sample analysis by Goff et al. (2004); Sample Type defined by Goff et al. (2004).

FIGURE 3.1 Grab Sample Cumulative Frequency Curves

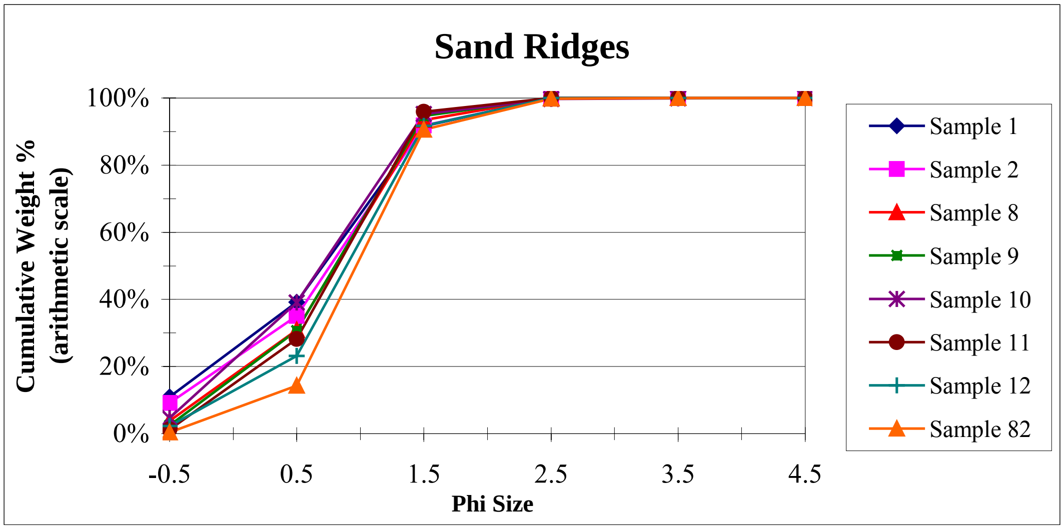

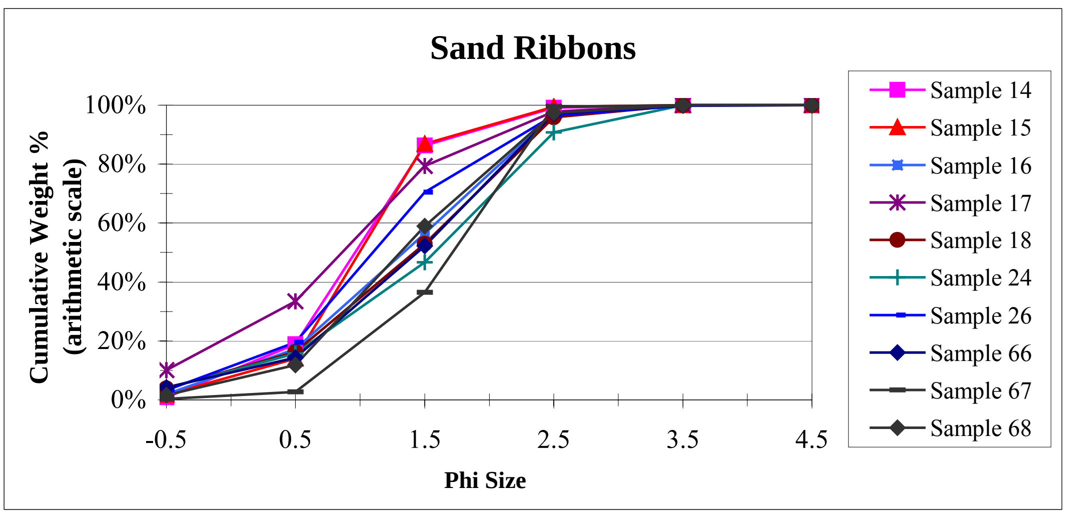

FIGURE 3.1 Grab Sample Cumulative Frequency Curves Continued

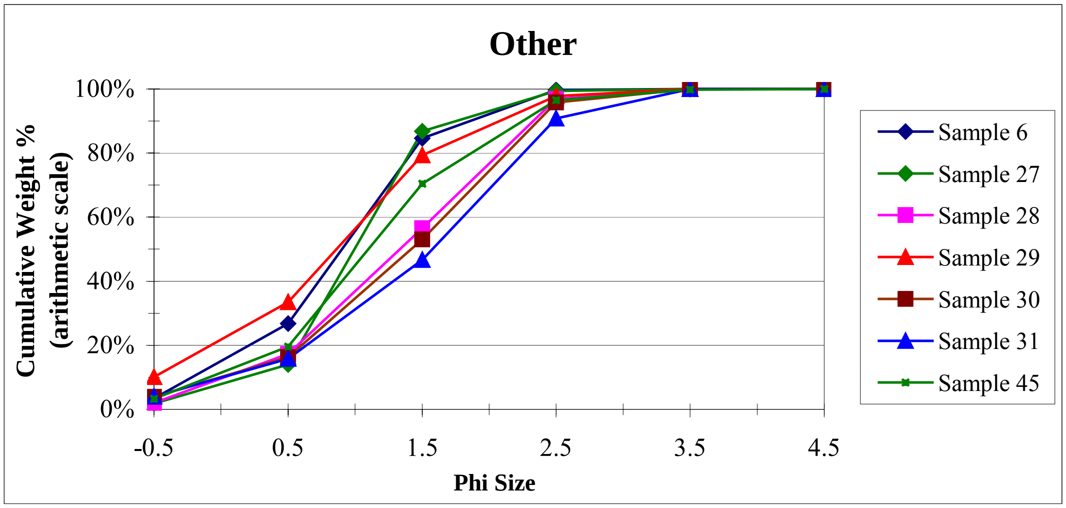

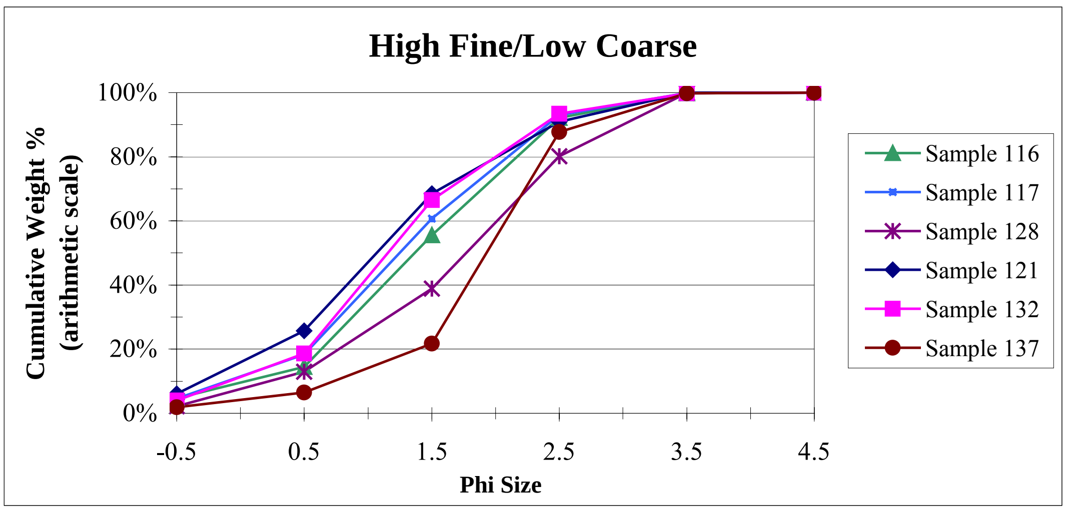

TABLE 3.3 Mass of Core Phi Size Fractions

Core	Depth (cm)	**Sand Fraction Mass (grams)** Sample	coarser than 0 phi	1 phi	2 phi	3 phi	4 phi	Bulk Sample* Total Mass (g)	% finer than 4 phi
Site 1	16	16.25	1.90	1.93	7.17	4.18	1.06	23.07	29.6%
Site 1	60	7.75	0.27	1.48	4.42	0.97	0.57	28.48	72.8%
Site 1	150	30.85	1.04	4.64	16.99	5.54	2.59	41.64	25.9%
Site 3	141	16.80	0.72	1.17	10.56	4.27	0.04	17.66	4.9%
Site 3	358	19.49	0.05	0.73	5.28	10.47	2.96	40.23	51.6%
Site 3	767	19.79	0.07	0.04	0.34	17.84	1.49	40.42	51.0%

* Bulk sample weight was before washing of fines (<63 µm).

TABLE 3.4 Cumulative Weight Percent of Sand Fraction at Core Sites

			Cumulative weight percent			
Sample	Depth (cm)	coarser than 0 phi	1 phi	2 phi	3 phi	4 phi
Site 1	16	11.7%	23.6%	67.7%	93.4%	99.9%
Site 1	60	3.5%	22.7%	79.9%	92.5%	99.9%
Site 1	150	3.4%	18.4%	73.6%	91.5%	99.9%
Site 3	141	4.3%	11.3%	74.2%	99.7%	99.9%
Site 3	358	0.3%	4.0%	31.1%	84.8%	99.9%
Site 3	767	0.4%	0.6%	2.3%	92.5%	100.0%

FIGURE 3.2 Core Cumulative Frequency Curves

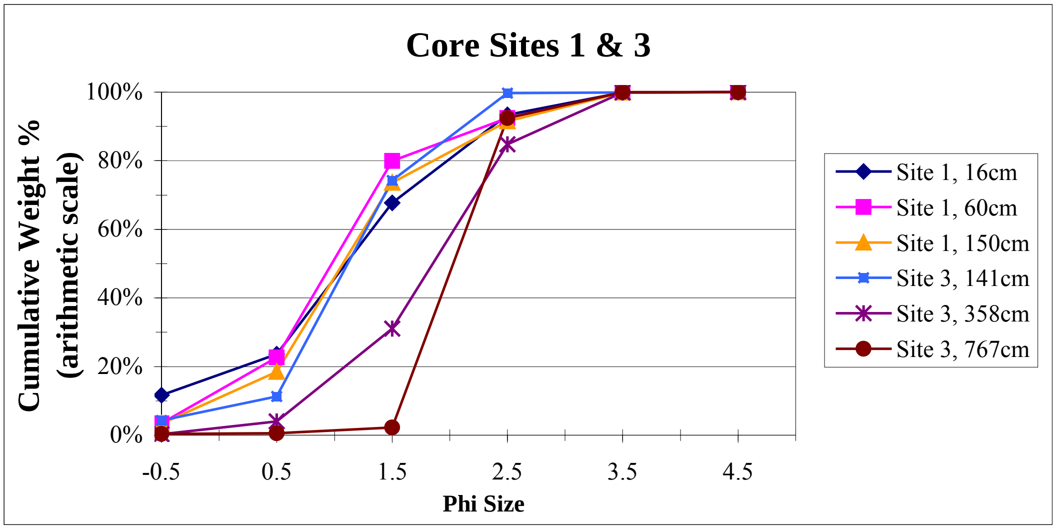

3.1 Heavy Mineral Fraction Results

Heavy minerals were separated from light minerals for the 2ϕ and 3ϕ size fractions from 31 grab samples and six core samples. The mass fractions of heavy minerals from the grab samples are provided in Table 3.5 and Figure 3.3. Average heavy mineral content of the 2ϕ size fraction across all grab sample types is 2.0%. Average heavy mineral content of the 3ϕ fraction by weight is 13.1%. The total average HM content for the bulk grab samples is 2.87%. This value is slightly lower than the result of 3.61% reported by Uptegrove et al. (1994). The heavy mineral analyses show that the average heavy mineral contents of both size fractions are greater in transect sand ridge samples than in all other groups. Average heavy mineral content for sand ridge samples for the 2ϕ and 3ϕ size fractions are 2.9% and 29.3% by weight respectively. Average HM content for transect sand ribbons for the 2ϕ and 3ϕ size fractions by weight is 1.1% and 7.9% respectively. The high fine / low coarse samples have average heavy mineral concentrations of 1.5% and 5.6% for the 2ϕ and 3ϕ size fractions, respectively. The grab samples classified as "other" samples have average heavy mineral concentrations of 2.8% and 8.5% for the 2ϕ and 3ϕ size fractions, respectively.

The mass fractions of heavy mineral in the core samples are provided in Figure 3.5 and Table 3.6. The average HM content in core samples are 2.9% and 9.1% for the 2ϕ and 3ϕ size fractions, respectively. The average HM percentage for core samples is 4.7% of the sand fraction and 2.1% of the bulk sample. The bulk HM percentage arrived in this study is comparable to the results of 1.94% by weight percent reported by Uptegrove et al. (1994). The 2ϕ size fractions have lower heavy mineral contents than the 3ϕ size fractions in all samples except one. The exception, Site 3: 767 cm, was the smallest sample analyzed with a total sample

mass of 0.34 g, of which 0.02 g comprised the heavy mineral concentrate. If this sample had been substantially larger, the observed heavy mineral contents would likely not be anomalous.

TABLE 3.5 Grab Sample Sand Fraction Heavy Mineral Results

Sample	Type	2ϕ	3ϕ	Sample Total
1	Ridge (TR)	2.45%	19.78%	3.06%
2	Ridge (TR)	4.25%	30.26%	4.86%
6	Other (TR)	3.34%	12.11%	3.76%
8	Ridge (TR)	4.88%	55.32%	6.68%
9	Ridge (TR)	2.50%	29.90%	3.17%
10	Ridge (TR)	3.50%	34.00%	3.48%
11	Ridge (TR)	1.92%	22.14%	2.21%
12	Ridge (TR)	2.94%	33.22%	4.77%
14	Ribbon (TR)	0.56%	14.39%	2.39%
15	Ribbon (TR)	1.27%	6.05%	2.75%
16	Ribbon (TR)	0.82%	15.92%	1.68%
17	Ribbon (TR)	0.51%	8.95%	2.49%
18	Ribbon (TR)	0.58%	3.73%	1.41%
24	Ribbon (TR)	0.81%	9.80%	1.16%
26	Ribbon (TR)	0.71%	5.35%	1.16%
27	Other (TR)	1.01%	8.65%	1.81%
28	Other (TR)	1.71%	3.03%	1.88%
29	Other (TR)	3.40%	14.70%	4.28%
30	Other (TR)	1.89%	4.17%	2.47%
31	Other (TR)	1.89%	4.26%	2.47%
45	Other	6.04%	12.50%	6.36%
66	Ribbon	3.84%	5.53%	3.95%
67	Ribbon	0.46%	2.06%	1.45%
68	Ribbon	1.89%	7.59%	3.80%
82	Ridge	0.53%	9.84%	1.31%
116	HF/LC	1.43%	5.88%	2.76%
117	HF/LC	1.76%	7.56%	3.19%
121	HF/LC	1.98%	7.70%	2.57%
128	HF/LC	1.59%	4.34%	2.20%
132	HF/LC	0.94%	6.28%	2.15%
137	HF/LC	1.32%	1.83%	1.40%
All	Average	2.02%	13.12%	2.87%

Note: Sample types defined by Goff et al. (2004);
TR = Transect samples.

FIGURE 3.3 Grab Sample Heavy Mineral Distribution

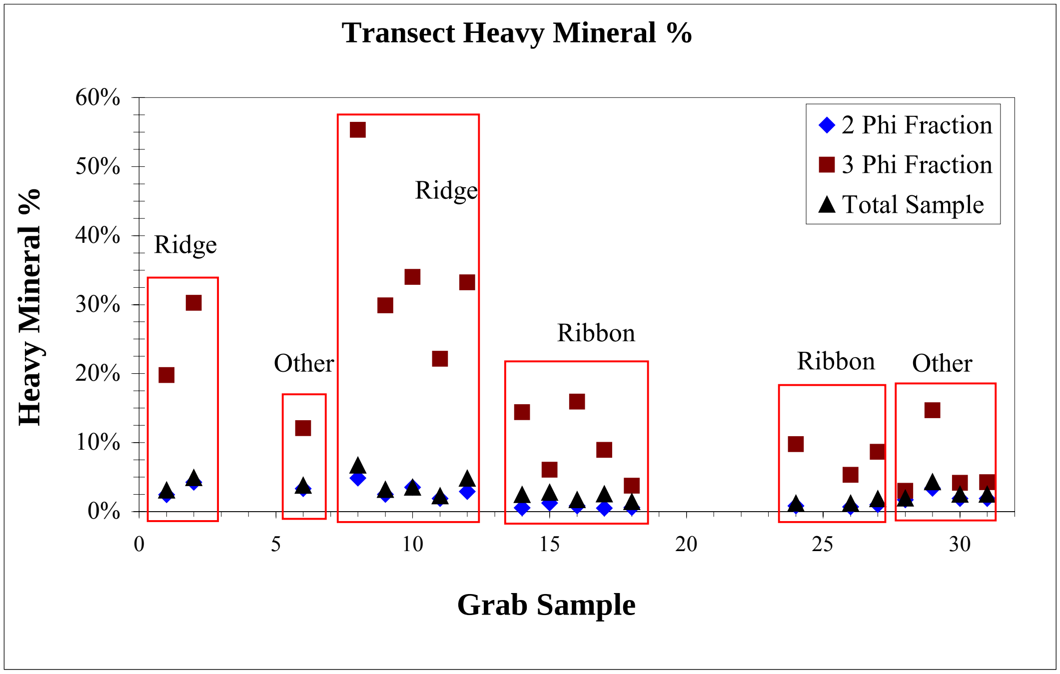

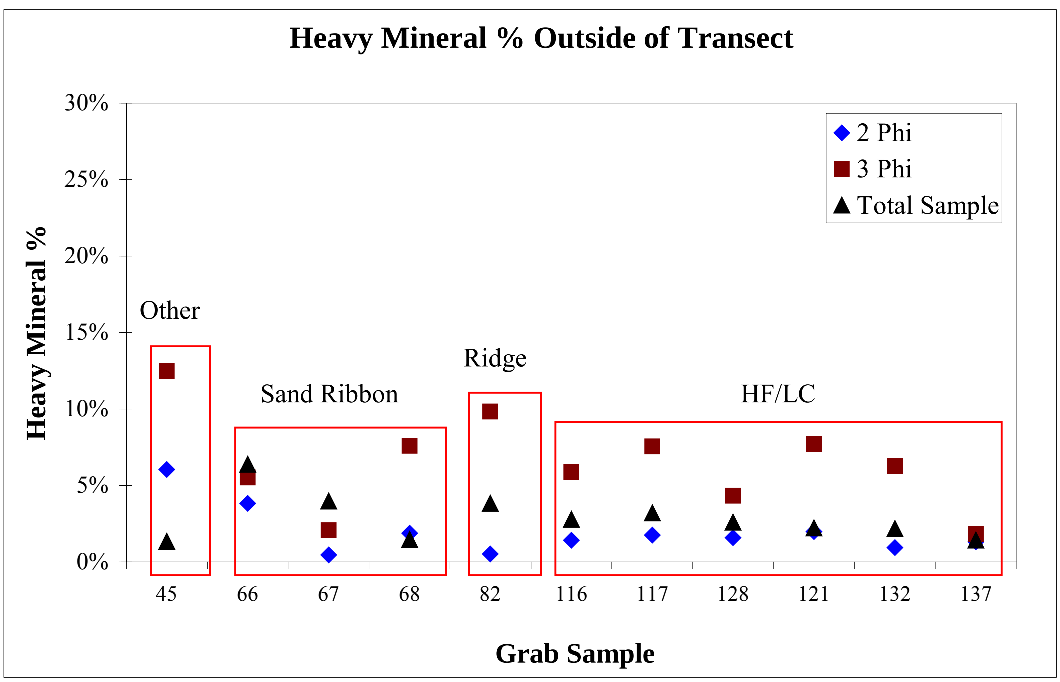

TABLE 3.6 Heavy Mineral Results Averaged

Samples	2ϕ	3ϕ	Total Sample	# of Samples
	(Average)			
Sand Ridges	2.9%	29.3%	3.7%	8
Sand Ribbons	1.1%	7.9%	2.2%	10
Other	2.8%	8.5%	3.3%	7
High Fine/Low Coarse	1.5%	5.6%	2.4%	6
Core	1.4%	5.3%	0.2%	6

TABLE 3.7 Core Sand Fraction Heavy Mineral Results

	Sand Fraction			
Sample	2ϕ	3ϕ	Sample Total	Bulk Sample
Site 1, 16 cm	3.5%	8.9%	5.5%	2.7%
Site 1, 60 cm	5.4%	11.3%	6.5%	1.2%
Site 1, 150 cm	0.2%	11.7%	3.1%	1.7%
Site 3, 141 cm	0.6%	10.1%	3.3%	2.8%
Site 3, 358 cm	1.9%	9.9%	7.2%	2.8%
Site 3, 767 cm	5.9%	2.6%	2.6%	1.2%
Average	2.9%	9.1%	4.7%	2.1%

3.2 Magnetic Mineral Results

The results of the heavy mineral magnetic susceptibility analyses are shown in Table 3.8. The two fractions having the lowest magnetic susceptibility (the fractions magnetic at 1.8 A and the residuum) are for all samples much large in mass than the fractions having larger magnetic susceptibility. Of the latter, the most magnetic fraction (that magnetic at 0.05 A) is generally the largest. The ferromagnetic mineral grains, or those magnetic at 0.05 A, include populations of magnetite, ilmenite, and pyroboles (undifferentiated pyroxenes and amphiboles) (Uptegrove et al., 1991). The mineral grains magnetic at 1.8 A are only slightly paramagnetic (weakly accelerated in a strong magnetic field) but this group is the largest in mass of the magnetic groups and has the largest diversity of minerals. The minerals found in this fraction include abundant hornblende and minor amounts of visually identified leucoxene, biotite, and aluminosilicates such as sillimanite, kyanite, and andalusite. The heavy mineral grains found in the fractions magnetic at 0.2 A, 0.4 A, and 0.6 A include garnet, easily identifiable because of its color, as well as tourmaline, epidote, and staurolite. These results resemble those of Uptegrove et al. (1991) except in respect to abundance of hornblende found in the grab samples.

The distribution of magnetic minerals across the transect samples analyzed is shown in Figure 3.4. Grab samples 8, 9, 10, 11, and 12 span a sand ridge, with sample 8 most landward. The percentage of magnetic minerals at all susceptibilities is greatest on the landward side of the sand ridge and decreases toward the center of the ridge, rising slightly toward the other side. The patterns of magnetic distribution across the two sand ribbons (grab samples 14-18 and 24-26) are similar to one another. Grab sample 14 is at the landward side of the first sand ribbon analyzed. Samples 15 and 16 have somewhat higher percentages of magnetically susceptible heavy mineral

grains than the other samples from that ribbon, but the overall variability within most of the susceptibility groups is small. The two samples from the second sand ribbon analyzed have similar susceptibility percentages to those in the first sand ribbon. Grab samples 27, 29, and 30 are samples labeled as “other” and show a pattern of increasing percentage of magnetic mineral grains seaward.

TABLE 3.8 Magnetic Heavy Mineral Mineral Results

Sample	Type	$2\phi + 3\phi$ weight (g)	0.05 A %	0.2 A %	0.4 A %	0.6 A %	1.8 A %	Residuum %	Loss %
2	Ridge	1.387	4.9%	1.0%	1.7%	1.7%	48.2%	42.9%	-0.4%
6	Other	0.719	0.7%	0.3%	0.4%	0.6%	25.6%	72.2%	0.3%
8	Ridge	2.377	2.5%	0.8%	0.6%	0.9%	55.4%	40.0%	-0.3%
9	Ridge	1.276	1.4%	0.5%	0.6%	0.8%	35.1%	61.1%	0.5%
10	Ridge	0.998	1.3%	0.3%	0.3%	0.5%	26.9%	69.8%	0.9%
11	Ridge	0.742	0.4%	0.4%	0.5%	0.5%	12.5%	85.6%	0.0%
12	Ridge	1.676	1.6%	0.6%	0.5%	0.6%	17.8%	78.2%	0.8%
14	Ribbon	0.478	0.6%	0.2%	0.4%	0.8%	22.4%	74.3%	1.3%
15	Ribbon	0.536	0.6%	0.2%	0.2%	0.9%	32.1%	64.6%	1.5%
16	Ribbon	0.400	1.3%	0.8%	0.5%	0.8%	29.8%	67.0%	0.0%
17	Ribbon	0.821	1.0%	0.2%	0.5%	0.5%	18.3%	78.3%	1.2%
18	Ribbon	0.383	0.8%	0.5%	0.8%	0.8%	12.8%	85.9%	-1.6%
24	Ribbon	0.463	0.9%	0.2%	0.4%	0.6%	20.5%	76.9%	0.4%
26	Ribbon	0.284	0.4%	0.4%	0.4%	0.4%	25.7%	72.2%	0.7%
27	Other	0.561	0.4%	0.2%	0.2%	0.5%	16.0%	80.7%	2.0%
29	Other	0.495	3.6%	1.2%	0.8%	1.6%	27.1%	64.8%	0.8%
30	Other	0.496	2.0%	0.6%	0.4%	0.6%	38.9%	55.4%	2.0%

FIGURE 3.4 Magnetic Mineral Distribution by Susceptibility Percentage

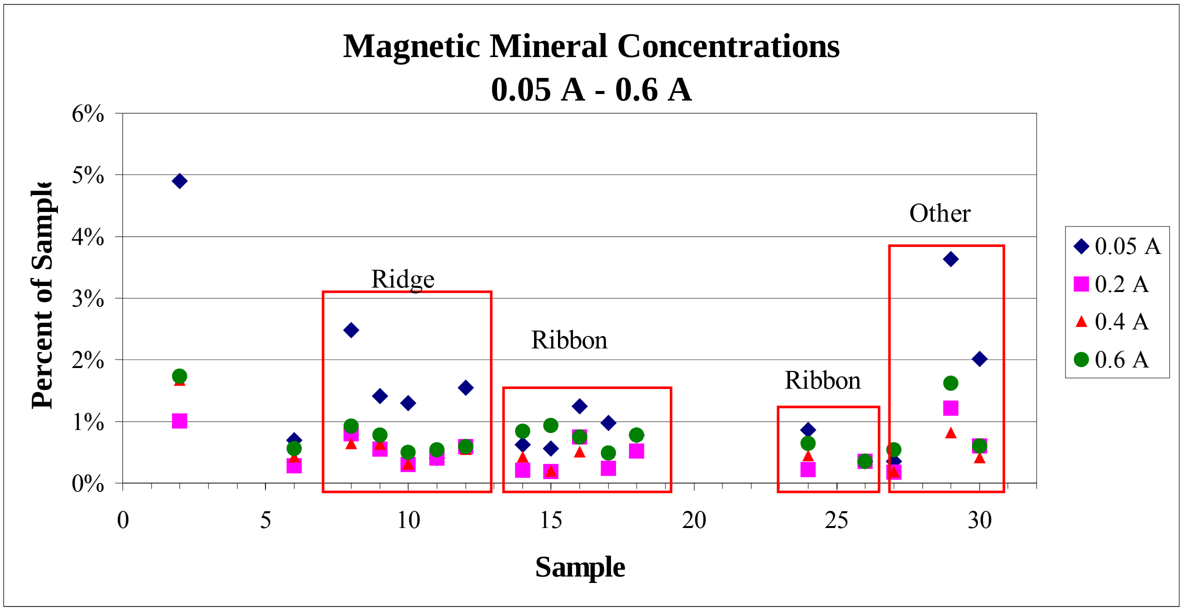

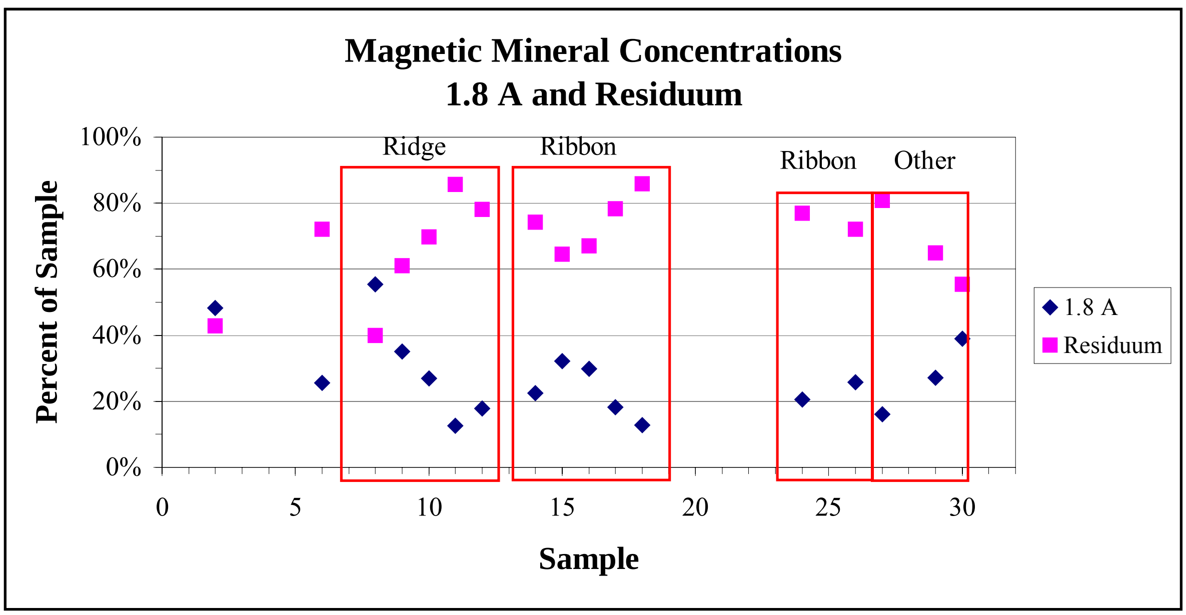

3.3 Hornblende Apparent Ages

Results from K-Ar isotopic analyses of hornblende grains are presented in Table 3.9. Two populations of hornblendes are apparent. Eight of the eleven age values group together in the range of 910 ± 30 My to 960 ± 30 My and the other three group in the range of 810 ± 40 My to 880 ± 30 My. The apparent ages greater than 900 My are consistent with a Grenvillian source. These age values, along with the pristine nature of the hornblende grains, suggests a proximal provenance of Precambrian amphibolites or gneisses such as the Reading Prong (Turner et al., 2004b). The dating by Gates and Krol (1998) and Gates et al. (2000) of hornblendes associated with the last stages of the Grenvillian orogeny in the Hudson and New Jersey Highlands provides good reason to expect that most hornblendes in rocks of the Highlands have K-Ar apparent ages somewhat greater than 915 My. Other samples returned age values somewhat less than those typical of the proximal Grenville sources, suggesting that a mixture of hornblendes from older and younger rocks was present in those samples. All hornblende grains selected for dating were very angular to subangular, indicating that they were freshly weathered.

Figure 3.5 illustrates the HM% and corresponding K-Ar hornblende age values for the six core samples from Sites 1 and 3. The areas shaded in blue indicate deposition within the current interglacial period (oxygen isotope stage 1) and in pink indicate earlier deposition (most likely oxygen isotope stage 3) based on radiocarbon data from Alexander et al. (2003).

TABLE 3.9 Results of K-Ar age determination analyses

Sample	Location (Lat, Long)	Depth	Size-Fraction (mm)	Potassium (weight %)	$^{40}Ar^*$ (%)	$^{40}Ar^*$ (pmol/g)	K-Ar Age (My)
1	39.35746, -73.067123	Seafloor	125 - 250	1.04 ± 0.04	96	2.29 ± 0.04	960 ± 30
28	39.238647, -72.786377	Seafloor	125 - 250	1.13 ± 0.02	98	2.46 ± 0.04	950 ± 20
31	39.203125, -72.753754	Seafloor	125 - 250	1.04 ± 0.04	97	2.15 ± 0.04	910 ± 30
116	39.224602, -72.660316	Seafloor	125 - 250	1.11 ± 0.05	89	1.98 ± 0.09	810 ± 40
117	39.22369, -72.65873	Seafloor	125 - 250	1.27 ± 0.04	98	2.80 ± 0.05	960 ± 30
Site 1, 16 cm	39.2391, -72.6863	16 cm	125 - 250	1.17 ± 0.02	90	2.47 ± 0.05	930 ± 20
Site 1, 60 cm	39.2391, -72.6863	60 cm	125 - 250	0.93 ± 0.03	97	1.97 ± 0.04	930 ± 20
Site 1, 150 cm	39.2391, -72.6863	150 cm	125 - 250	1.15 ± 0.02	97	2.17 ± 0.04	850 ± 20
Site 3, 141 cm	39.2533, -72.8998	141 cm	125 - 250	1.02 ± 0.02	95	2.27 ± 0.04	960 ± 20
Site 3, 358 cm	39.2533, -72.8998	358 cm	125 - 250	1.09 ± 0.03	97	2.38 ± 0.04	960 ± 30
Site 3, 767 cm	39.2533, -72.8998	767 cm	63 - 250	0.99 ± 0.03	90	1.93 ± 0.07	880 ± 30

FIGURE 3.5 Heavy mineral % of core samples with corresponding K-Ar age values for hornblende.

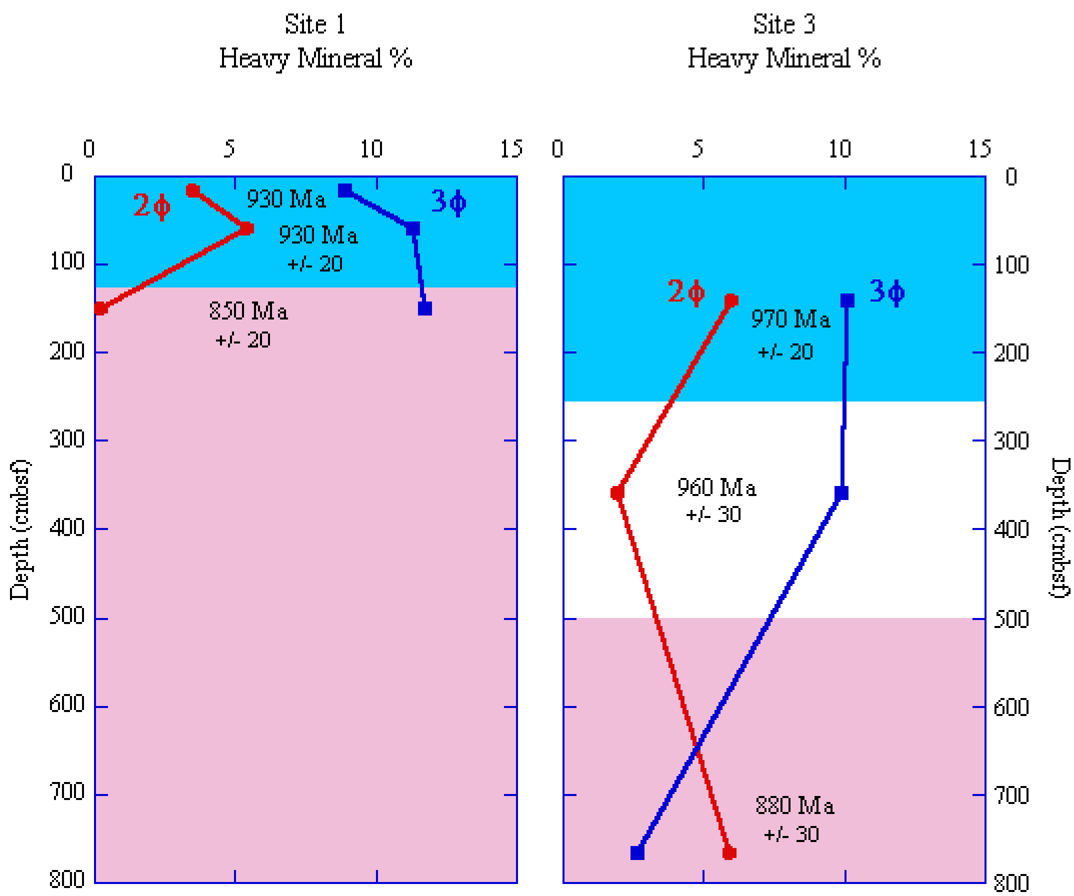

Note: Pink and blue shading represent ^{14}C dates as determined by Alexander et al. (2003). Pink = 40 ka– 31 ka B.P.; Blue = 10.7 – 4.0 ka B.P. Area not shaded does not have a radiocarbon date associated with it. Hornblende K-Ar apparent ages are shown in black beside the samples.

3.3 Foraminiferal Comparison

Summary results of the mineralogical assessments of certain grab samples of this study are shown in Table 3.10 for comparison with foraminiferal interpretations of the same samples by Christensen et al. (2003), which are also summarized in the table.

TABLE 3.10 Mineralogical Comparison to Foraminiferal Interpretation

Sample	Type	Foraminiferal Interpretation	Mineralogical Assessment
29	Other	Relict (Inner Neritic) & In-situ (Middle Neritic)	Poorly sorted grain size, high magnetic %
30	Other	Relict (Inner Neritic) & In-situ (Middle Neritic)	Moderately sorted grain size, excess coarse grains, high mag. %
45	Other	Relict (Inner Neritic) & In-situ (Middle Neritic)	Moderately sorted grain size with normal distribution
66	Ribbon	Relict (Inner Neritic) & In-situ (Middle Neritic)	Moderately sorted grain size with excess coarse grains
67	Ribbon	Relict (Inner Neritic) & In-situ (Middle Neritic)	Moderately well sorted grain size with excess coarse grains
68	Ribbon	Relict (Inner Neritic) & In-situ (Middle Neritic)	Moderately sorted grain size with normal distribution
82	Ridge	Relict (Inner Neritic) & In-situ (Middle Neritic)	Moderately well sorted grain size, even distribution of grains
128	HF/LC	In situ (Outer Neritic)	Poorly sorted grain size with coarse skewness
132	HF/LC	In situ (Outer Neritic)	Moderately sorted grain size with normal distribution
137	HF/LC	In situ (Outer Neritic)	Moderately sorted grain size with coarse skewness

Note: Foraminiferal interpretation completed by Christensen (2003), mineralogical assessment by Turner (this study).

CHAPTER 4: DISCUSSION

The objectives of this research were to determine 1) the age and provenance of New Jersey shelf sediments, 2) the transport history of the sediments, and 3) presence of IRD on the New Jersey shelf. The apparent age determinations of detrital hornblende grains have been used for provenance determinations. These sediment grains serve as representative members of the heavy mineral assemblage and provide information on the possible origins of sediments on the New Jersey shelf. The grain size, heavy mineral, and magnetic mineral analyses were completed to obtain data to support the interpretation of the transport and depositional history of sediments. The presence of IRD would be suggested if anomalous results were obtained for a sample using any combination of the analytical methods employed.

4.0 Age and Provenance of New Jersey Sediments

The data from this study indicate two sources: A, which is predominately Grenvillian terrane, and B, a mixed assemblage of Grenvillian and younger terranes. The age values of the New Jersey shelf hornblende grains suggests that the provenance of the majority of the sediments (Source A) are the proximal Grenville basement outcrops known as the New Jersey and Hudson Highlands (Figure 4.1). This area has been shown in numerous studies (Volkert and Drake, 1999; Drake, 1969; Ratcliffe, 1982) to be of Grenville age through various geochronological methods such as K-Ar, Rb-Sr, and U-Pb isotopic dating. In general, any granulite massif with an isotopic age between 1,300 Ma and 893 Ma in the Reading Prong of the north-central Appalachians is believed to have formed as a part of the Grenville orogeny (Gates et al., 2003).

For example, Gates et al. (2000) dated hornblende grains within a shear zone within the Tuxedo area of the Hudson Highlands that represent a late stage of the Grenville orogeny in this area. Apparent ages between 915 and 925 Ma for these late-stage hornblendes suggest that K-Ar ages of most of the hornblende in the Highlands should be a little greater than 915 My. Smith (1969) showed that the units within the Highlands comprised of hypersthene-quartz-andesine gneiss contain notable amounts of hornblende grains of about this age. Other Grenville rock units within the New Jersey and Hudson Highlands contain hornblende, but in less substantial quantities (Young and Icenhower, 1989). Additional potential Grenville source rocks exist further north along the Hudson River in the Adirondack Mountains.

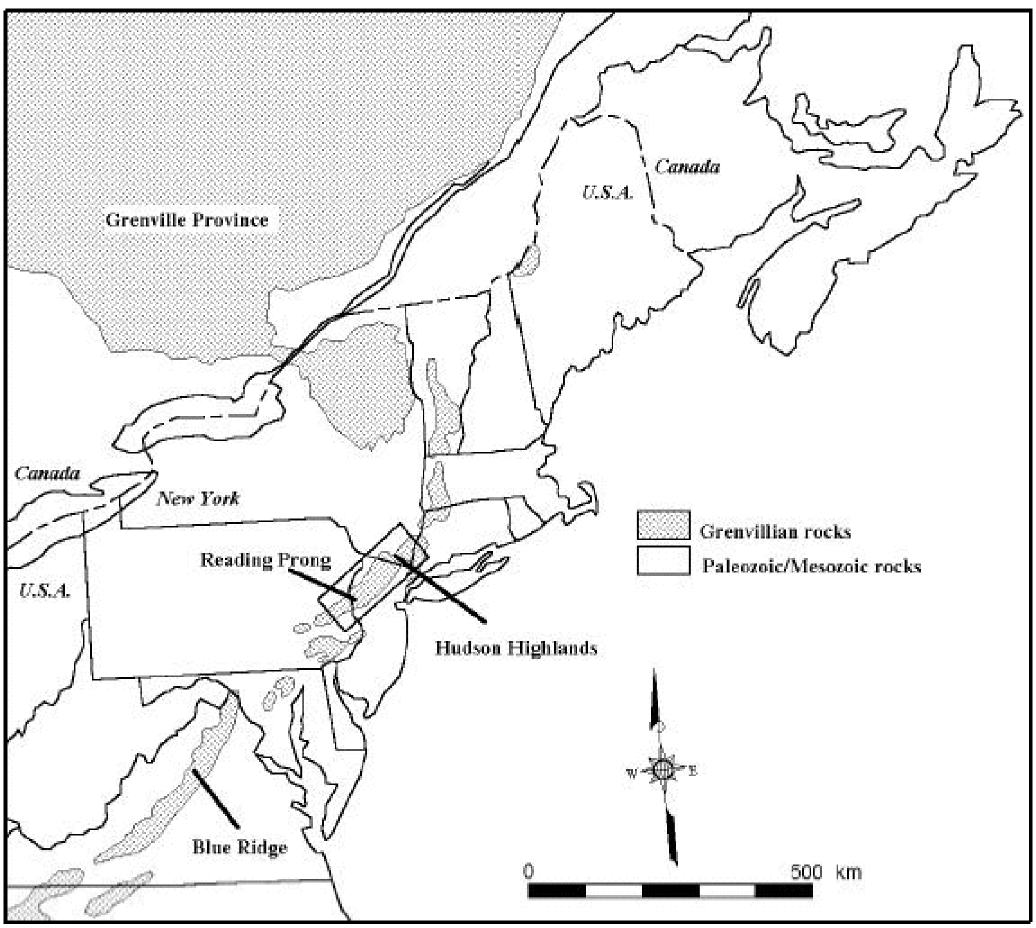

FIGURE 4.1 Map of Grenvillian basement outcrops and Paleozoic/Mesozoic rocks throughout the northeastern United States and Canada from Gates et al. (2003).

The three samples (grab sample 116, Site 1: 150 cm, Site 3: 767 cm) in this study with apparent ages less than 900 My are from Source B and interpreted have a mixed assemblage of hornblende from older (Grenville) and younger (Paleozoic) source rocks. The deepest two samples analyzed at Sites 1 and 3 (150 cm and 767 cm, respectively) are from sediment deposition before the LGM based on radiocarbon data collected by Alexander et al. (2003). These two core samples were deep enough not to have been affected by exposure, weathering, and redeposition of surficial sediment during the last glacial maximum. Grab sample 116, with an apparent age of 810 ± 40 My, is taken from a probable iceberg scour mark with high fine/low coarse material (Goff et al., 2004). The depth of the scouring has been measured up to 4 m into the seafloor (Duncan and Goff, 2001), deep enough to penetrate into the older depositional unit found below the Holocene sediment veneer. The younger source rocks are most likely the Cortlandt, Rosetown, and Stony Point complexes found along the Hudson River approximately 55 km north of New York City. Particles from these younger rocks could have been eroded from the bedrock and then transported via fluvial mechanisms downstream to the New Jersey shelf. Glacial transport is not an option for these sediments as the Laurentide Ice Sheet did not extend out onto the New Jersey shelf. In addition, the Illinoian glaciation that occurred approximately 150 ka extended past the maximum extent of the Wisconsinan glaciation, covering the younger Paleozoic units. The earlier glaciation could have eroded different source rocks with a younger apparent age. These younger sediments would then be mixed with the older Grenville sources to provide the younger mixed age of Source B.

Even younger Mesozoic rocks found in the Piedmont Province of New Jersey, such as those from Orange Mountain, Preakness, and Hook Mountain are additional possible contributors to the sediment on the New Jersey shelf. The oldest, Orange Mountain, was dated

to be 201 ± 2.1 My old, and the youngest, Hook Mountain was dated to 198.8 ± 2.0 My , by $^{40}Ar/^{39}Ar$ isotopic analyses of plagioclase (Hames et al., 2000). These rocks are not hornblende rich, but could have supplied other prominent detrital heavy mineral grains such as magnetite and ilmenite.

To constrain the provenance of hornblende grains found on the New Jersey shelf to more precisely, additional hornblende samples from the study area could be analyzed using single grain $^{40}Ar/^{39}Ar$ isotopic dating methods. An additional procedure that could be employed is determination of Na, Ca, Mg, total Fe, and Al in hornblende by atomic absorption and flame emission spectrophotometry. Such data could be compared to results from isotopic dating of amphibolites and gneisses throughout the New Jersey and New York Highlands and from studies using major chemical analyses, as described by Jappy et al. (2001).

4.1 Depositional History of New Jersey Shelf Sediments

Two issues to consider for interpreting transport history to the New Jersey shelf are 1) the delivery of sediment to the shelf as implied by hornblende data, and 2) the deposition and modification of surface features. The transport history of the New Jersey shelf sediments can be tentatively traced by considering the provenance determinations and results of the grain size, heavy mineral, and magnetic mineral analyses.

The paleo-drainage system from the Highlands across the Piedmont and Coastal Plain of New Jersey throughout the late Pleistocene carried sediments from the Highlands and Piedmont province directly to the continental shelf. Transport may have been through the ancestral Hudson River system or through any number of smaller river systems. Regardless of the precise riverine system that transported the sediments, the system did so in a manner that was direct and

swift. The pristine nature of the majority of hornblende grains analyzed suggests a freshly weathered and proximal source. Based on the results of Frank and Friedman (1972), the New Jersey shelf sediments do not match the signature of Coastal Plain sediments. The findings of this study support the conclusions drawn from Frank and Friedman (1972) as the majority of heavy mineral grains found on the shelf do not have the roundness found in sediment grains exposed to multiple weathering cycles.

Two independent studies completed recently address the question of glacial dam breaching. Fulthorpe and Austin (2004) have identified deep (up to 10 m) incisions on the New Jersey shelf interpreted to have been cut by flood events following glacial dam breaching. The incisions can be traced for up to 10 km along the shelf. In the other study, Donnelly et al. (2005) investigated a specific glacial dam breach. This second study indicates that Glacial Lake Iroquois breached its own terminal moraine dam before flowing into and breaching the dams of two other ancestral glacial lake dam systems, Glacial Lake Vermont and Glacial Lake Albany, creating an enormous surge of fresh water that flowed through the ancestral Hudson River valley. An event of this magnitude would be capable of carrying glacial erratics greater than 2 m in diameter (identified by Uchupi et al., 2001) and reducing the thermohaline circulation in the North Atlantic (Donnelly et al., 2005). The breaching of glacial Lake Iroquois is thought to have occurred between 13,280 and 13,050 year B.P. constrained by several ^{14}C-dated samples. A glacial surge of this extent would have cut the exposed continental shelf creating the deep incisions identified by Fulthorpe and Austin (2004) and would have provided a swift and direct transport mechanism for freshly eroded sediments from the New Jersey Highlands and more northern source areas such as the Adirondack and Catskill Mountains to the study area on the New Jersey shelf.

Once sediments reach the continental shelf, they are deposited onto an active surficial sand sheet that is mobile. Here, sediment grains are eroded and redeposited in a series of bedforms such as the sand ridges and sand ribbons. The deposition of sediments occurred predominately towards the end of and following the glacial maximums in the late Pleistocene, in close proximity to the shorelines of those times. Trends in the results of grain size, heavy mineral, and magnetic mineral analyses of the sand size fraction can be used to draw conclusions on the depositional history of sediments once they reach the shelf.

The surface grab samples and the samples in the uppermost portions of the cores are from Source A. These include grab samples 1, 28, 31, 117, and Site 1: 16 cm, Site 1: 60 cm, Site 3: 141 cm, and Site 3: 358 cm. The timing of surficial sediment deposition is constrained to less than 13 ka by radiocarbon data (Alexander et al., 2003) and thus, follows the retreat of the Laurentide ice sheet. Each of these sample sites returned a K-Ar hornblende age value of 910 $\pm$ 30 Ma or older.

Variations in the mean size of the sand size fractions of grab samples are, in part, related to the movement of surface and bottom currents across the shelf. Grain size distributions in the grab samples show that all samples are medium or fine sands. Samples 1-12 in the transect are coarser (between 1.0ϕ and 1.5ϕ) than those found further seaward in the transect. Samples 14, 15, 18 and 28, 30, 31 are medium-to-fine sands (between 1.5ϕ and 2.0ϕ) that are categorized by Goff et al. (2004) as sand ribbons or other samples. Grab samples from outside of the transect are fine to fine-to-medium sands (>1.5ϕ). Goff et al. (2005) showed that erosion is active on the New Jersey shelf in water depths up to 50 m. However, the sand ribbon features are also interpreted to be erosional surfaces, and several occur in this study area in water depths greater than 50 m.

Those samples closest to the shoreline in the transect show a trend of higher heavy mineral concentration. These samples are generally classified as sand ridge samples with one or two exceptions. The majority of these samples are found in water depths of 70 m or below. While it has been reported that erosion is most likely to affect samples in water depths of 50 m or less, the evidence of concentrated HMs in water depths between 50 m and 70 m suggests preferential movement of lighter density grains. Preferential transport of sediments could also result from bottom current activity. A possible explanation for the varying HM content in the transect sand ridge verses transect sand ribbon samples is that the HMs were deposited during times of differing sea levels in the past. Alternatively, currents could have winnowed out the lighter mineral grains, such as quartz. A third possible explanation is that the sand ridge represented by grab samples 8 through 12 could be a relict barrier island, as suggested by Rine et al. (1991). Concentrations of heavy mineral layers can be found in modern barrier islands systems along the east coast of the United States today.

Magnetic mineral analyses were completed for the majority of the transect grab samples. It was found that magnetic grain concentrations are generally higher in sand ridges and almost always less in sand ribbon samples. This finding correlates well with the interpretation of Goff et al. (2004) that sand ribbons are erosional bedforms. Samples rich in magnetite grains (2, 8, 29, 30) indicate two distinct areas of concentration. The sand ridge samples (2 and 8) are areas of concentrated coarse and dense mineral grains with majority of fines having been winnowed away. Samples 29 and 30, described as "other" had a high percentage of coarse-grained material (>4 mm) when collected (Goff et al., 2004). Perhaps this gravel population aids in the preservation of magnetic mineral grains at these sites.

When considering the stratigraphic samples at Sites 1 and 3, a trend can be seen as highlighted in the blue and pink areas in Figure 3.5. The samples from the areas shaded in blue are interpreted to be recent deposition during transgression since the LGM. The grain size, heavy mineral concentration, and hornblende apparent ages of the uppermost two samples at Sites 1 and 3 concur with those of grab samples analyzed in and around these areas. Samples at Site 1: 150 cm and Site 3: 767 cm indicate a trend different than that seen in the surface sand sheet, particularly with respect to hornblende apparent ages. These samples, along with grab sample 116, are from Source B.

A map of grab sample sites with hornblende apparent ages is shown in Figure 4.2. The seismic profiles at Sites 1 and 3 are shown with the hornblende apparent ages in Figures 4.3 and 4.4. When considering the stratigraphic data in context with the seismic reflectors, distinct units of deposition can be identified. At Site 1, the uppermost two samples are within the surface sand sheet. The sample at Site 1: 150 cm is at or below the first major reflector. The sample at Site 3: 150 cm was collected within the recently deposited sediment within the channel scour. The sample at Site 3: 358 cm is between the channel scour but above the regional reflector "R." Site 3: 767 cm is from below the regional reflector "R". Thus, the deepest samples from Site 1 and 3 are interpreted to have been deposited before the LGM, and, based on ^{14}C dates provided by Alexander et al. (2003), are at least 31.5 ky and 36.6 ky old, respectively.

FIGURE 4.2 Hornblende apparent age distribution at grab sample site.

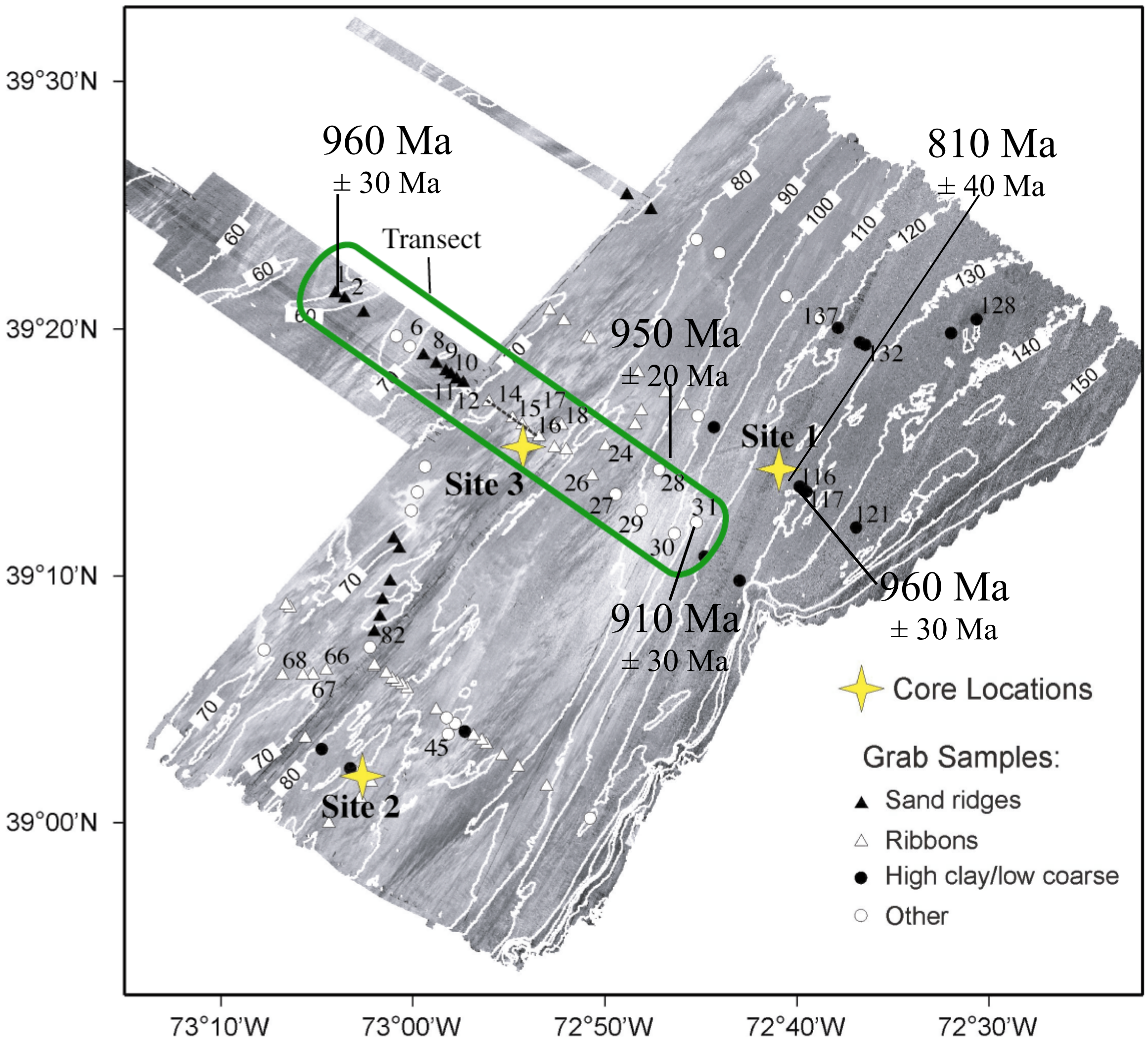

FIGURE 4.3 Seismic profile at Site 1 along the red line at water depth of 127 m, core penetration 6.8 mbsf (from Alexander et al., 2003); hornblende apparent ages marked.

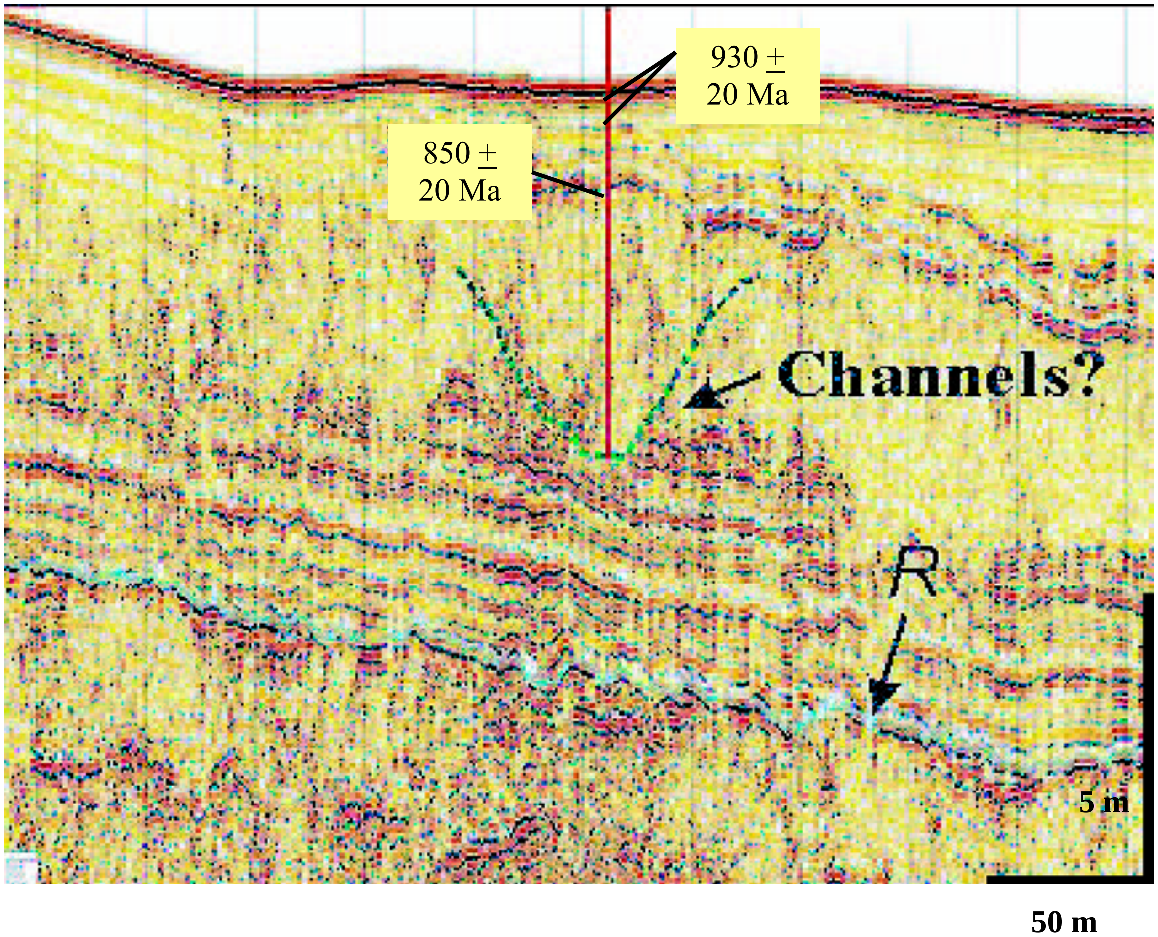

FIGURE 4.4 Seismic profile at Site 3 (Core 3 along the red line) at water depth of 75 m, core penetration 7.7 mbsf (from Alexander et al., 2003); hornblende apparent ages marked.

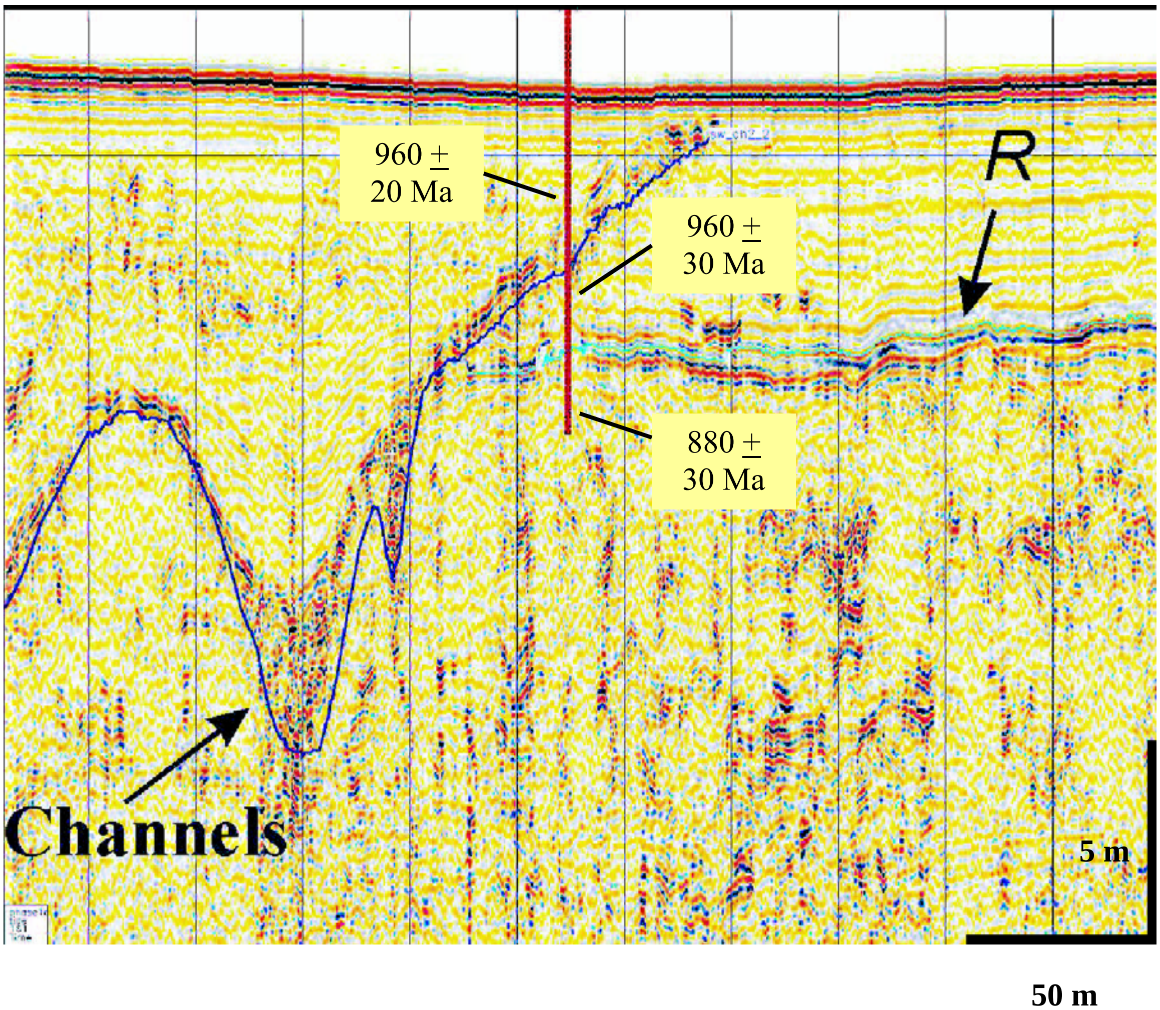

4.2 Possible Presence of IRD on the New Jersey Shelf

Based on the mineralogical evidence and the abundance of regional probable source rocks of both old (Grenville) and young (Paleozoic) hornblende grains, IRD has not been identified on the New Jersey shelf through this study. The source terrain originally suspected for contributing to IRD to the NJ shelf is Maine bedrock, however, based on the sea-level at the time of the Laurentide Ice Sheet contact with the ocean south of Maine, this is unlikely. A more northerly source of IRD is more likely. A definitive source of IRD cannot be identified because individual hornblende grains could not be dated in this study. Maine bedrock has varied ages of predominately Paleozoic crystallization and Canadian bedrock ages vary widely depending on the region considered. Single grain $^{40}Ar/^{39}Ar$ isotopic analyses could be employed on hornblende grains from these samples in the future in an effort to better constrain provenance. U-Pb isotopic apparent ages could also be pursued if zircon grains can be identified within the sediment samples.

CHAPTER 5: CONCLUSIONS

The results of this study indicate:

1) The majority of hornblende grains in Late Pleistocene New Jersey continental shelf sediments are derived from units in the Hudson and New Jersey Highlands, but in the oldest of the sediments sampled some hornblende grains are likely from the Cortlandt complex and related mafic intrusions;

2) The transport history of New Jersey shelf sediments begins at the source rock, most likely in the New Jersey and Hudson Highlands, and continues through fluvial transport in the ancient Hudson River system or other paleodrainage channels;

3) Sedimentological analysis of New Jersey shelf sediments support the catashrophic glacial lake dam breaching hypothesis. Pristine grains of hornblende, garnet, and quartz are found on the New Jersey shelf along with other detrital grains that are abraded and rounded, apparently survivors of multiple weathering episodes;

4) Grain size analysis using graphic mean, standard deviation, and kurtosis allows for identification of trends associated with bedforms. Sand ridges have moderately to moderately-well sorted sand of medium mean grain size and are usually coarse-skewed. Sand ribbons and areas of high fine/low coarse material are more variable in grain size parameters but seem to have been influenced by active erosion through bottom currents;

5) IRD has not been identified through mineralogical assessment. Further geochronological methods need to be employed in the future.

REFERENCES

Ahern, S. M., 1995, Protocol for heavy liquid separation of heavy minerals and recovery of separation liquids, via Uptegrove, Jane, New Jersey Department of Environmental Protection, Geological Survey, gray paper, p. A2-A5.

Alexander, C., C. Sommerfield, J. Austin, B. Christensen, C. Fulthorpe, J. Goff, S. Gulick, S. Nordfjord, D. Nielson, S. Schock. 2003. Sedimentology and Age control of late Quaternary New Jersey Shelf deposits. AGU Fall Meeting Abstracts, San Francisco, CA.

Alexander, C., Austin, Jr., J. A., 2002, Cruise Report – KN167-KN168A/B: "AHC-800 Coring on the New Jersey Shelf for ONR's Geoclutter Initiative", R/V Knorr.

Anderson, W. A., Kelley, J. T., Thompson, W. B., Borns, H. W., Jr., Sanger, D., Smith, D. C., Tyler, D. A., Anderson, R. S., Bridges, A. E., Crossen, K. J., Ladd, J. W., Andersen, B. G., and Lee, F. T., 1984, Crustal warping in coastal Maine: Geology, v. 12, p. 677-680.

Austin Jr., J. A., Fulthorpe, C. S., Mountain, G. S., Orange, D. L., Field, M. E., 1996, Continental-margin seismic stratigraphy: assessing the preservation potential of heterogeneous geological processes operating on continental shelves and slopes, Oceanography, v. 9, p. 173-177.

Bender, J. F., Hanson, G. N., Bence, A. E., 1982, The Cortlandt complex: evidence for large-scale liquid immiscibility involving granodiorite and diorite magmas, Earth and Planetary Science Letters, v. 58, p. 330-344.

Bender, J. F., 1980, Petrogenesis of the Cortlandt complex, Ph.D. thesis, State University of New York at Stony Brook, 306 p.

Boggs Jr., S., 2001, Principles of Sedimentology and Stratigraphy 3rd ed., Prentice-Hall Inc., New Jersey, p. 64-74.

Carver, R. E., 1971, Heavy mineral separation, in Carver, R. E. (ed.) *Procedures in Sedimentary Petrology*, Wiley-Interscience, New York, p. 427-452.

Christensen, B. A., Goff, J. A., Alexander, C. R., Austin, J. A., Gulick, S. P., Fulthorpe, C. S., Nordfjord, S., Sommerfield, C., Venherm, C., Schock, S., Nielson, D. L., 2003, Late Pleistocene depositional environments of the New Jersey continental shelf: foraminiferal evidence, *Eos Trans. AGU, 84*(46), Fall Meet. Suppl., Abstract OS52B-0907.

Cronin, T. M., 1999, *Principles of Paleoclimatology*, Columbia University Press, New York, 560 p.

Dallmeyer, R. D., 1975, $^{40}Ar/^{39}Ar$ release spectra of biotite and hornblende from the Cortlandt and Rosetown plutons, New York, and their regional implications, Journal of Geology, v. 83, p. 629-643.

Dalrymple, G. B., and Lanphere, M. A., 1969, *Potassium-argon dating: Principles, techniques, and applications to geochronology*, W. H. Freeman, San Francisco, 258 p.

Davies, T. A., and Austin Jr., J. A., 1997, High-resolution 3D seismic reflection and coring techniques applied to late Quaternary deposits on the New Jersey shelf, Marine Geology, v. 143, p. 137-149.

Dickin, A. P., 1995, *Radiogenic Isotope Geology*, Cambridge University Press, Cambridge, United Kingdom, 490 p.

Diekmann, B. and Kuhn, G., 1998, Provenance and dispersal of glacial-marine surface sediments in the Weddell Sea and adjoining areas, Antarctica: ice-rafting verses current transport, Marine Geology, vol. 158, p. 209-231.

Dill, H. G., 1998, A review of heavy minerals in clastic sediments with case studies from the alluvial-fan through the nearshore-marine environments, Earth Science Reviews, v. 45, p. 103-132.

Domenick, M. A., and Basu, A. R., 1982, Age and origin of the Coutlandt Complex, New York: Implications from Sm-Nd data, Contributions to Mineral Petrology, v. 79, p. 290-294.

Donnelly, J. P., Driscoll, N. W., Uchupi, E., Keigwin, L. D., Schwab, W. C., Theiler, E. R., Swift, S. A., 2005, Catastrophic meltwater discharge down the Hudson Valley: A potential trigger for the Intra-Allerod cold period, Geology, v. 33 (2), p. 89-92.

Duncan, C. S., Goff, J. A., 2001, Relict iceberg keel marks on the New Jersey outer shelf, Hudson apron, Geology, v. 29 (5), p. 411-414.

Duncan, C. S., Goff, J. A., Austin Jr., J. A., 2000, Tracking the last sea-level cycle: seafloor morphology and shallow stratigraphy of the latest Quaternary New Jersey middle continental shelf, Marine Geology, v. 170, p. 395-421.

Eby, G. N., Petrology, geochronology, mineralogy, and geochemistry of the Beemerville alkaline complex, northern New Jersey, in Puffer, J. H., and Volkert, R. A. (eds.) Neoproterozoic, Paleozoic, and Mesozoic Intrusive Rocks of Northern New Jersey and Southeastern New York, Twenty-first Annual Meeting Geological Association of New Jersey, Mahwah, NJ, p. 52-68.

Emery, K. O., Uchipi, E., 1984, *The Geology of the Atlantic Ocean*, Springer, New York, 105 p.

Ewing, J., Le Pichon, X., Ewing, M., 1963, Upper stratification of Hudson Apron region, Journal of Geophysical Research, v. 68, p. 6303-6316.

Figueiredo, A. G., Swift, D. J. P., Stubblefield, W. L., Clarke, T. L., 1981, Sand ridges on the inner Atlantic shelf of North America: Morphometric comparisons with Huthnance stability model, Geo-Marine Letters, v. 1, p. 187-191.

Folk, R. L., 1974, Petrology of sedimentary rocks, Hemphill, Austin, TX, 182 p.

Folk, R. L., and Ward, W. C., 1957, Brazos River bar: A study in the significance of grain-size parameters, Journal of Sedimentary Petrology, v. 27, p.3-26.

Frank, W. M., and Friedman, G. M., 1972, Continental-shelf sediments off New Jersey, NAPS Document number 02000, National Auxiliary Publications Service, ASIS, CCM Information Corporation, p. 224-237.

Friedman, G. M. and Johnson, K. G., 1983, *Exercises in Sedimentology*, John Wiley and Sons, New York.

Fulthorpe, C. S., and Austin, J. A., 2004, Shallowly buried, enigmatic seismic stratigraphy on the New Jersey outer shelf: Evidence for latest Pleistocene catastrophic erosion? Geology, v. 32, p. 1013-1016.

Galehouse, J. S., 1971, Point counting, in *Procedures in Sedimentary Petrology*, R. E. Carver ed., Wiley-Interscience, New York, p. 385-407.

Gates, A. E., Valentino, D. W., Gorring, M. L., Chiarenzelli, J. R., Hamilton, M. A., 2003, Field trip to the western Hudson Highlands, New York, Long Island Association of Professional Geologists, http://pbisotope.ess.sunysb.edu/lig/Field_Trips/index.htm.

Gates, A. E., Krol, M. A., Valentino, D. W., 2000, Dextral strike-slip tectonic escape in the final assembly of Rodinia in the Appalachians, Hudson Highlands, NY, GSA Abstracts with Programs, v. 32 (1), p. 20.

Gates, A. E., Krol, M. A., 1998, Kinematics and thermochronology of late Grenville escape tectonism in the Central Appalachians, GSA Abstracts with Programs, v. 30 (7), p. 124.

Goff, J. A., Austin Jr., J. A., Gulick, S., Nordfjord, S., Christensen, B., Sommerfield, C., Olson, H., Alexander, C., 2005, Recent and modern marine erosion on the New Jersey outer shelf, Marine Geology, in press.

Goff, J. A., Kraft, B. J., Mayer, L. A, Schock, S. G., Sommerfield, C. K., Olsen, H. C., Gulick, S. P. S., Nordfjord, S., 2004, Seabed characterization on the New Jersey middle and outer shelf: Correlability and spatial variability of seafloor sediment properties, Marine Geology, v. 209, p. 147-172.

Goff, J. A., Swift, D., J. P., Duncan, C. S., Mayer, L. A., Hughes-Clarke, J., 1999, High-resolution swath sonar investigation of sand ridge, dune and ribbon morphology in the offshore environment of the New Jersey margin, Marine Geology, v. 161, p. 307-337.

Grosz, A. E., Berquist, C. R., Jr., and Fischler, C. T., 1990, A procedure for assessing heavy-mineral resources potential of continental shelf sediments, in Heavy Mineral Studies – Virginia Inner Continental Shelf, C. R., Berquist, Jr., ed., Virginia Division of Mineral Resources, Publication 103, p. 13-30.

Gulick, S. P. S., Goff, J. A., Austin Jr., J. A., Alexander, C. R., Nordfjord, S., Fulthorpe, C. S., 2005, Basal inflection-controlled shelf-edge wedges off New Jersey track sea-level fall, Geology, v. 33 (5), p. 429-432.

Hallsworth, C. R., Morton, A. C., Claoue-Long, J., Fanning, C. M., 2000 Carboniferous sand provenance in the Pennine Basin, UK: constraints from heavy mineral and detrital zircon age data, Sedimentary Geology, v. 137 (3-4), p. 147-185.

Hart, S. R., 1964, The petrology and isotopic mineral age relations of a contact zone in the Front Range, Colorado, Journal of Geology, v. 72, p. 493-525.

Hemming, S. R., Vorren, T. O., Kleman, J., 2002, Provinciality of ice rafting in the North Atlantic: application of $^{40}Ar/^{39}Ar$ dating of individual ice rafted hornblende grains, Quaternary International, v. 95-96, p. 75-85.

Hemming, S. R., Broecker, W. S., Sharp, W. D., Bond, G. C., Gwiazda, R. H., McManus, J. F., Klas, M., and Hajdas, I., 1998, Provenance of Heinrich layers in core V28-82, northeastern Atlantic: $^{40}Ar/^{39}Ar$ ages of ice-rafted hornblende, Pb isotopes in feldspar grains, and Nd-Sr-Pb isotopes in the fine sediment fraction, Earth and Planetary Science Letters, v. 164, p. 317-333.

Hubert, J. F., 1962, A zircon-tourmaline-rutile maturity index and the interdependence of the composition of heavy mineral assemblages with the gross composition and texture of sandstones, Journal of Sedimentary Petrology, v. 32, p. 440-450.

Isphording, W. C., 1970, Late Tertiary paleoclimate of eastern United States, American Association of Petroleum Geologists Bulletin, v. 54, p. 334-343.

Jappy, T. G., Leake, B. E., Fallick, A. E., 2001, Relationships between hornblende K-Ar ages, chemical composition and hydrogen isotopes, Connemara, western Ireland: evidence for a massive extinct hydrothermal system, Journal of the Geological Society, London, v. 158, p. 843-854.

Kaplan, M. R., 1999, Retreat of a tidewater margin of the Laurentide ice sheet in eastern coastal Maine between ca. 14000 and 13000 ^{14}C yr B.P.: Geological Society of America, Bulletin, v. 111, no. 4, p. 620-632.

Lambeck, K., and Chappell, J., 2001, Sea level change through the last glacial cycle, Science, v. 292, p. 679-686.

Long, L. E., and Kulp, J. L., 1962, Isotopic age study of the metamorphic history of the Manhattan and Reading prongs, GSA Bulletin, v. 73, p. 969-996.

Maine Geological Survey, 2004, Generalized Surficial Geologic Map of Maine, and A Geologic History of Maine, http://www.state.me.us/doc/nrimc/pubedinf/factsht/surfical/surfmap.gif, http://www.state.me.us/doc/nrimc/pubedinf/factsht/surf-fact.htm.

Marvinney, R. G., and Thompson, W. B., 2000, A geologic history of Maine, Maine Geological Survey, Department of Conservation, http://www.state.me.us/doc/nrimc/pubedinf/factsht/bedrock/megeol.htm.

McBride, E. F., 1971, Mathematical treatment of size distribution data, in Carver, R. E. (ed.) *Procedures in Sedimentary Petrology*, Wiley-Interscience, New York, p.109-127.

McHone, J. G., 1992, Mafic dike suites within Mesozoic igneous provinces of New England and Atlantic Canada, *in* Puffer, J. H., and Ragland, P. C., (editors), Eastern North American Mesozoic magmatism: Geological Society of America, Special Paper 268, p. 1-12.

McMaster, R. L., 1954, Petrography and genesis of the New Jersey beach sands, State of New Jersey Department of Conservation and Economic Development, Geological Survey Bulletin, 63, 239 p.

Merguerian, Charles; and Sanders, J. E., 1995b, Late syn-intrusive clastic dikes at the base of the Palisades intrusive sheet, Fort Lee, NJ, imply a shallow (~3 to 4 km) depth of intrusion, p. 54-63 *in* Hanson, G. N., *chm*., Geology of Long Island and metropolitan New York, 22 April 1995, State University of New York at Stony Brook, NY, Long Island Geologists Program with Abstracts, 135 p.

Morton, A. C., Claoue-Long, J. C., Hallsworth, C. R., 2001, Zircon age and heavy mineral constraints on provenance of North Sea Carboniferous sandstones, Marine and Petroleum Geology, v. 18, p. 319-337.

Morton, A.C. & Hallsworth, C.R., 1999, Processes controlling the composition of heavy mineral assemblages in sandstones, Sedimentary Geology, v. 124, 3-29.

New Jersey Geological Survey, 1999, Geologic Map of New Jersey, Department of Environmental Protection, http://www.state.nj.us/dep/njgs/enviroed/freedwn/psnjmap.pdf.

Nordfjord, S., Goff, J. A., Austin Jr., J. A., Sommerfield, C. K., 2005, Seismic geomorphology of buried channel systems on the New Jersey outer shelf: assessing past environmental conditions, Marine Geology, v. 214, p. 339-364.

Ockay, C. and Hubert, J. F., 1996, Mineralogy and provenance of Pleistocene outwash-plain and modern beach sands of outer Cape Cod, Massachusetts, USA, Marine Geology, v. 130, p. 121-137.

Osberg, P. H., Hussey, A. M., II, and Boone, G. M., 1985, Bedrock geologic map of Maine: Maine Geological Survey, scale 1:500,000.

Owens, J. P., and Sohl, N. F., 1969, Shelf and deltaic paleoenvironments in Cretaceous-Tertiary formations of the New Jersey coastal plain, p. 235-278, in. Subutsky, S. (ed.), Geology of selected areas in New Jersey and eastern Pennsylvania, New Brunswick, Rutgers University Press, 382 p.

Pettijohn, F. J., Potter, P. E., and Siever, R., 1987, *Sand and Sandstone*, 2nd ed., Springer-Verlag, New York, 553 p.

Ratcliffe, N. M., Armstrong, R. L., Mose, D. G., Seneschal, R., Williams, R., and Baramonte, M. J., 1982, Emplacement history and tectonic significance of the Cortlandt complex, related plutons, and dike swarms in the Taconide Zone of southeastern New York based on K-Ar and Rb-Sr investigations, American Journal of Science, v. 282, p. 358-390.

Rine, J. M., Tillman, R. W., Culver, R. W., Swift, D. J. P., 1991, Generation of late Holocene sand ridges on the middle continental shelf of New Jersey, USA – evidence for formation in a mid-shelf setting based on comparisons with a nearshore ridge, Spec. Publs Int. Ass. Sediment. v. 14, p. 395-423.

Simmons, W. B., Foord, E. E., Falster, A. U., and King, V. T., 1995, Evidence for an anatectic origin of granitic pegmatites, western Maine, USA [abstract]: Geological Society of America, Abstracts with Program, v. 27, p. 411.

Sirkin, L., 1986, Pleistocene stratigraphy of Long Island, New York, *in* Cadwell, D. H. (editor), The Wisconsinan stage of the first geological district, eastern New York: New York State Museum, Bulletin 455, p. 6-21.

Smith, B. L., 1969, The Precambrian geology of the central and northeastern parts of the New Jersey Highlands, in Subitzky, S. (ed.), Geology of Selected Areas in New Jersey and Eastern Pennsylvania and Guidebook of Excursions, Rutgers University Press, New Jersey, p. 35-47.

St. John, K. E. K., and Krissek, L., 1999, Regional patterns of Pleistocene ice-rafted debris flux in the North Pacific, Paleoceanography, vol. 14 (5), p. 653-662.

Stubblefield, W. L., McGrail, D. W., Kersey, D. G., 1984, Recognition of transgressive and post-transgressive sand ridges on the New Jersey continental shelf, in Tillman, R. W. (ed) Siliciclastic shelf sediments, Society of Economic Paleontologists and Mineralogists, Special Pub. 34, Tulsa, OK, p. 1-23.

Stubblefield, W. L., and Swift, D. J. P., 1981, Grain size variation across sand ridges, New Jersey continental shelf, Geo-Marine Letters, v. 1, p. 45-48.

Swanson, M. T., 1992, Structural sequence and tectonic significance of Mesozoic dikes in southern coastal Maine, *in* Puffer, J. H., and Ragland, P. C. (ed.), Eastern North American Mesozoic magmatism: Geological Society of America, Special Paper 268, p. 37-62.

Swift, D. J. P., McKinney, T. F., and Stahl, L., 1984, Recognition of transgressive and post-transgressive sand ridges on the New Jersey continental shelf: Discussion, in Tillman, R. W. (ed) Siliciclastic shelf sediments, Society of Economic Paleontologists and Mineralogists, Special Pub. 34, Tulsa, OK, p. 25-36.

Swift, D. J. P., Field, M. E., 1981, Evolution of a classic sand ridge field: Maryland sector, North American inner shelf, Sedimentology, v. 28, p. 461-482.

Turner, R. J., Christensen, B. A., Goff, J. A., Uptegrove, J., 2004a, Late Pleistocene IRD on the New Jersey Shelf? GSA Abstracts with Programs, v. 36 (2), p. 70.

Turner, R. J., Christensen, B. C., Wampler, J. M., Uptegrove, J., Goff, J. A., 2004b, Identification of Late Pleistocence IRD on the New Jersey Shelf, EOS Trans., AGU, v. 85 (47), Fall Meeting Supplement, Abstract OS41D-0524.

Uptegrove, J., Muessig, K. W., Grosz, A. E., Muller, F. L., Maharaj, S. V., 1994. Distribution of heavy minerals and gravel in sediments of the New Jersey Shelf as determined from grab and vibracore samples, from Proceedings of the Third Symposium on Studies Related to Continental Margins – A Summary of Year-Five and Year-Six Activities, ed. Dellagiarino, George, Masterson, Amanda, and Miller, Lynda, Minerals Management Service, US Department of the Interior.

Uptegrove, J., Grosz, A. E., Maharaj, S. V., Muller, F. L., Muessig, K., Farnsworth, J., Burbank, G. P., Cheung, T., 1991, Preliminary textural and mineralogical analyses of vibracore samples collected between Absecon and Barnegat Inlets, New Jersey, New Jersey Open-File Report OFR 91-3.

Walker, K. R., Ware, N. G., Lovering, J. F., 1973, Compositional variations in the pyroxenes of the differentiated Palisades Sill, New Jersey, GSA Bulletin, v. 84, no. 1, p. 89-110.

White, R. W., 1998, Glacial sediment and the ice age in New Jersey, New Jersey Geological Survey Information Circular, State of New Jersey.

United States Geological Survey (USGS) Cascades Volcano Observatory (CVO), 2004, America's volcanic past, Maine, http://vulcan.wr.usgs.gov/LivingWith/VolcanicPast/Places/volcanic_past_maine.html

United States Geological Survey (USGS), 2003, NYC Regional Geology, http://3dparks.wr.usgs.gov/nyc/highlands/hudson.htm.

Veatch, A. C., Smith, P. A., 1939, Atlantic submarine valleys of the United States and the Congo submarine valley, GSA Supplemental Paper 7, p. 1-101.

Young, D. A., and Icenhower, J. P., 1989, A metamorphosed sill in the New Jersey Highlands, Northeastern Geology, v. 11 (1), p. 56-64.

APPENDIX

Grain size histograms by bedform:

- Sand Ridges
- Sand Ribbons
- High Fine/ Low Coarse
- Other
- Core

Results of grain size measurements by moment statistics

- TABLE A-1 Results of moment statistics
- TABLE A-2 Results of moment statistical analysis

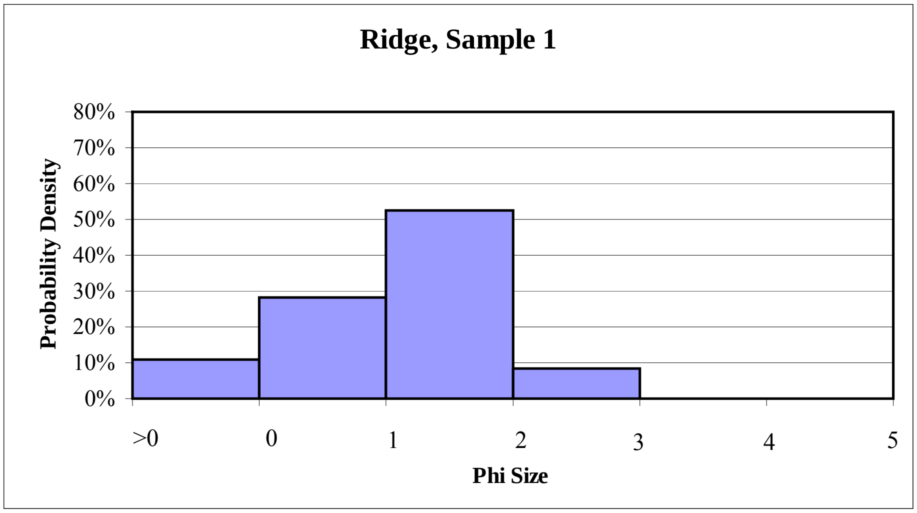
Ridge, Sample 1
Probability Density
80%
70%
60%
50%
40%
30%
20%
10%
0%
>0
0
1
2
3
4
5
Phi Size

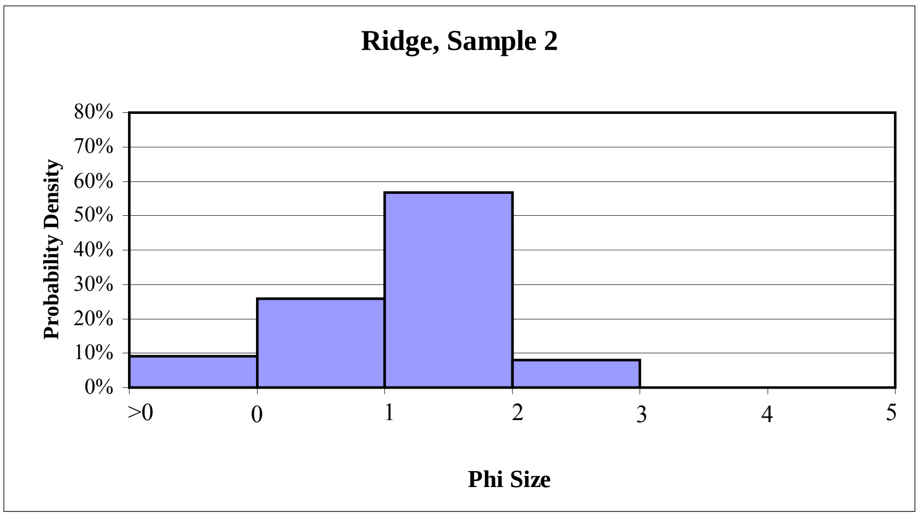
Ridge, Sample 2
Probability Density
80%
70%
60%
50%
40%
30%
20%
10%
0%
>0
0
1
2
3
4
5
Phi Size

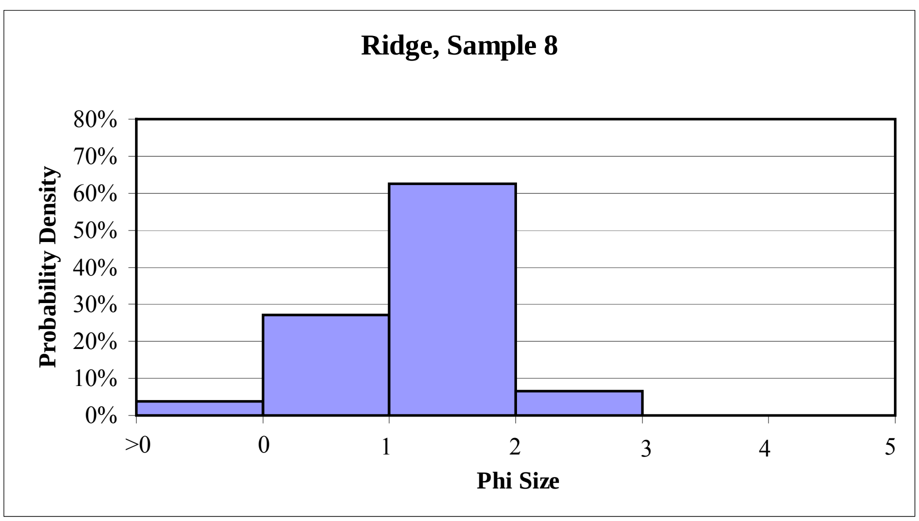
Ridge, Sample 8
Probability Density
80%
70%
60%
50%
40%
30%
20%
10%
0%
>0
0
1
2
3
4
5
Phi Size

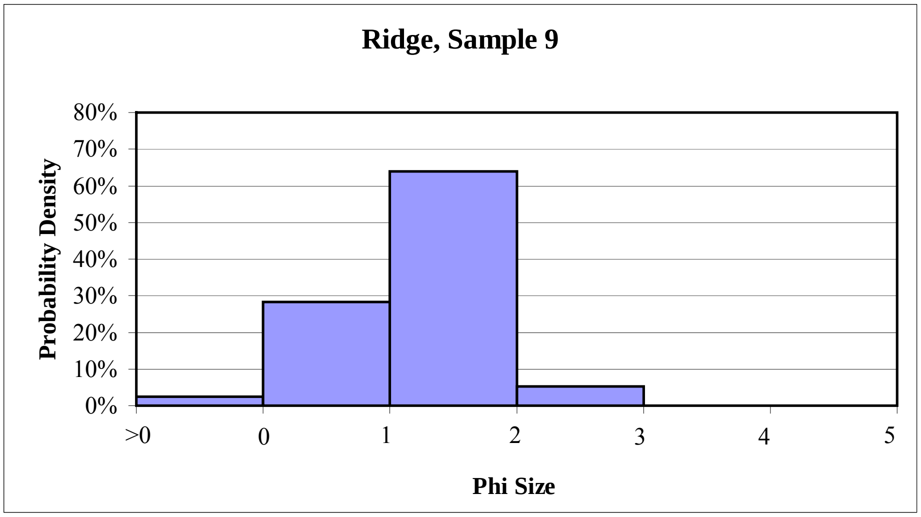
Ridge, Sample 9
Probability Density
80%
70%
60%
50%
40%
30%
20%
10%
0%
>0
0
1
2
3
4
5
Phi Size

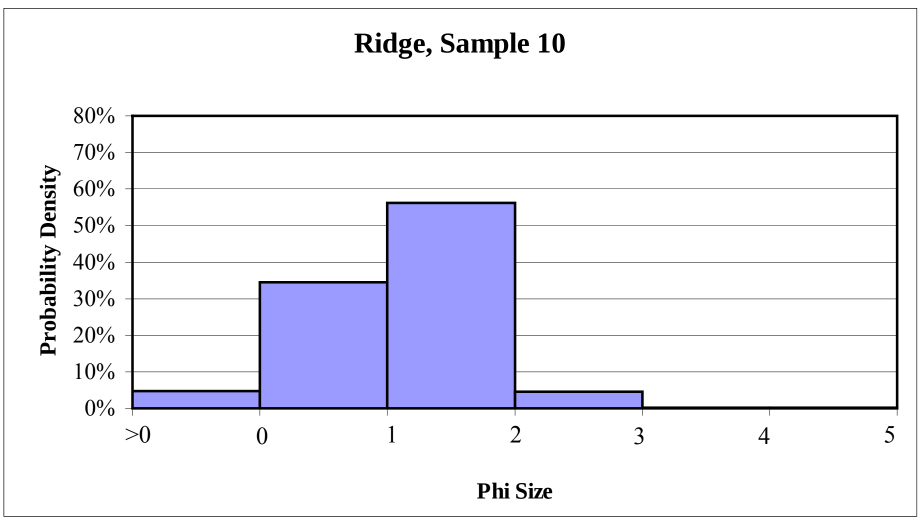
Ridge, Sample 10
Probability Density
80%
70%
60%
50%
40%
30%
20%
10%
0%
>0
0
1
2
3
4
5
Phi Size

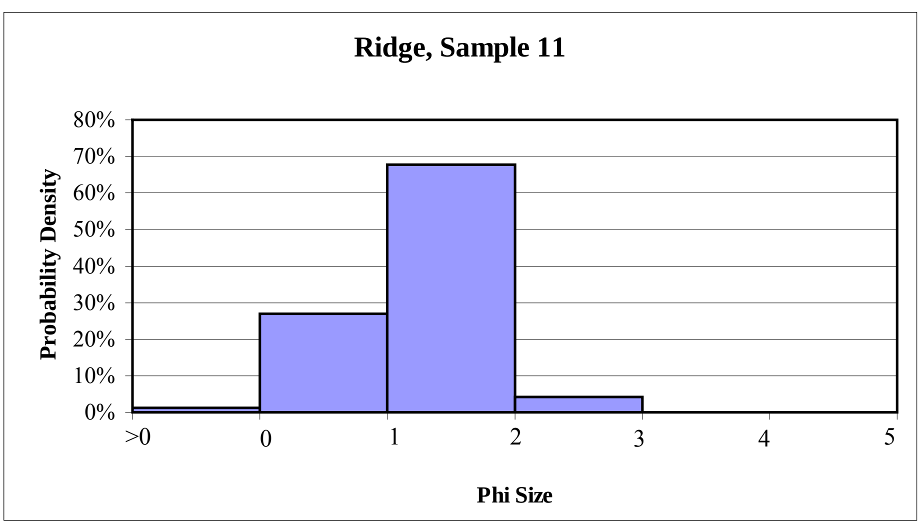
Ridge, Sample 11
Probability Density
80%
70%
60%
50%
40%
30%
20%
10%
0%
>0
0
1
2
3
4
5
Phi Size

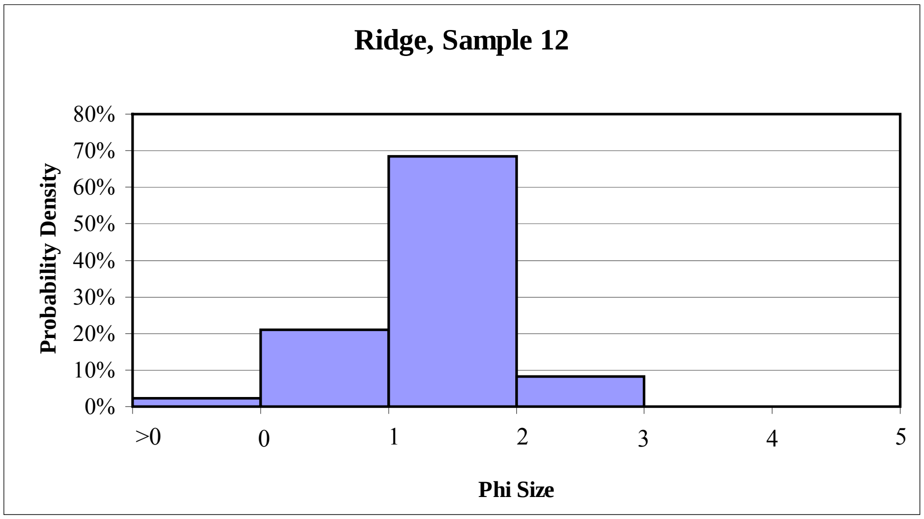
Ridge, Sample 12
Probability Density
80%
70%
60%
50%
40%
30%
20%
10%
0%
>0
0
1
2
3
4
5
Phi Size

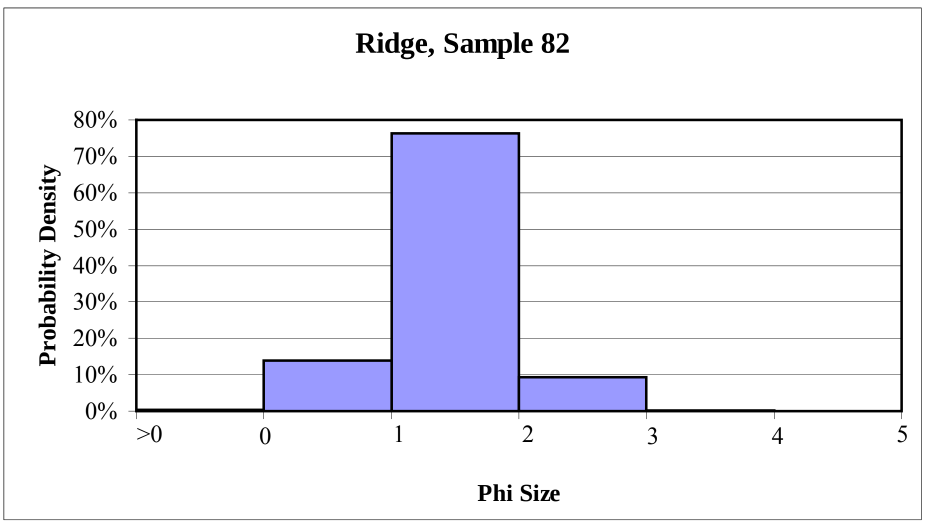
Ridge, Sample 82
Probability Density
80%
70%
60%
50%
40%
30%
20%
10%
0%
>0
0
1
2
3
4
5
Phi Size

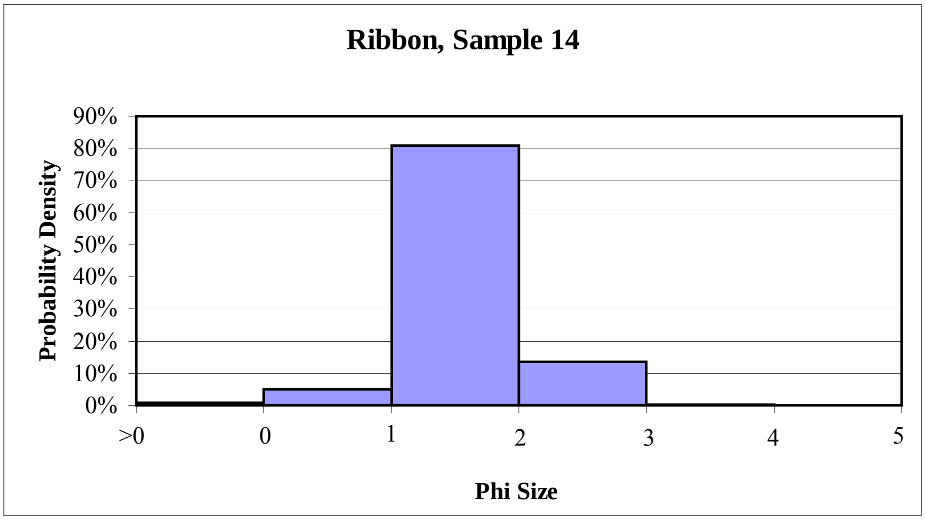
Ribbon, Sample 14
Probability Density
90%
80%
70%
60%
50%
40%
30%
20%
10%
0%
>0
0
1
2
3
4
5
Phi Size

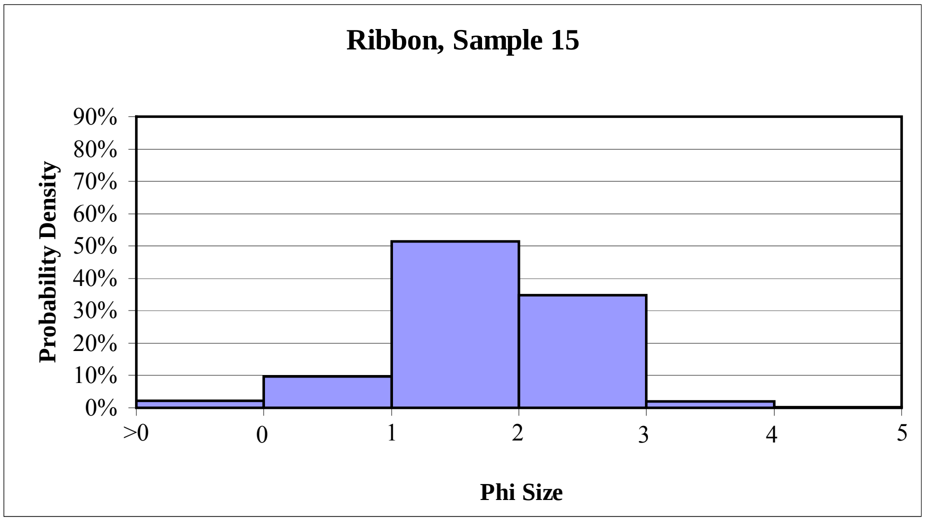
Ribbon, Sample 15
Probability Density
90%
80%
70%
60%
50%
40%
30%
20%
10%
0%
>0
0
1
2
3
4
5
Phi Size

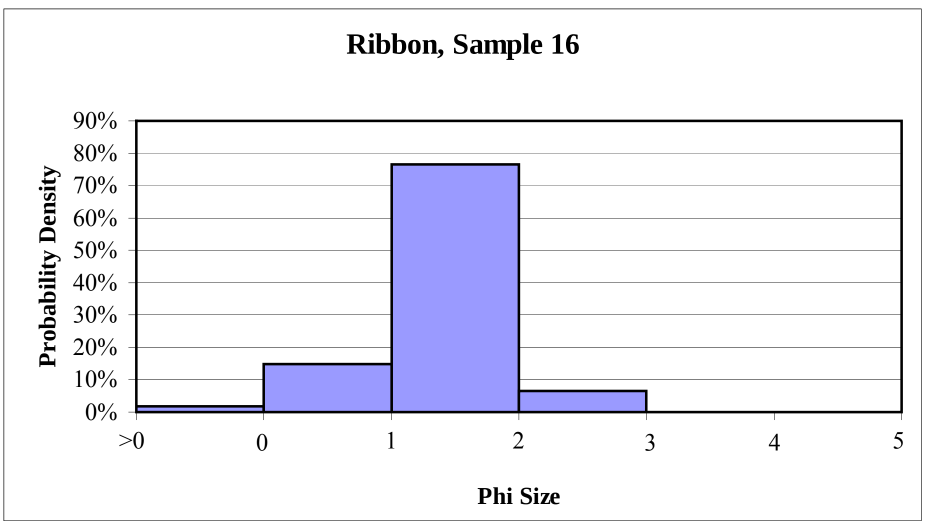
Ribbon, Sample 16
Probability Density
90%
80%
70%
60%
50%
40%
30%
20%
10%
0%
>0
0
1
2
3
4
5
Phi Size

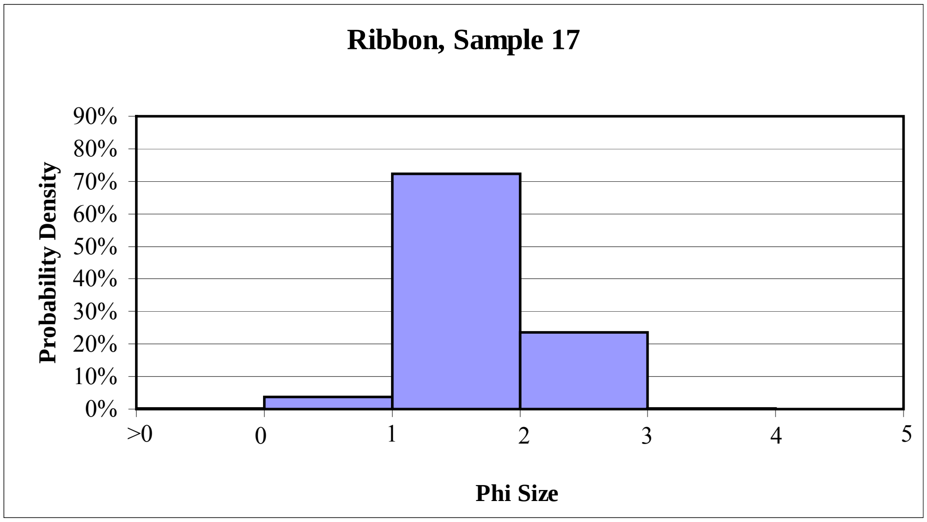
Ribbon, Sample 17
Probability Density
90%
80%
70%
60%
50%
40%
30%
20%
10%
0%
>0
0
1
2
3
4
5
Phi Size

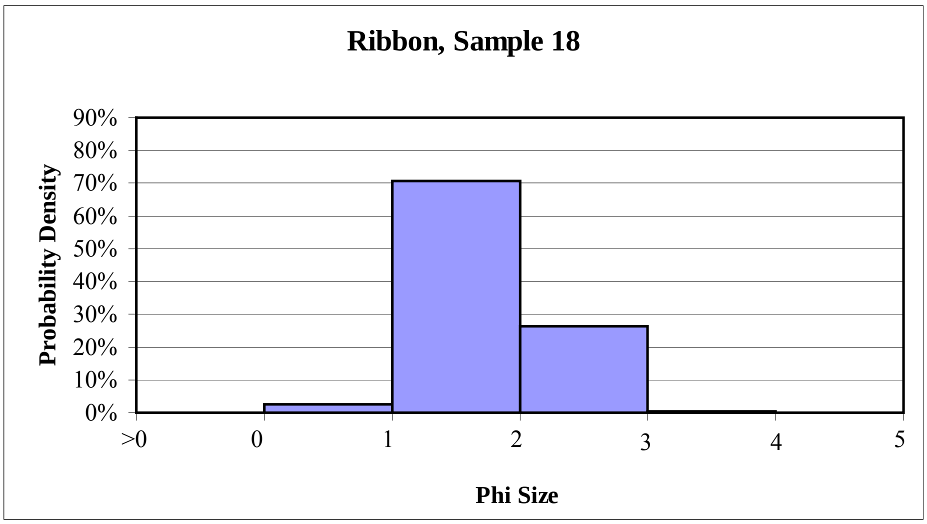
Ribbon, Sample 18
Probability Density
90%
80%
70%
60%
50%
40%
30%
20%
10%
0%
>0
0
1
2
3
4
5
Phi Size

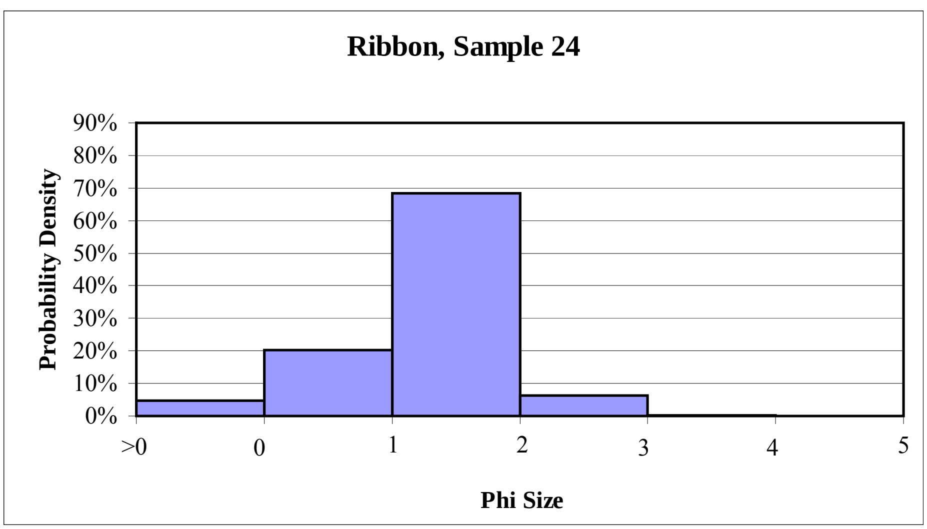
Ribbon, Sample 24
Probability Density
90%
80%
70%
60%
50%
40%
30%
20%
10%
0%
>0
0
1
2
3
4
5
Phi Size

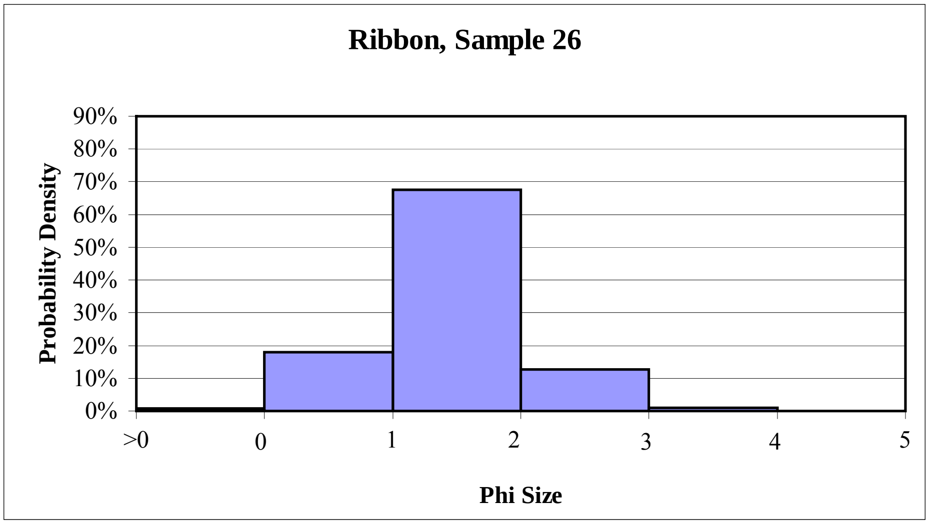
Ribbon, Sample 26
Probability Density
90%
80%
70%
60%
50%
40%
30%
20%
10%
0%
>0
0
1
2
3
4
5
Phi Size

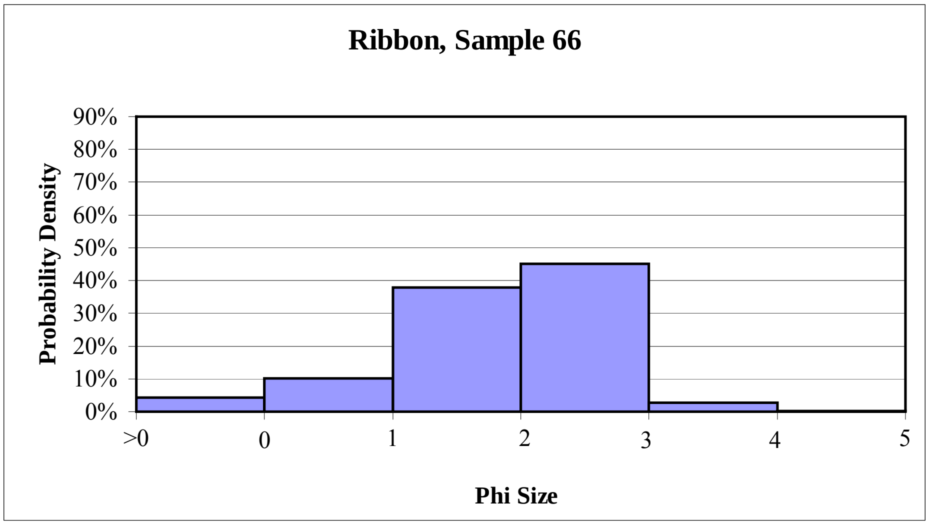
Ribbon, Sample 66
Probability Density
90%
80%
70%
60%
50%
40%
30%
20%
10%
0%
>0
0
1
2
3
4
5
Phi Size

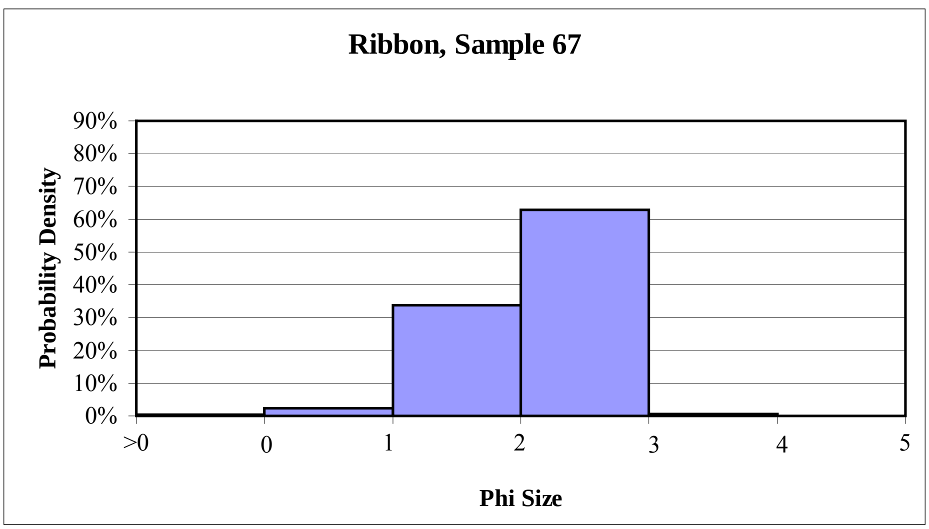
Ribbon, Sample 67
Probability Density
90%
80%
70%
60%
50%
40%
30%
20%
10%
0%
>0
0
1
2
3
4
5
Phi Size

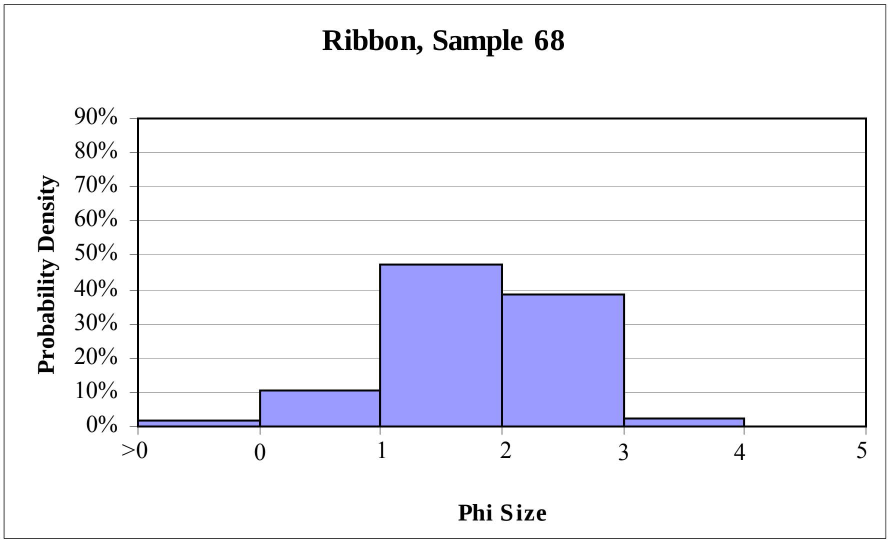

Ribbon, Sample 68
Probability Density
90%
80%
70%
60%
50%
40%
30%
20%
10%
0%
>0
0
1
2
3
4
5
Phi Size

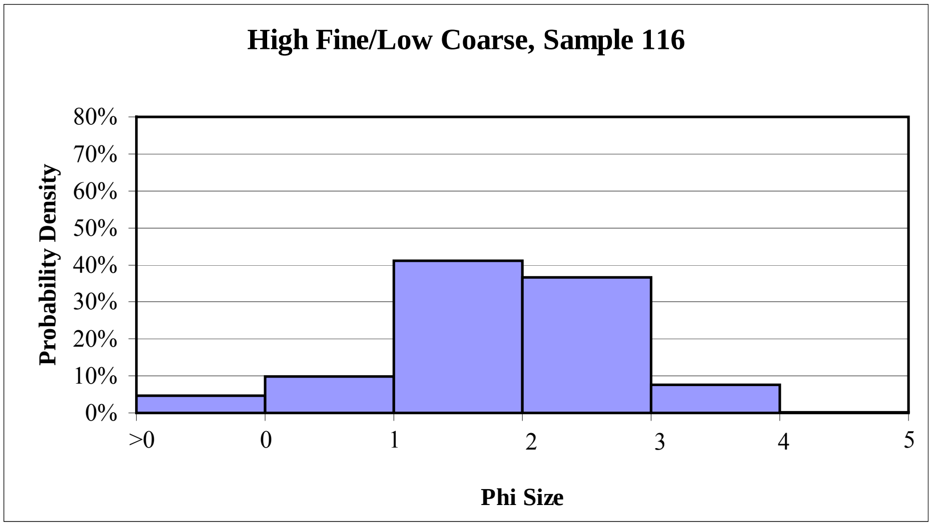
High Fine/Low Coarse, Sample 116
80%
70%
60%
50%
40%
30%
20%
10%
0%
Probability Density
>0
0
1
2
3
4
5
Phi Size

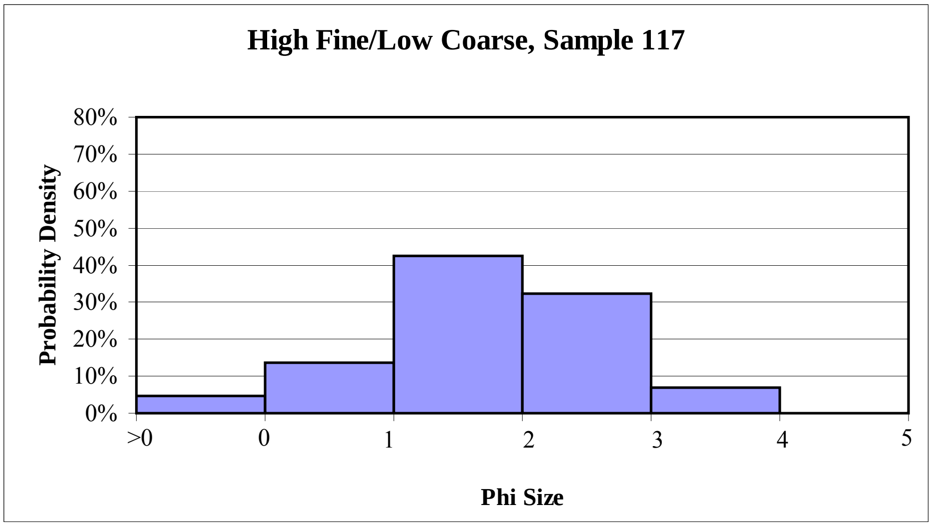
High Fine/Low Coarse, Sample 117
80%
70%
60%
50%
40%
30%
20%
10%
0%
Probability Density
>0
0
1
2
3
4
5
Phi Size

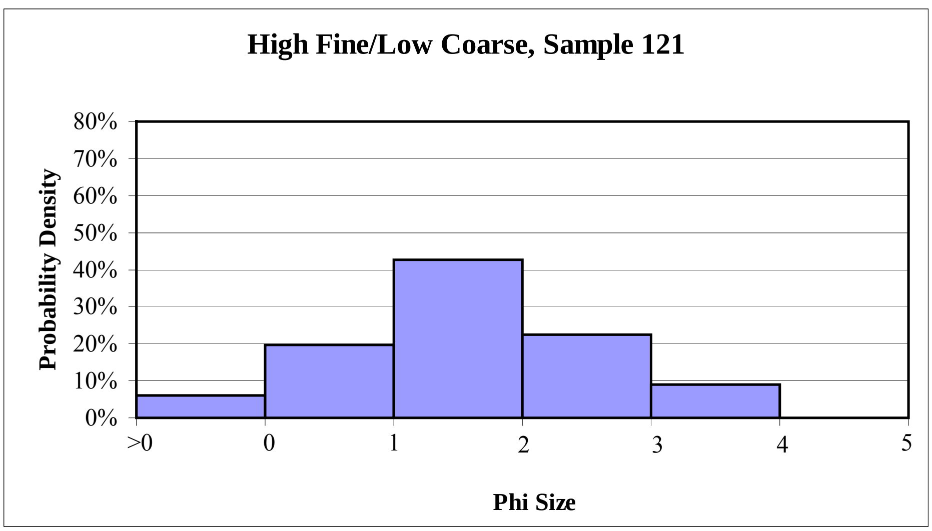
High Fine/Low Coarse, Sample 121
80%
70%
60%
50%
40%
30%
20%
10%
0%
Probability Density
>0
0
1
2
3
4
5
Phi Size

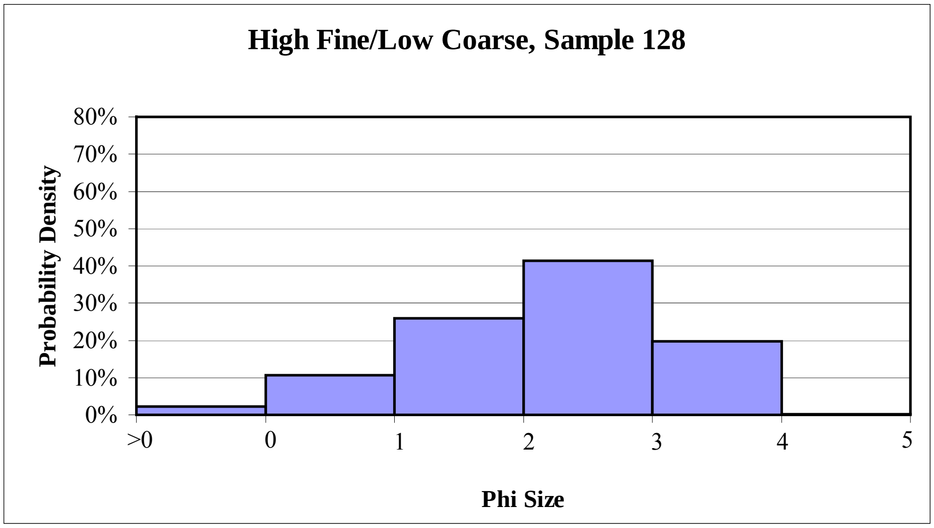
High Fine/Low Coarse, Sample 128
Probability Density
80%
70%
60%
50%
40%
30%
20%
10%
0%
>0
0
1
2
3
4
5
Phi Size

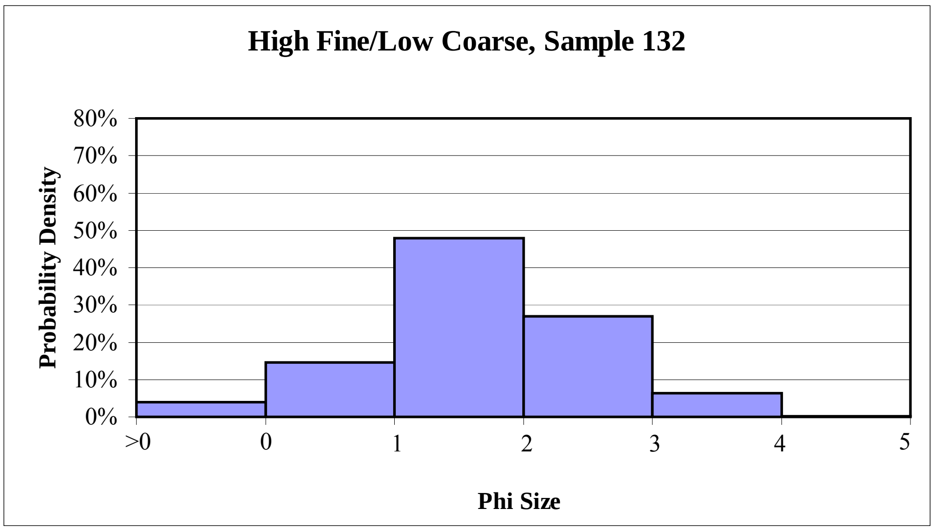
High Fine/Low Coarse, Sample 132
Probability Density
80%
70%
60%
50%
40%
30%
20%
10%
0%
>0
0
1
2
3
4
5
Phi Size

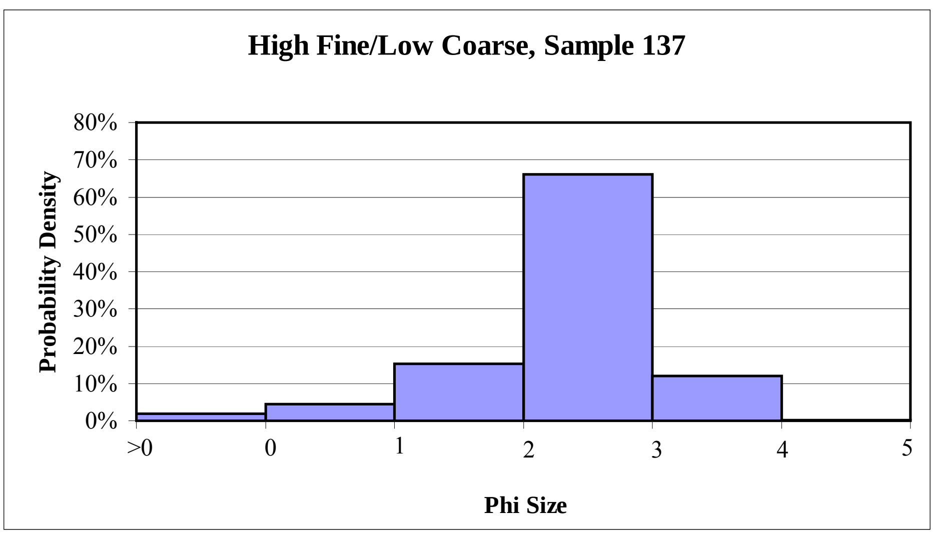
High Fine/Low Coarse, Sample 137
Probability Density
80%
70%
60%
50%
40%
30%
20%
10%
0%
>0
0
1
2
3
4
5
Phi Size

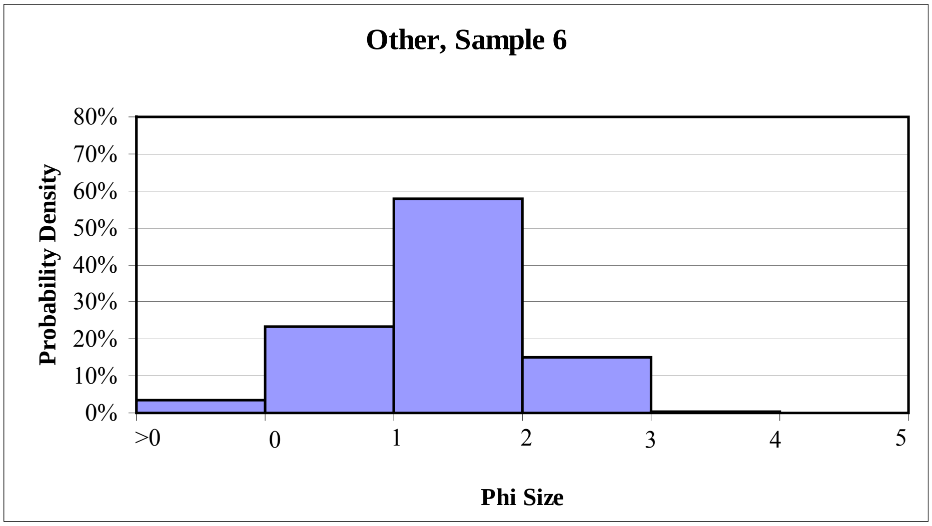
Other, Sample 6
Probability Density
80%
70%
60%
50%
40%
30%
20%
10%
0%
>0
0
1
2
3
4
5
Phi Size

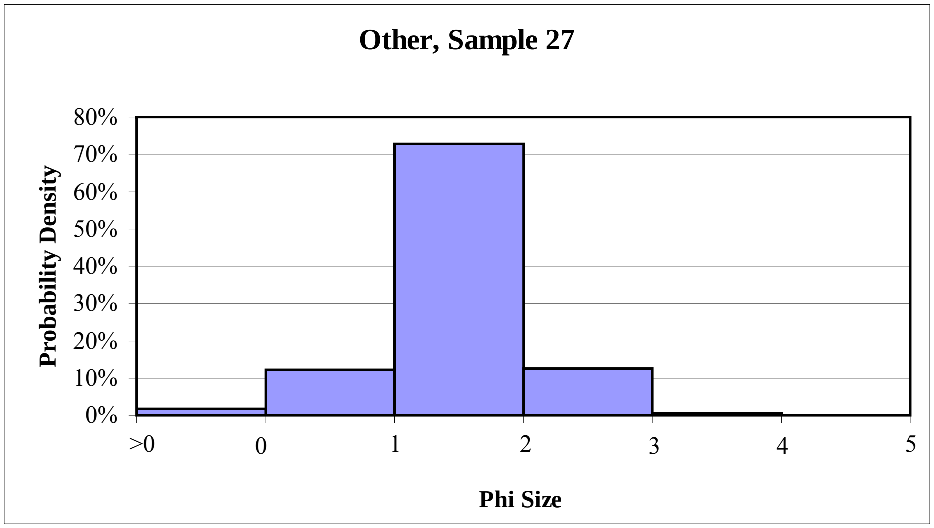
Other, Sample 27
Probability Density
80%
70%
60%
50%
40%
30%
20%
10%
0%
>0
0
1
2
3
4
5
Phi Size

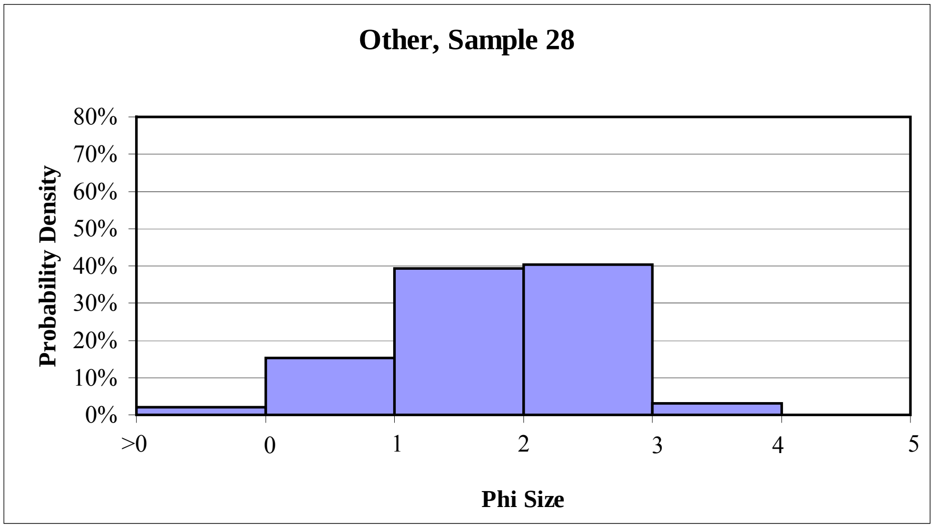
Other, Sample 28
Probability Density
80%
70%
60%
50%
40%
30%
20%
10%
0%
>0
0
1
2
3
4
5
Phi Size

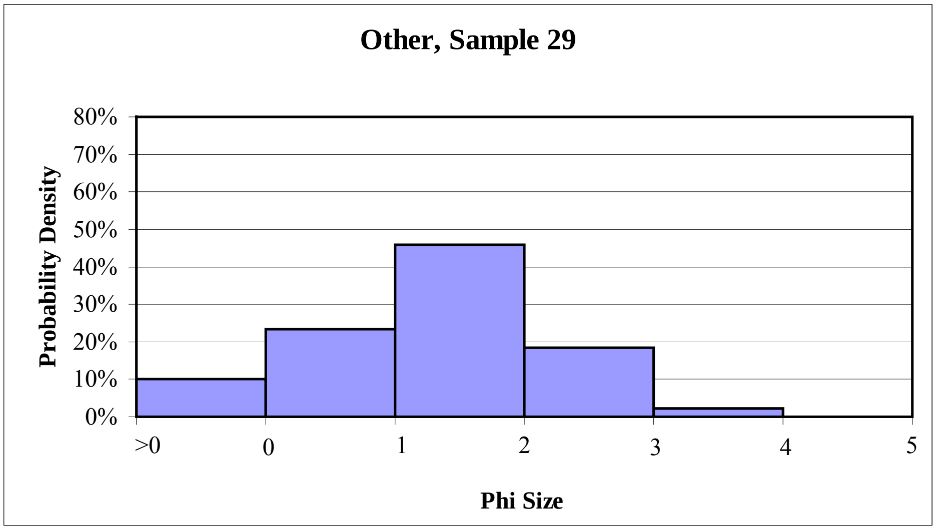
Other, Sample 29
80%
70%
60%
50%
40%
30%
20%
10%
0%
Probability Density
>0
0
1
2
3
4
5
Phi Size

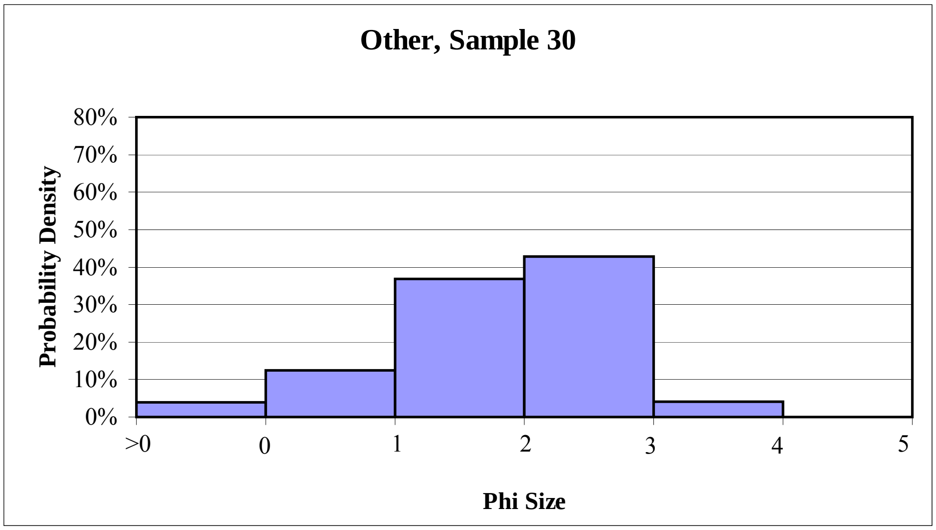
Other, Sample 30
80%
70%
60%
50%
40%
30%
20%
10%
0%
Probability Density
>0
0
1
2
3
4
5
Phi Size

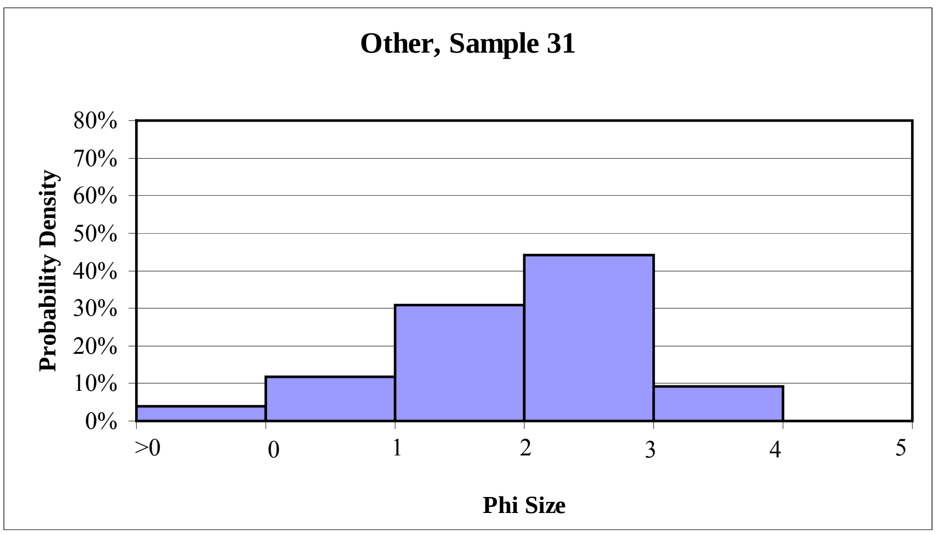
Other, Sample 31
80%
70%
60%
50%
40%
30%
20%
10%
0%
Probability Density
>0
0
1
2
3
4
5
Phi Size

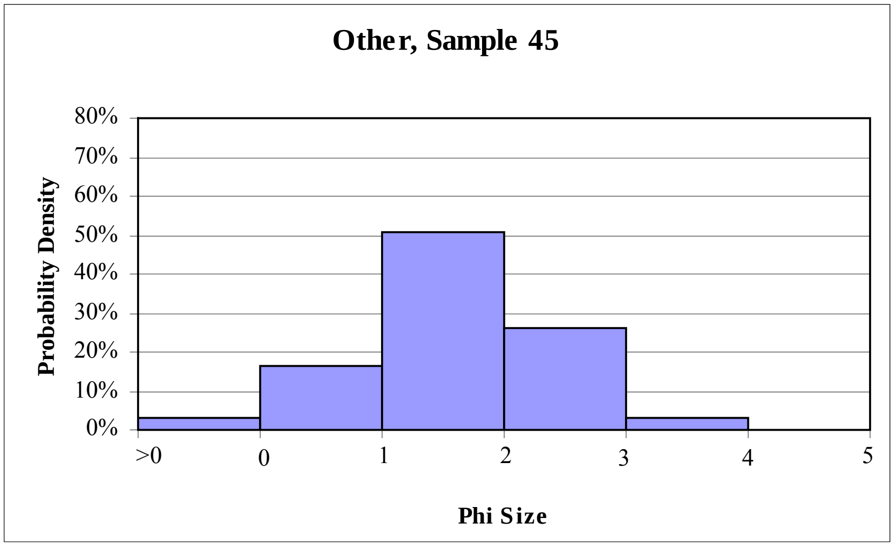
Other, Sample 45
Probability Density
80%
70%
60%
50%
40%
30%
20%
10%
0%
>0
0
1
2
3
4
5
Phi Size

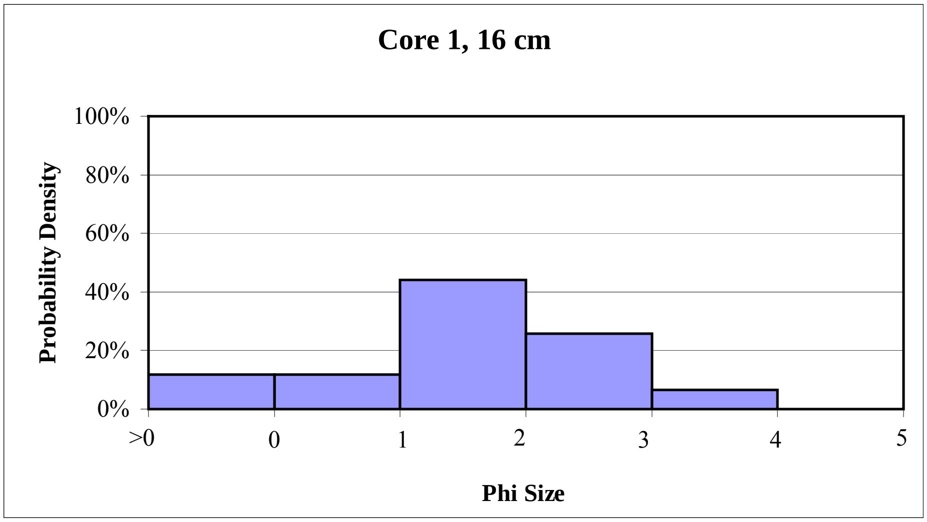
Core 1, 16 cm
Probability Density
100%
80%
60%
40%
20%
0%
>0
0
1
2
3
4
5
Phi Size

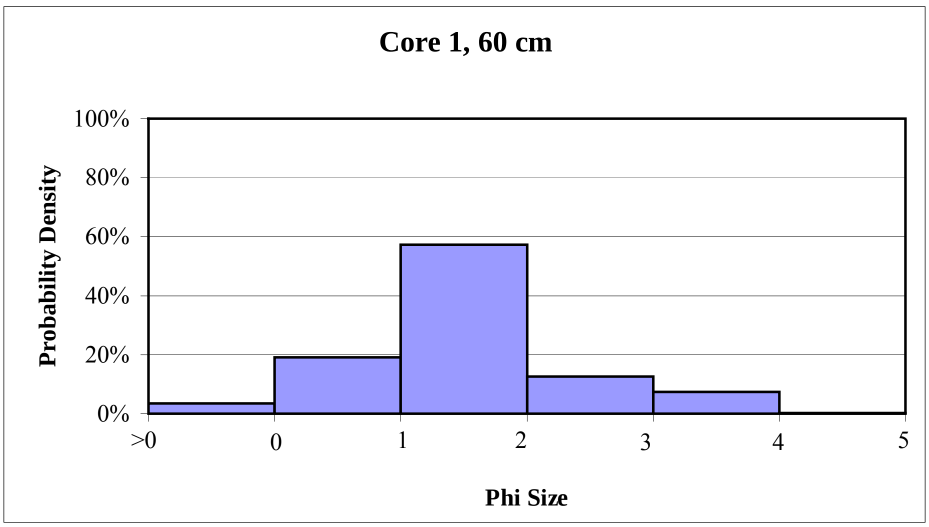
Core 1, 60 cm
Probability Density
100%
80%
60%
40%
20%
0%
>0
0
1
2
3
4
5
Phi Size

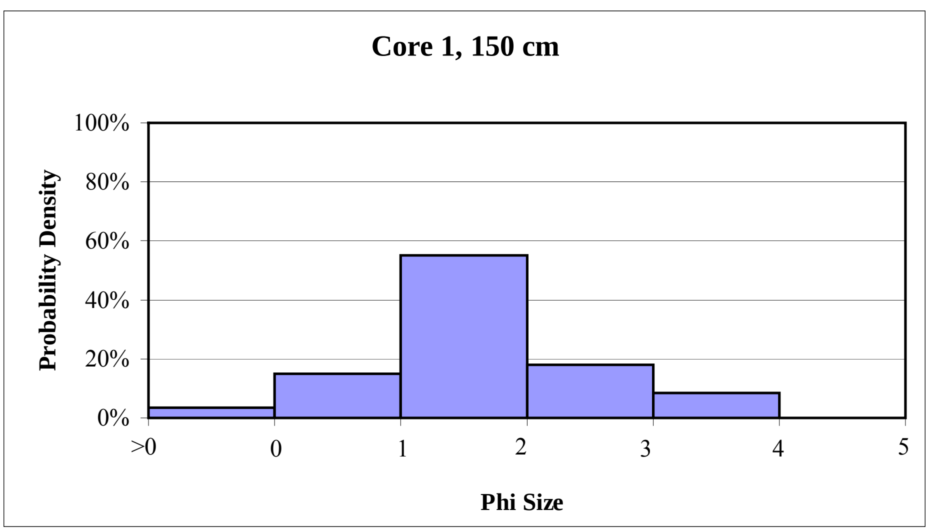
Core 1, 150 cm
Probability Density
100%
80%
60%
40%
20%
0%
>0
0
1
2
3
4
5
Phi Size

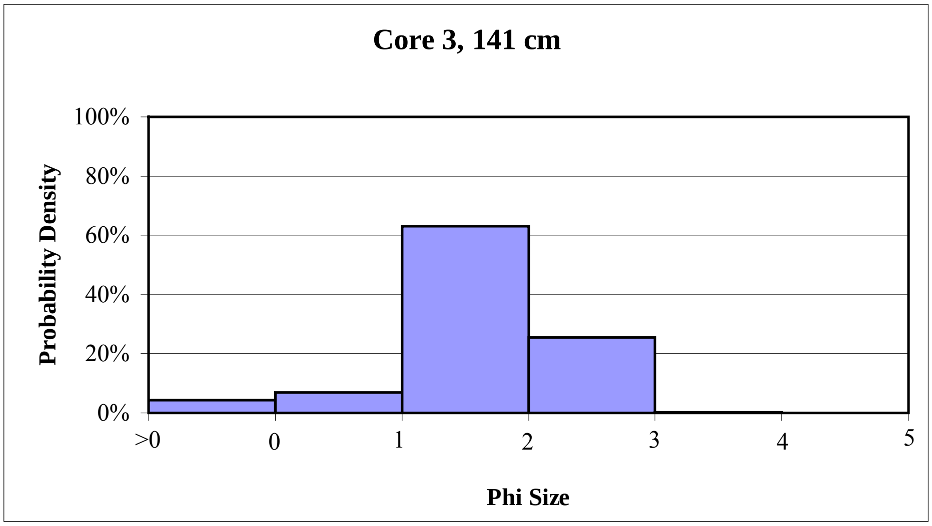
Core 3, 141 cm
Probability Density
100%
80%
60%
40%
20%
0%
>0
0
1
2
3
4
5
Phi Size

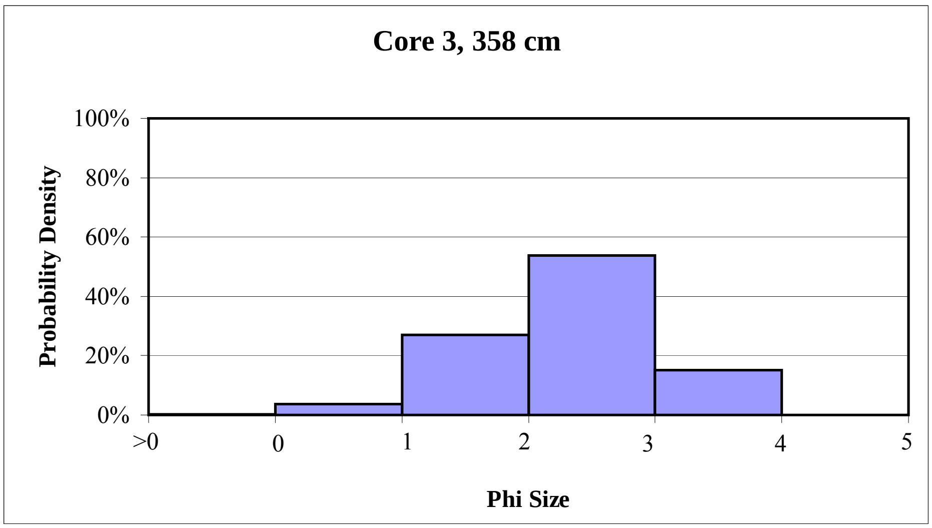
Core 3, 358 cm
Probability Density
100%
80%
60%
40%
20%
0%
>0
0
1
2
3
4
5
Phi Size

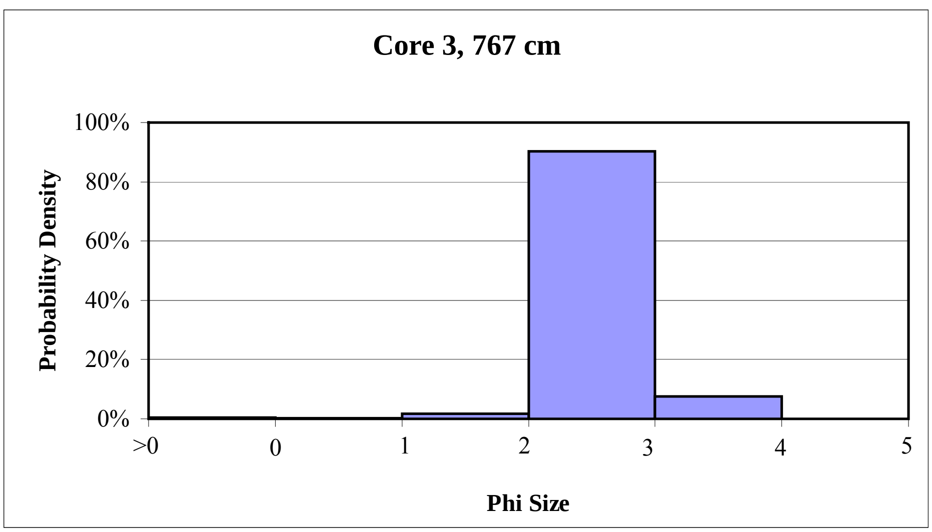
Core 3, 767 cm
Probability Density
100%
80%
60%
40%
20%
0%
>0
0
1
2
3
4
5
Phi Size

TABLE A-1 Results of moment statistics

Sample	Type	Mean	Standard Deviation	Skewness	Kurtosis
1	Ridge	1.08	0.79	-0.42	2.72
2	Ridge	1.14	0.76	-0.50	3.12
6	Other	1.35	0.72	-0.29	3.26
8	Ridge	1.22	0.64	-0.52	3.51
9	Ridge	1.22	0.60	-0.48	3.51
10	Ridge	1.11	0.67	-0.16	3.91
11	Ridge	1.25	0.55	-0.54	3.47
12	Ridge	1.33	0.60	-0.56	4.09
14	Ribbon	1.57	0.46	-0.09	6.92
15	Ribbon	1.75	0.75	-0.42	3.72
16	Ribbon	1.38	0.52	-0.83	5.70
17	Ribbon	1.70	0.50	0.36	3.87
18	Ribbon	1.75	0.50	0.61	3.13
24	Ribbon	1.27	0.64	-0.77	4.37
26	Ribbon	1.45	0.61	0.05	4.16
27	Other	1.48	0.58	-0.35	5.28
28	Other	1.77	0.83	-0.42	2.84
29	Other	1.29	0.93	-0.17	2.72
30	Other	1.81	0.88	-0.61	3.18
31	Other	1.93	0.95	-0.57	3.06
45	Other	1.60	0.83	-0.12	3.36
66	Ribbon	1.82	0.86	-0.78	3.54
67	Ribbon	2.11	0.57	-1.00	4.14
68	Ribbon	1.80	0.75	-0.40	3.37
82	Ridge	1.45	0.50	-0.17	4.95
116	HF/LC	1.83	0.93	-0.43	3.30
117	HF/LC	1.73	0.93	-0.29	3.01
121	HF/LC	1.59	1.01	0.00	2.70
128	HF/LC	2.16	0.99	-0.49	2.79
132	HF/LC	1.68	0.90	-0.09	3.20
137	HF/LC	2.32	0.78	-1.22	5.67
Core 1, 16 cm	Core 1	1.54	1.05	-0.33	2.76
Core 1, 60 cm	Core 1	1.52	0.87	0.37	3.68
Core 1, 150 cm	Core 1	1.63	0.89	0.19	3.39
Core 3, 148 cm	Core 3	1.61	0.71	-0.80	4.74
Core 3, 358 cm	Core 3	2.30	0.75	-0.34	3.18
Core 3, 767 cm	Core 3	2.54	0.36	-1.50	24.77

TABLE A-2 Results of moment statistical analysis

Sample	Type	Mean	Sorting Interpretation	Skewness Interpretation
1	Ridge	1.08	Moderately sorted	Strongly coarse skewed
2	Ridge	1.14	Moderately sorted	Strongly coarse skewed
6	Other	1.35	Moderately sorted	Coarse skewed
8	Ridge	1.22	Moderately well sorted	Strongly coarse skewed
9	Ridge	1.22	Moderately well sorted	Strongly coarse skewed
10	Ridge	1.11	Moderately well sorted	Coarse skewed
11	Ridge	1.25	Moderately well sorted	Strongly coarse skewed
12	Ridge	1.33	Moderately well sorted	Strongly coarse skewed
14	Ribbon	1.57	Well sorted	Near symmetrical
15	Ribbon	1.75	Moderately sorted	Strongly coarse skewed
16	Ribbon	1.38	Moderately well sorted	Strongly coarse skewed
17	Ribbon	1.70	Moderately well sorted	Strongly fine skewed
18	Ribbon	1.75	Moderately well sorted	Strongly fine skewed
24	Ribbon	1.27	Moderately well sorted	Strongly coarse skewed
26	Ribbon	1.45	Moderately well sorted	Near symmetrical
27	Other	1.48	Moderately well sorted	Strongly coarse skewed
28	Other	1.77	Moderately sorted	Strongly coarse skewed
29	Other	1.29	Moderately sorted	Coarse skewed
30	Other	1.81	Moderately sorted	Strongly coarse skewed
31	Other	1.93	Moderately sorted	Strongly coarse skewed
45	Other	1.60	Moderately sorted	Coarse skewed
66	Ribbon	1.82	Moderately sorted	Strongly coarse skewed
67	Ribbon	2.11	Moderately well sorted	Strongly coarse skewed
68	Ribbon	1.80	Moderately sorted	Strongly coarse skewed
82	Ridge	1.45	Well sorted	Coarse skewed
116	HF/LC	1.83	Moderately sorted	Strongly coarse skewed
117	HF/LC	1.73	Moderately sorted	Strongly coarse skewed
121	HF/LC	1.59	Poorly sorted	Symmetrical
128	HF/LC	2.16	Moderately sorted	Strongly coarse skewed
132	HF/LC	1.68	Moderately sorted	Near symmetrical
137	HF/LC	2.32	Moderately sorted	Strongly coarse skewed
Core 1, 16 cm	Core 1	1.54	Poorly sorted	Strongly coarse skewed
Core 1, 60 cm	Core 1	1.52	Moderately sorted	Strongly fine skewed
Core 1, 150 cm	Core 1	1.63	Moderately sorted	Fine skewed
Core 3, 148 cm	Core 3	1.61	Moderately sorted	Strongly coarse skewed
Core 3, 358 cm	Core 3	2.30	Moderately sorted	Strongly coarse skewed
Core 3, 767 cm	Core 3	2.54	Well sorted	Strongly coarse skewed